

CORNELL FSAE

Development, Manufacture, and Testing of a Monolithic Automotive CFRP Wheel

Spring 2014 M.Eng. Report

By Nathaniel F. Gilbert
With contributions by Paul D. Giannelis
Advised by Albert R. George
5/16/2014

Contents

Introduction	8
Acknowledgements	8
Report Intent.....	8
Motivation.....	9
The State of the Art	9
Past Cornell FSAE Composite Wheels.....	10
2006-2007 (ARG 07)	10
2007-2008 (ARG 08)	10
2008-2009 (ARG 09)	11
2009-2010 (ARG 10)	11
2010-2011 (ARG 11)	12
Summary of Unresolved Issues	14
Designing the ARG14 Composite Wheels.....	14
Establishing Design Requirements and Criteria	14
Relevant Competition Rules.....	14
Requirements.....	15
Interfaces.....	15
Structural.....	15
Other	16
Design Drivers.....	16
Selecting an Approach to Design.....	16
Limiting the Scope	17
Choice of Geometry.....	17
Two Piece Composite Rim.....	18
Two Piece Composite Wheel.....	19
One Piece Composite Rim	19
One Piece Composite Wheel	20
Choice and Rationale	20
Design Process.....	21
Defining Loading and Fixtures	21

Isotropic Design	23
Simple Wheel.....	23
U-Channel Wheels	26
Anisotropic Design	29
Initial Model	29
Maximum Load Simulation.....	29
Comparative Simulation	33
Layup Optimization	35
Carbon Selection	35
Design for Stiffness	36
Wheel Center and Spokes.....	36
Rim	38
Design Guide Adherence	39
Final Layup Schedule.....	40
Lug Attachment Design	43
Laminate Testing and Validation	46
Resin System Compatibility Testing.....	46
Sample Preparation and Test Process.....	46
Test Results.....	47
Lug Attachment Design Testing	48
Test Panel Preparation	48
Load Calculations	49
Test Setup	50
Test and Results	52
Manufacturing Process Selection and Design	53
Methods of Pressure Application	53
Autoclave.....	53
Silicone Pressure Intensifier	54
Theory and Process	54
Potential Use for Wheels.....	55
Testing	55
Lessons Learned.....	60

Silicone Vacuum Bag	60
Testing	60
Lessons Learned	61
Bladders.....	61
Mold Design	62
Splits.....	62
Design, Materials, and Manufacturing Process Selection	62
Rim Mold	62
Center Mold.....	64
ARG14 Wheel Manufacture	66
Mold Manufacture	66
Foam Machining and Assembly.....	66
Foam Surface Preparation.....	67
Rim Mold Layups	69
Alignment and Evaluation of Dimensional Tolerances	73
Rim Mold Post Processing and Assembly.....	74
Lesson Learned	77
Layup Process.....	78
Rim Layup.....	78
Center Layup	82
Joining the Molds.....	84
Noodle Application	86
Combined Layup.....	87
Curing.....	88
Initial Cure	88
Post-Cure.....	91
Lessons Learned	92
Carbon Application Techniques	92
Splicing and Conformity	92
Contamination	93
Prepreg Life.....	93
Tack	94

Debulking.....	94
Time	95
Laminate Quality.....	96
Mold Durability.....	99
Post Processing.....	100
Trimming	100
Manually.....	100
Waterjet	102
Sealing and Surface Preparation	103
Washer Installation.....	104
Tire Stem Installation.....	105
Lessons Learned	106
ARG14 Wheel Testing and Evaluation	107
CMM Evaluation	107
Clearance Verification.....	108
Tire Mounting.....	109
Leak Testing.....	110
Weighing	110
Load Testing	110
Test Rig Design	111
Test Rig Manufacture.....	114
Test Setup and Procedure	115
Conclusion.....	117
Lessons Learned	118
Molds	118
Manufacturing Time	118
Future Development.....	119
Testing and Analysis.....	119
Tire Bead Seat Load Testing	119
ANSYS Model Sophistication	119
Impact and Fatigue Resistance	120
Manufacturing and Molds.....	120

Silicone Pressure Intensifier	120
Bladders.....	120
Core.....	120
Tackifier.....	120
Appendix A: Wheel Load Distribution Calculations.....	122
Appendix B: 2010 Wheel Compliance Testing	124
Spring 2010 Testing	124
Fall 2010 Testing.....	125
Procedure.....	125
Results.....	126
Appendix C: Flexural Bending Testing	127
Appendix D: ANSYS Layup Optimization Results.....	128
Maximum Wheel Deflection using T800H and T800S Carbon Fiber	128
Maximum Wheel Deflection using M46J Carbon.....	130
Main Cylinder (Optimized 1st)	130
Inner Rim (Optimized 2nd).....	131
Outer Rim (Optimized 3rd).....	134
Maximum Wheel Deflection using M46J Carbon and T300 Carbon.....	134
Main Cylinder (Optimized 1st)	135
Inner Rim (Optimized 2nd).....	135
Outer Rim (Optimized 3rd).....	136
Appendix E: Layup Schedule Development	137
Wheel Layup Schedule v1	137
Wheel Layup Schedule v2	137
Wheel Layup Schedule v3	138
Wheel Layup Schedule v4	138
Total Plies	138
Independent Plies.....	138
Wheel Layup Schedule v5	139
Total Plies	139
Independent Plies.....	139
Appendix F: Final Layup Checklist	140

Appendix G: Ryan Kennett Emails	141
Appendix H: Wheel Rim Mold CMM Results	143
Outer Rim Bead Surface.....	143
Inner Rim Bead Surface	146
Appendix I: Noodle Instructions.....	148
Appendix J: Wheel CMM Results	151
Appendix K: Tackifier Solution	151
Bibliography	154

Introduction

A one-piece CFRP (Carbon Fiber Reinforced Polymer) wheel was developed, manufactured, and tested. The wheel was intended to replace Cornell FSAE's existing aluminum alloy rims and wheel centers while providing greater wheel stiffness and decreasing mass. This reduction in mass has a particularly notable impact on vehicle performance and handling because wheels are both unsprung and rotating. Previously, Cornell FSAE unsuccessfully attempted to manufacture two-part carbon fiber rims that interfaced with the existing metallic wheel centers. This year, a monolithic design was pursued. While utilizing a one-piece design greatly increases the manufacturing complexity, it eliminates the issues related to the mechanical joining of multi-part wheels and it has the potential to allow even further reduction of wheel weight.

Isotropic Solidworks Simulation models were created to first compare various wheel geometries. Second, once a geometry was selected, a ANSYS Composite PrepPost model of the wheel was used to iteratively optimize its layup schedule. Then coupon and element-scale physical testing was conducted to verify aspects of the ANSYS model and layup design. The suitability of a variety of specialized manufacturing processes for molding the wheel was evaluated. Ultimately, a novel four-part female mold and multiphase layup process was developed and implemented in order to allow for the complex geometry of the wheel to be fabricated while maintaining adequate dimensional control of critical surfaces. The wheel was manufactured and tested to validate its dimensional accuracy, and sealing. Preparations for testing the wheel's stiffness and ability to endure all anticipated loads were completed, but testing was delayed due to the breakdown of the only suitable Instron machine. The wheel was found meet all tested primary design requirements while providing a roughly 20% reduction in wheel weight and allowing for a 1% decrease in overall vehicle mass.

Acknowledgements

This report represents the culmination of a yearlong Master of Engineering project by Nathaniel Gilbert. The report as well as the bulk of the design and manufacturing represents the work of Nathaniel Gilbert. Paul Gianellis was also a major contributor to the project during the fall semester. Paul focused on mold design and evaluating manufacturing techniques during the fall semester. He also was heavily involved with the manufacture of the wheel during January and the beginning of February. This project was only possible with the assistance of the Cornell FSAE team. In particular, Lucas Sganderlla and Larry Lenkin deserve particular mention for assisting with part of the wheel layup and welding the wheel load test rig. In addition, Luke Moll, the unsprung team lead, and Jesse Greene, the team lead, provided invaluable assistance and advice throughout the process. Lastly, but certainly not least, Professor Al George oversaw the project and provided essential guidance throughout the year.

Report Intent

This report has been written with the intent of providing the information necessary for other students to replicate and build upon the work completed this year. Effort has been made include comprehensive information, explain the motivation behind the various decisions, and highlight lessons learned to guide future CFRP wheel development. As of the time of writing, a single proof-of-concept wheel has been designed, manufactured, and validated. The hope is that this report will provide the

basis necessary to allow the wheel design to be further refined and a complete set of competition-ready wheels to be manufactured during the coming school year.

Motivation

CFRP wheels have the potential to provide equal or greater strength and stiffness than the existing alloy wheels, while significantly reducing the mass of the wheels. Wheels are one of the few areas of Cornell's FSAE car where it is still possible to achieve further weight savings measured in multiple pounds. This is particularly beneficial, because it reduces the un-sprung mass of the vehicle while simultaneously reducing the rotational inertia of the car's spinning components (Koenigsegg). This positively impacts almost all measures of the performance of the vehicle and its handling characteristics. At least one source estimates that every pound of wheel weight loss is functionally equivalent to a reduction of 1.6 lb of static mass elsewhere on the car (Mason).

The State of the Art

Composite automotive wheels remain a largely experimental developing technology that has not gained wide acceptance. Both in the FSAE competition and the wider world, few teams and companies have produced composite wheels. Information related to the development of CFRP wheels is largely unavailable. From what information is publically available, it is clear that there is no standardized manner of construction or design and that CFRP wheels vary widely.

In the past, Cornell FSAE has attempted to produce three-piece wheels with a two part composite rim and metallic wheel center. The rims have been composed of unidirectional and/or woven carbon fiber and have been laid up on female molds. After being baked or, in some years, autoclaved, the rims have been bolted to the wheel center to produce the finished wheel.

A handful of other FSAE teams have demonstrated functional composite wheels of varying sophistication. These include TU Graz, RIT, UTA, McGill, University of Toronto, Stuttgart, Kansas University, and Deakin University. Of these, TU Graz, Stuttgart, University of Toronto and Deakin University have produced single-piece wheels while the remaining teams use various types of multi-part wheels. Some teams utilize prepreg laminates and others RTM (Resin Transfer Molding). Some may even use wet layups to produce their wheels.

There are few professional teams or companies which have produced CFRP wheels and little technical information is available about those that have. Composite wheels are banned in most racing series, including F1, likely due to concerns about the potential hazards of composite wheels catastrophically failing. A few manufacturers have recently begun to commercially produce and sell automotive composite wheels. Koenigsegg now sells the first production vehicle to include CFRP wheels (Koenigsegg) while Carbon Revolution sells aftermarket CFRP wheels for a bargain \$15,000 per set (Carbon Revolution Pty Ltd.). Among mainstream manufacturers, BMW has demonstrated concept carbon fiber wheels and reportedly hopes to bring them to the market in the next several years (Ramsey). Motorcycle composite wheels are slightly more common and have been available for purchase longer, but remain rare and expensive.

Past Cornell FSAE Composite Wheels

By the fall of 2013, the team's institutional memory of past attempts to produce composite wheels could be described as hazy. Some of the team's most senior members had memories of the last few attempts to produce carbon wheels, but surviving information on previous composite wheels was primarily found in past technical reports. At the start of the school year, the overriding belief among current team members seemed to be that that composite wheels were too difficult to be worth attempting.

With varying levels of intensity, the team worked on producing composite wheels from 2006-2011. The wheels produced in this period were all of a three piece design. After five years of effort, the team had still not produced wheels that could be reliably used in competition. Most of the issues related to mold sealing, layup reliability, and wheel stiffness had been resolved, however issues relating to wheel leakage, mechanical fastening, and tire mounting were never overcome. The ARG11 (2011) wheels were the most successful, but still leaked unacceptably and proved to be easily damaged when installing tires. It is clear that many of the problems the team encountered with manufacturing the molds and doing layups were related to the team's relative lack of experience with working with composites at the time. Much effort had been invested in developing ANSYS models of the wheels. This process has since been greatly simplified by enhancements to the capabilities and user interface of ANSYS.

Using available technical reports, the team's previous attempts to produce composite wheels have been summarized below. For more detail, consult the relevant technical reports.

2006-2007 (ARG 07)

"Ryan Sills worked on the wheels this year. He worked on laying up wheels and physically testing laminate designs (the two mentioned in the ARG08 summary). He spent a lot of time with manufacturing and dealing with the autoclave. More details about the autoclave can be found in the Spring 2007 technical report as well as Zack Eakin's (first one to suggest carbon fiber wheel flanges) report from 2006." (Rotondo, ARG11 Spring 2011 Technical Report 8)

"A plug was machined for the two piece design, and a mold was made. This mold was not of very good quality, though, with numerous air pockets that led to cracking gel coat. He had also constructed a primitive autoclave from a water heater and several hotplates. As well, after competition last year, we laid up the first several layers of a wheel [in 2007].... Of the three small flange halves laid up in spring of 2007, only one was acceptable for use. The other two either deformed in the autoclave or could not be removed from the mold. The large flange half also had issues during the removal process." (Maduskuie 1) "The layup was just with radial (0 degree) and circumferential (90 degree) orientations, with varying amounts of each. These proved to be too compliant." (Rotondo, ARG11 Spring 2011 Technical Report 3)

2007-2008 (ARG 08)

"In '08 Andrew Maduskie worked on the wheels. At this time the layup schedule was based in radial (0 degree) and circumferential (90 degree) layers. The layup schedules were $[0\ 90\ 0_3]_{sym}$ for a total

of 10 layers and $[0\ 90_2\ 0_2]_{sym}$ for a total of 10 layers. These layup schedules and T700 carbon with E765 epoxy prepreg from Nelcote proved to be less stiff than the aluminum rims.... Maduskie manufactured a full set of carbon wheel flanges using a makeshift autoclave that was built in '06. However, this was the year that they discovered the wheels leaked by about 1 psi an hour and the wheels were not run for competition. " (Rotondo, ARG11 Spring 2011 Technical Report 8)

2008-2009 (ARG 09)

"Alison Nalven worked on the wheels this year. The fall technical report from this year is on the archive and contains mainly the same information as previous years' reports. I don't believe any wheels were manufactured, only attempts were made to seal the wheels from the previous year. All of these attempts failed, as only 5-minute epoxy was used to try and seal them." (Rotondo, ARG11 Spring 2011 Technical Report 8)

2009-2010 (ARG 10)

"For ARG 2010, a graduate student in MAE, Kyle Meier, designed and manufactured a full set of carbon fiber wheel flanges. The laminate design was found by trial [and] error in ANSYS, as well as by a prototype wheel (12 layers) that was tested and determined to be too compliant. Therefore, for the final layup, a wheel with 20 layers, $[weave\ 0\ 45\ 90\ -45\ 0\ 45\ 0\ 45\ 90]_{sym}$ (unidirectional T650 carbon with outer layers of woven carbon) was manufactured. This laminate design has been tested numerous times and is 40% stiffer than the Keizer aluminum wheel flanges.

In terms of manufacturing, Kyle machined the plugs on the lathe and CAD-ed the correct bead geometry. Kyle's CAD geometry is based off of tire specs from Hoosier.... There were some issues regarding the bead seat, as the first wheel manufactured refused to seat. When contacted about this issue, Kyle does not think it is the CAD geometry, but rather a manufacturing error, as the same geometry was used to manufacture the plug again, which worked for all other wheels.



Figure 1: ARG 10 Wheel Mold Preparation



Figure 2: 2010 Carbon Fiber Tools



Figure 3: ARG 10 Inner Wheel Layup



Figure 4: ARG 10 Outer Wheel Layup

Also, in manufacturing, Kyle found and used a surface film during the layup, which improved the leakage issue. The wheels still leaked in the corners of large flange and in some corners of the small flanges. Different people did each layup and different types of vacuum bag were used in the lay ups of each of the flanges. Kyle also perfected a method in the manufacture of the molds and wheels, as many failed attempts at molds due to poor mold surface finish (the epoxy tooling board was porous). The tooling board was sealed with a very thin layer of thin epoxy, and the method in using the PTM&W surface coat was detailed as well. Kyle's report includes these details.

In terms of performance, the wheels still had small leaks at the corners, and were therefore not used during competition. They were run a few times throughout the semester and seemed to perform well, but the leakage prevented extensive testing." (Rotondo, ARG11 Spring 2011 Technical Report 6-8) An example of the completed 2010 wheels can be seen in Figure 9, Figure 10, and Figure 11.

2010-2011 (ARG 11)

Megan Rotondo, an MEng student, led the effort to produce carbon wheels for ARG 11. As with previous years, a three piece design was used. Megan developed a genetic algorithm that implemented in Matlab and ANSYS (Rotondo, ARG11 Spring 2011 Technical Report 34). The algorithm automatically optimized the layup schedule of the wheel in terms of maximum deflection, Tsai-Wu failure criterion values, and number of plies (Rotondo, ARG11 Spring 2011 Technical Report 34). The final layup schedule was manually modified to "to reduce stacking of plies and free edge effects leading to inter-laminar stresses" (Rotondo, ARG11 Spring 2011 Technical Report 35). The specifics of Megan's process for modeling and optimizing the wheels are included in her Spring 2011 technical report.

Foam plugs (40lb/ft³) were turned on a lathe. After several failed attempts to seal the plugs using epoxy, the plugs were ultimately sealed with automotive primer (Rotondo, ARG11 Spring 2011 Technical Report 15-17). The plugs were glued to a sheet of glass using silicone caulk (Rotondo, ARG11 Spring 2011 Technical Report 17-18). The plugs were sealed with Frekote PMC, FMS-100. and WOLO before being sprayed with gelcoat. Fiberglass veil and ten layers of chopped strand mat were applied along with vinyl ester resin. Once removed from the plugs, the molds were cleaned, sealed, and released (Rotondo, ARG11 Spring 2011 Technical Report 19).

"The order of the layup for ARG11 was [surfacing film, weave, 0 15 0 -15 10 0 -10 -45 90]_{sym}" (Rotondo, ARG11 Spring 2011 Technical Report 20). T650 carbon was used (Rotondo, ARG11 Spring 2011 Technical Report 20). Each wheel required 90 ft² of unidirectional carbon (Rotondo, ARG11 Spring 2011 Technical Report 20). Megan provides a detailed explanation of the layup process she used in her Spring '11 report. The wheels were post machined using a CNC mill in the Physics Graduate Shop and trimmed with a Dremel (Rotondo, ARG11 Spring 2011 Technical Report 21-22).



Figure 5: ARG 11 Outer Wheel Layup



Figure 7: Debulking a ARG 11 Outer Wheel Flange



Figure 6: ARG 11 Outer Wheel Layup



Figure 8: Debulking a ARG 11 Inner Wheel Flange

After manufacturing these flanges it was found that they leaked air. "The bolts and washers when torqued down so much, end up cracking the flange, which caused the wheel to leak air" (Rotondo, ARG11 Spring 2011 Technical Report 6). While the leakage problems were never fully resolved, the

wheels were run on the car for several weeks (Rotondo, ARG11 Spring 2011 Technical Report 11). The final composite wheels each weighed 1.5lbs less than the aluminum wheels and were 43% stiffer (Rotondo, ARG11 Spring 2011 Technical Report 34-35). Megan estimated that a total of 240 hours of work were required to manufacture the four wheels (Rotondo, ARG11 Spring 2011 Technical Report 31).

Summary of Unresolved Issues

All previous attempts by Cornell FSAE to produce composite wheels have utilized a three-piece design. Despite six years of work, reliable wheels were never successfully produced. However, when composite wheels were abandoned in 2011, the only unresolved problems were:

- Reliability problems with the gel-coats, mold manufacturing processes, and layup quality control
- Leakage due to porosity
- Cracking and leaking at mechanically fastened joints
- Damage as a result of tire changing

All of these issues would need to be addressed to successfully produce composite wheels.

Designing the ARG14 Composite Wheels

At the start of the design process, a decision was made design the wheels from scratch and reinvent the wheel rather than attempting to build off of Cornell FSAE's past wheel designs. All aspects of the design were reconsidered. Past technical reports were referenced, but not relied upon.

Establishing Design Requirements and Criteria

The first step was to determine the requirements that designs would be required to meet and the criteria against which different designs would be compared.

Relevant Competition Rules

In contrast to most motorsports, which ban composite wheels, FSAE has no rules which disallow composite wheels and few rules related to wheels whatsoever . Relevant 2014 rules relating to wheels are listed below:

- T6.3 Wheels
 - T6.3.1 The wheels of the car must be 203.2 mm (8.0 inches) or more in diameter.
 - T6.3.3 Standard wheel lug bolts are considered engineering fasteners and any modification will be subject to extra scrutiny during technical inspection. Teams using modified lug bolts or custom designs will be required to provide proof that good engineering practices have been followed in their design.
 - T6.3.4 Aluminum wheel nuts may be used, but they must be hard anodized and in pristine condition.
- S4.23 Tires and Wheels
 - S4.23.3 Only one set of tires and wheels needs to be included in the Cost Report...

As can be seen above, FSAE rules have little bearing on the design of composite wheels.

Requirements

Interfaces

It decided initially that the composite wheels would need to be directly interchangeable with the existing alloy rims and tires. This ensures that the alloy rims can be swapped with the composite wheels with no further modification or changes to the car. Until the team has far more experience with composite wheels and is more confident about their long-term reliability, this is prudent. It also means that the car is not dependent on the successful manufacture of composite wheels, which is important because composite wheels remain a highly experimental project. For the composite wheels to function as intended and be interchangeable with the alloy rims, the following requirements must be met:

- The wheels rims must interface with the beads of the tire
- The wheels must interface with the hub and associated lugs
- The wheel must have the appropriate offset
- The wheels must not come in contact with other un-sprung components

These requirements largely specify the geometry of the wheel. The wheel offset is set by the design of the car's suspension and un-sprung components. The center of the wheel is dictated by the design of the hubs and selection of lugs. The outer surface of the rim must be designed to interface with the tire and thus is specified. The necessary geometry of the outer rim surface and its tolerances can be found in the appropriate Tire and Rim Association standard (The Tire and Rim Association) which was obtained from Hoosier, the tire manufacturer. Since the outer surface of the rim is specified, the location of the inner surface is dependent on the thickness of the layup. The layup thickness is likely to be thicker than the aluminum wheels in areas, so it is important to ensure that adequate clearance between fixed components and the wheel is provided during the design phase of un-sprung components.

Structural

The wheels must meet several structural requirements. These can be split into those relating to strength and those relating to stiffness. The strength requirements are straightforward:

- The wheel must not fail
- *In particular*, the wheel must not catastrophically fail
- The wheels must withstand 1 year of normal usage by the team

The requirements for stiffness are less clear. Indubitably, the wheels must withstand all anticipated loading scenarios without deflecting in such a way that the tire bead seal is compromised or the wheel comes in contact with stationary un-sprung components. That is not a particularly stringent requirement however. The other limitation and possibly the limiting factor is that the wheels cannot

deflect to an extent which would negatively impact the handling of the car. The bottom line, however, is that the team simply does not know how wheel deflection impacts the handling characteristics of the car. The softness of the tires and springiness of the suspension seems to suggest that any wheel deflection effect is negligible. However, the team lacks the testing to back that up and searches of literature for relevant information have not proved fruitful. For that reason the following criteria was imposed:

- The wheels must have a stiffness equal or greater than that of the existing alloy wheels to maintain un-sprung stiffness

From years of usage, it is clear that the stiffness of the existing Kiezer alloy wheels is adequate, so this criteria ensure that the composite wheels will have sufficient stiffness. What is not clear, however, is if additional stiffness benefits the handing of the car or if this requirement could be relaxed without impacting the vehicle's performance.

Other

The wheels must also meet the additional miscellaneous requirements:

- The wheels must allow for the repeated changing of tires without damage
- The wheels must not leak
- The manufacturing process must be reliable and repeatable
- The wheels must not unacceptably obstruct airflow around the brake rotors

While seemingly simple, the first three of these requirements have proved to be problematic in the past. The last requirement could prove relevant for a design that lacked spokes or ventilation holes. A quick test that involved taping over the holes on one of the existing alloy wheels and then roughly comparing the brake temperature of that wheel with another after driving using an IR thermometer showed notably elevated brake temperatures. For any given brake design, it will be necessary to ensure the composite wheels do not unacceptably inhibit brake ventilation.

Design Drivers

In addition to the above requirements, the design of composite wheels should be optimized to achieve the following:

- The wheels should have the minimum possible weight
- The manufacturing process should be minimally time intensive and costly

Selecting an Approach to Design

There are many possible approaches to designing a composite wheel. There is a wide array of different manufacturing processes, materials, and wheel architectures that could potentially be used. Some approaches are easier than others and some have the potential for greater weight savings than others. That said, there is no obvious ideal process. The first step, however, of the design process is to outline the general design and methods of manufacture.

Limiting the Scope

This year, the design process was started from scratch and all aspects of the design were reconsidered. Within the time frame of a year, there were limits to the scope of what could be considered for the design. For this reason, after some initial research, consideration of the following was ruled out:

- the use of core
- secondary bonding
- extensive post-machining
- non-prepreg composites

While the team has extensive experience using core, the team lacks the experience necessary to evaluate the susceptibility of core to impact and fatigue damage. With the monocoque, this is less of the concern, but with wheels these issues are potentially highly relevant. In addition, core adds complexity to the layup process. For it be possible to use core in the wheels, further research and testing would be necessary, so a decision was made not to consider the use of core for wheels this year.

Structural secondary bonding, where already-cured composite parts are bonded to other composite or metallic parts, can be deceptively temperamental (Hoke) (Niu 330-348). The team has plenty of experience doing this, but not in highly stressed locations. There is also anecdotal evidence on online forums of commercially produced carbon fiber motorcycle wheels catastrophically failing at bond joints (matt#corse). If reputable commercial manufacturers are unable to ensure bond reliability, it certainly does not bode well for the team. Again, extensive research and testing would be needed to establish the necessary confidence for secondary bonding to be used on the wheels, so secondary bonding was ruled out during the design process.

Post machining cured composite parts is more of an art form than a science. The heat, vibration, and loads generated by conventional machining can cause delimitation or damage the matrix (Sloan, Machining carbon composites: Risky business). If the fibers are being cut, a localized loss of strength necessarily occurs (Sloan, Machining carbon composites: Risky business). Due to the risks involved with post-machining composites, the team's lack of experience in doing so, and the prohibition on the machining of composites in the Emerson shop, efforts were made to limit post-machining (excluding that which could be done with a water-jet) to an absolute minimum and avoid doing so in highly stressed locations.

Manufacturing processes that do not utilize pre-impregnated composite materials, such as resin transfer molding (RTM), were not considered. The team has no experience using these manufacturing methods and would have to develop the necessary skills.

Choice of Geometry

There are several different approaches to designing composite wheels which are in essence dependant on if the wheel is manufactured as a single part or as several parts which must then be bolted together. The decision of how, or if, to split the wheel into different Sections determines the

overall architecture of the design. Ultimately, it becomes a choice between potential weight savings and manufacturing complexity.

Two Piece Composite Rim

A two piece composite rim was considered. In this design, a metallic wheel center is used and bolted to a two piece carbon fiber flange. This type of three-piece wheel was manufactured for ARG11, and was used for all previous Cornell composite wheels. This approach makes the tool design much simpler because two separate tools can be used for each part of the wheel. The two composite pieces can each be manufactured using conventional one piece female molds while providing tooled surfaces at the bead seats and joint between the sections of the rim. Once manufactured, the two parts of the wheel can be bolted together.



Figure 9: 2010 Two-Piece Flange After Lay-Up



Figure 10: 2010 Two-Piece Flange Bolted Together



Figure 11: Assembled 2010 Three-Piece Wheel

From a manufacturing standpoint, a three piece wheel is unquestionably the simplest. The molds are straight forward and no special processes are required. However, a three piece wheel is less than ideal from a weight perspective since the use of a metallic wheel center and hardware adds mass. The use of mechanical fasteners to join the sections provides a potential additional failure point since each bolt represents a stress concentration and it is difficult to design mechanically fastened composite joints. This proved to be a critical problem for the ARG 11 wheels: “The bolts and washers when torqu-

ed down so much, end up cracking the flange, which caused the wheel to leak air” (Rotondo, ARG11 Spring 2011 Technical Report 6). The joint between the rim sections also can potentially leak if not properly sealed or aligned. One advantage of a three piece design is that it allows for the tire to be mounted before the flanges are bolted together, eliminating the need to worry about damaging the carbon fiber during manual tire installation.

Two Piece Composite Wheel

A two-piece composite wheel design would be similar to that of a three-piece wheel with a two part rim, except that one piece of the rim would also extend inwards to serve as the wheel center. A bolt ring would likely still be required to join the two pieces. The manufacturing processes, advantages, and disadvantages of this approach are largely the same as for a three-piece wheel, except that the use of carbon fiber for the wheel center could potentially save additional weight. While this approach would only be marginally more complicated to manufacture than a three-piece wheel, it is not entirely clear that this design would in fact save enough additional weight to justify its use.



Figure 12: Inner Side of a McGill Two-Piece Composite Wheel - Source: zencomposites.com/design.html



Figure 13: Outer Side of a McGill Two-Piece Composite Wheel - Source: fsae.mcgill.ca

One Piece Composite Rim

A one piece composite rim was also considered. The composite rim would be manufactured as a single part and then attached to a metallic wheel center. This design eliminates the mechanically fastened joint between the two rim pieces that would be used in a three piece design. This, in theory, ensures that there can be no leakage between segments of the rim. Still, the metallic center would need to be bolted to the rim, so the bolt ring and issues associated with mechanical fastening remain. This design would likely require the inclusion of an internal lip to which the wheel center could bolt. In contrast to a rim composed of two pieces, it is not possible to produce a one piece rim using a one-piece mold. Any one-piece mold, either male or female, would have negative draft and therefore be unusable. Two male molds (similar to those shown in Figure 9) that were bolted together during the layup could

be used. Alternatively, two or three female molds with split plane(s) parallel to the central axis could be used. A set of female molds would be more difficult to manufacture while maintaining the cylindricity of the wheel, but would provide the bead seats of the wheel with tooled surfaces. While a one piece rim would only be slightly more difficult to manufacture than a two piece rim, the benefits to doing so are limited. It is unclear that a two piece wheel would weigh less than a three piece wheel. The only notable advantage of a one piece rim over a two piece rim is that there is no possibility of leakage through the joint between rim sections.

One Piece Composite Wheel

A one-piece wheel design in which a single monolithic composite part serves as both the rim and center of the wheel offers tantalizing benefits. A one piece wheel has the potential to be lighter than a multi-part wheel due to the elimination of bonded joints and/or mechanical fasteners. In addition, the elimination of these joints eliminates the risk of joint failure. However, a one part wheel requires sophisticated multi-part molds and potentially could necessitate the use of exotic manufacturing processes. As is the case for a two-part wheel with a one-piece rim, a one-piece wheel cannot be manufactured with a one-part mold due to draft angle issues. Significant manufacturing complexity is added by the intersection of the wheel center and the rim. Since, locally this joint has a "T" cross section, it is necessary to have sections of mold on both sides of a surface in order to mold the part. This either requires precise thickness matching of the layup and opposing mold surfaces or non-rigid tooling.



Figure 14: A One Piece RTM Molded Deakin University Wheel - Source: FSAE.com Forums



Figure 15: A One Piece TU Graz Wheel - Source: Mazdaspeedforums.org

Choice and Rationale

A decision was made to pursue manufacturing a one piece wheel. A one piece wheel is the 'ideal' design in the sense that the greatest possible weight savings can be achieved due to the absence of mechanical joints. As the most elegant approach, a one piece wheel also presented the opportunity to gain the most points during design judging. A one piece wheel also eliminated the potential issues related to mechanical joints failing or leaking. While a one piece wheel introduces additional

complexities to the manufacturing process, it was believed that this approach was feasible given the team's abilities and resources.

All of the team's past attempts to produce composite wheels have utilized a three-piece design. While after six years of trying, the team still never produced a reliable set of wheels, the unresolved issues fell into two categories: independent of overall wheel geometry (e.g. wheel porosity, tire changing damage, etc.) or mitigated by the selection of a one-piece design (e.g. cracking and leakage around the mechanical fasteners connecting sections). None of the issues that would remain for a one-piece design appeared particularly daunting. Despite the added complexity of a one-piece wheel, it was concluded to be reasonable to pursue a one piece design rather than simply replicating the 2011 wheels with minor corrections to address the past problems.

Design Process

Once the decision had been made to pursue a one-piece design, the next steps were to define the geometry and layup schedule of the wheel. To do this, the wheel was modeled and simulated as an isotropic part in Solidworks Simulation to establish the geometry of the wheel and gain a sense of the expected distribution of stresses through the wheels and modes of deformation. Once the exact geometry of the wheel had been selected, anisotropic models of the wheel were simulated in ANSYS to select the optimal layup schedule.

No attempt was made to analytically analyze the designs of the wheel, as has been done for the car chassis (Wu, Badu and Tia 7-8). While analytical analysis can serve as a useful baseline against which to compare FEM analysis, in the case of the wheels the areas of greatest interest have complex geometry and/or multi-axial loading, so any simple analytical analysis would be a gross simplification. Furthermore, the team's past wheel simulation and testing results were available and considered a far more reliable baseline against which to compare the design.

Defining Loading and Fixtures

In order to run both the isotropic and anisotropic FEM simulations, it was necessary to first define the loading scenarios and fixtures that would be simulated. The team's understanding of the external loads applied to the wheels is actually quite detailed, however the team's understanding of how these loads are applied to the wheel is far more limited.

The maximum braking, acceleration, cornering, and bump loads had previously been calculated by the un-sprung team and were available in the ARG13 Link Loads spreadsheet. The minimum and maximum loads for both the front and rear wheels are shown in Table 1. Rather than simulating the loads for both the front and rear wheels under each individual loading scenario, the worst-case loads defined for the vehicle suspension were combined. The largest load components in the X, Y, and Z axes predicted for the vehicle suspension were simultaneously applied to the wheel. It should be noted that this loading scenario is in excess of that predicted for the wheels. This single load case was used when running simulations to represent the range of loads that the wheels could experience. While this single case is a simplification, by using only a single conservative load case, the required number of simulations is greatly reduced.

Table 1: External Wheel Load Components

	X-Axis (lbf)	Y-Axis (lbf)	Z-Axis (lbf)
Maximum Front Wheel Loads	0	0	1259.54
Minimum Front Wheel Loads	-300.26	-422.79	187.66
Maximum Rear Wheel Loads	285	0	1186.54
Minimum Rear Wheel Loads	-155.74	-615.6	97.34
Largest Loads	-300.26	-615.6	1259.54

The suspension loads are applied through the tire where it contacts the wheel at the bead seat. Tires are highly elastic, anisotropic, and thin-walled. While possible, creating a FEM model of a tire to calculate bead loads is extremely complex and requires a detailed understanding of the mechanical properties of the tire (M. Chawla) (N. T. Tseng) (X. Yang). After looking into tire FEM models, it quickly became apparent that generating an FEM model for the tire was not a feasible undertaking. Attempting the experimentally measure the loads at the tire bead seat was briefly considered, but was ruled out due to time limitations. This left finding an approximation for tire bead load distributions. Hoosier, the tire manufacturer was unable to provide any information on this. An extensive literature search yielded only the somewhat odd article, "Simplified Stress Analysis of Large-scale Harbor Machine's Wheel" (Wubin Xu), which had been used as a guide during past years. The article gives a cosine distribution with a spread angle of 60° around the circumference of the wheel as the bead seat load distribution (Wubin Xu 355, 359). This distribution was used for the wheel simulations in ANSYS, however a uniform distribution was used for the Solidworks simulations. See Appendix A: Wheel Load Distribution Calculations for the calculations associated with determining this load distribution. The distribution of load across the width of the bead seat is not specified and was assumed to be uniform for the purposes of the simulations.

These loads are supported where the wheel bolts to the hub. As was the case for tire bead loads, developing a detailed model for the mechanical fastening of composites was found to be excessively complicated (J.E. Jam) (Th. Kermanidis) (McClendon) (S. Venkateswarlu) and no generalized approximation for load distribution around bolts in composites was found. For this reason, in the FEM simulations the areas beneath the heads of the wheel lugs were specified as fixed. This is, of course, a rough approximation, but no better solution was identified at time.

In addition to the external loads applied to the wheel, there are also internal loads. The internal air pressure within the tire was specified as a pressure acting upon the outside surface of the wheel. Variations or spikes in this pressure resulting from tire deformation under load were not accounted for. The pressure imposed by the tire on the bead seat due to internal stresses in the tire after installation was assumed to be negligible.

The loads that were applied in the simulations and their distributions are shown in Table 2.

Table 2: Combined Worst-Case Scenario Simulation Loads

Load	Total	Distribution (as defined in ANSYS)	Direction (as defined in ANSYS)	Location
Air Pressure	N/A	12 PSI	Normal	Outer surface between tire bead seats
Vertical Load (Bump)	1260 lbf	$190.9 * \cos((3/2) * \arctan(y / \sqrt{30.25 - y^2}))$ PSI	Normal	Bottom half of tire bead seats
Lateral Load (Cornering)	620 lbf	N/A	X-Direction	Bottom half of side of a tire bead seat on one side
Tangential Load (Braking)	300 lbf	N/A	Tangential and Perpendicular to Central Axis	Bottom half of tire bead seats

Isotropic Design

A variety of one-piece wheel geometries were modeled in Solidworks and simulated using Solidworks Simulation to comparatively evaluate the different designs. Solidworks was used because, while Solidworks Simulation is not as versatile as ANSYS, it provides convenient FEM analysis of isotropic parts. Wheels were modeled as zero-thickness surfaces and then thickened to give a constant thickness throughout the wheel of 0.1 inch. The models were assigned the material properties of 6061 Al for the simulations. These simulations were intended to be rough approximations that could be used to identify stress concentrations and modes of deformation. The simulated maximum displacement was used as a measure of wheel stiffness and used to compare the designs.

Simple Wheel

The simplest of the tested wheel geometries were the ‘simple’ wheel designs which in essence consist of the wheel rim with a conical face connecting the rim to the circular surface at the center of the wheel where the hub attaches. This design was initially intended as a baseline to which other designs could be compared.

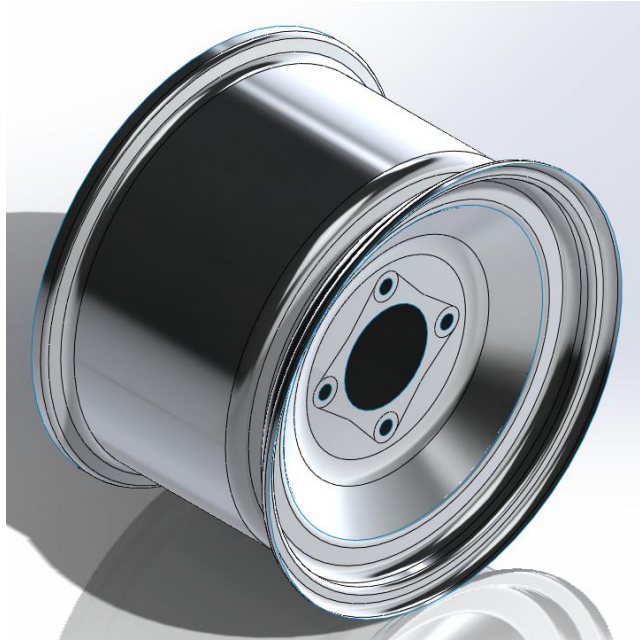


Figure 16: Simple Wheel Design Without Holes

Model name: Thickened Simple Wheel
Study name: Static Loading
Plot type: Static displacement Displacement1
Deformation scale: 32.8992

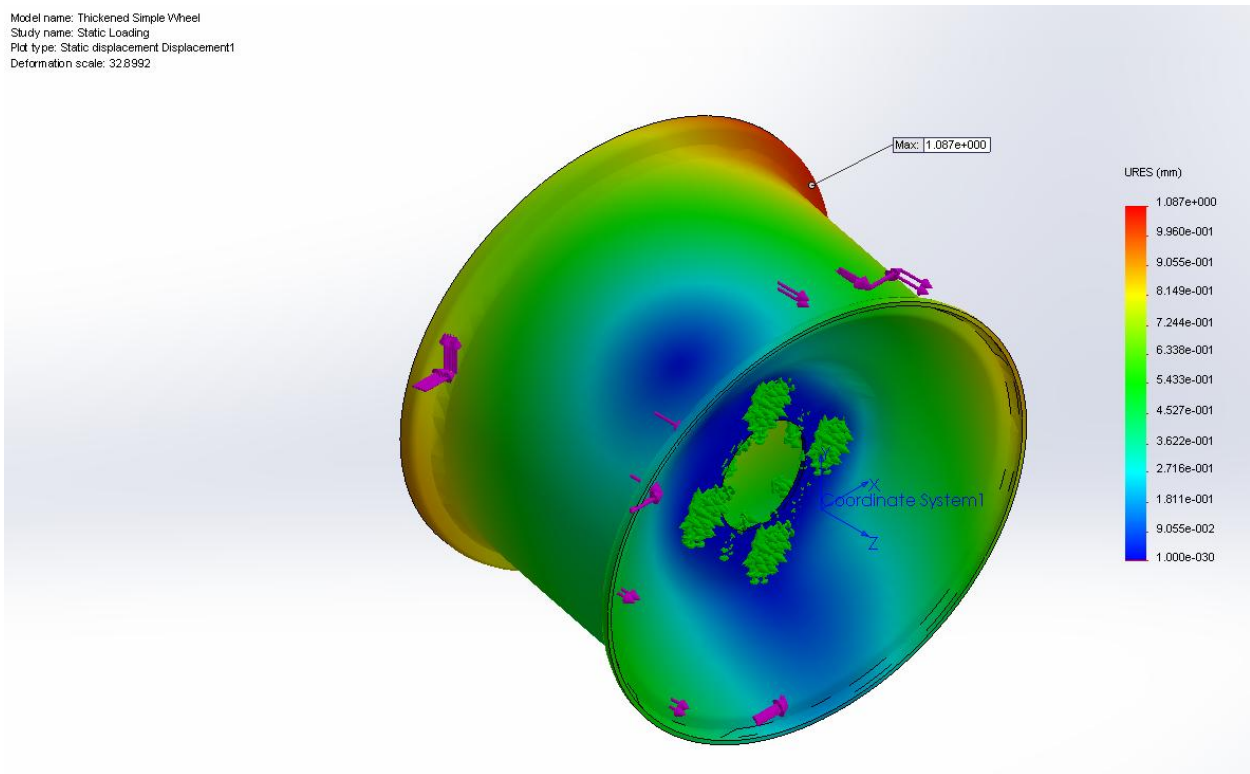


Figure 17: Displacement Results from Simplified Solidworks Simulation of Isotropic Simple Wheel

Model name: Thickened Simple Wheel
Study name: Static Loading
Plot type: Static strain Strain1
Deformation scale: 32.8992

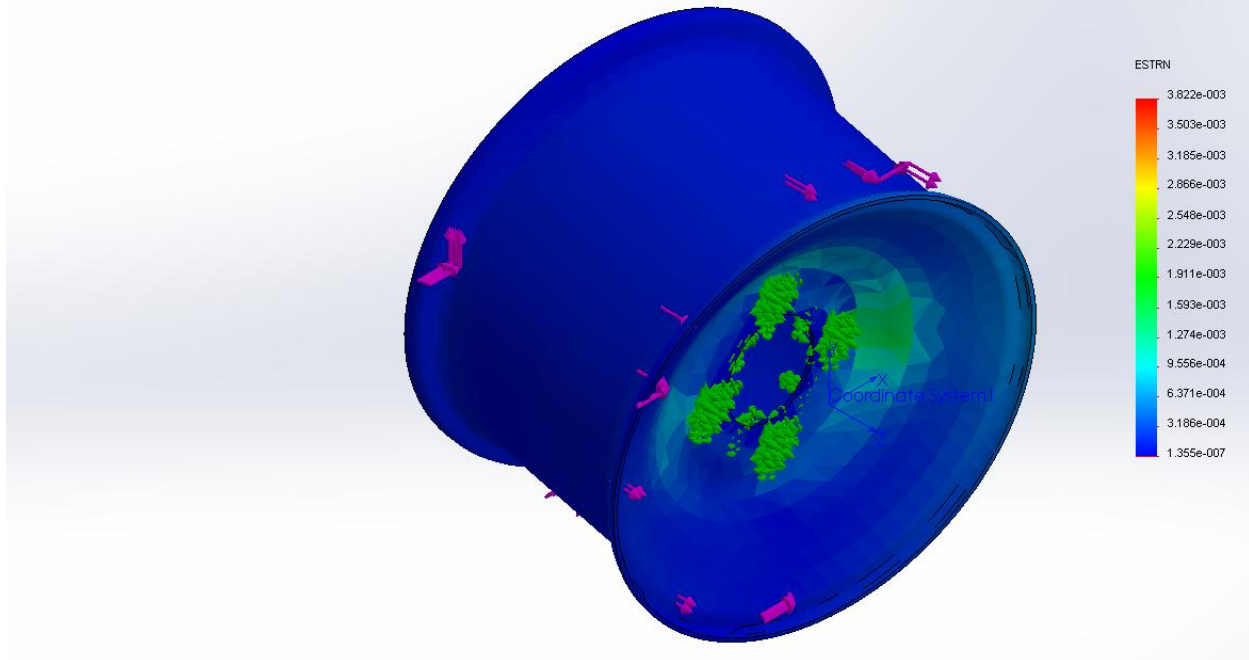


Figure 18: Strain Results from Simplified Solidworks Simulation of Isotropic Simple Wheel

Due to concerns about brake rotor ventilation, the simple wheel was modeled with several different types of holes in the conical face. It was initially considered desirable to avoid holes in this face, due to concerns about stress concentrations and delamination at the edges. However, testing of the existing alloy wheels with the holes taped over resulted in elevated brake temperatures, so holes were incorporated into the design.

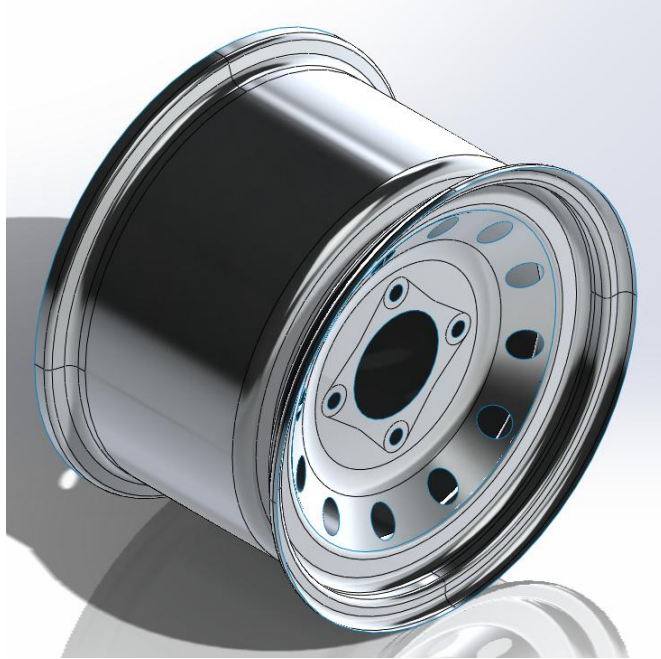


Figure 19: Simple Wheel Design With Round Holes

U-Channel Wheels

A variety of more complex U-channel spoked wheels were also considered. Due to the significant complexity and risk that enclosed spokes would have presented during the manufacturing process, wheels with enclosed spokes were not considered. For this reason, wheels with spokes with a cross-section of a ‘U’ shape were evaluated. These wheels, while more complex than the simple wheel designs, did not require additional mold sections. A variety of wheel shapes were modeled and tested in Solidworks Simulation.

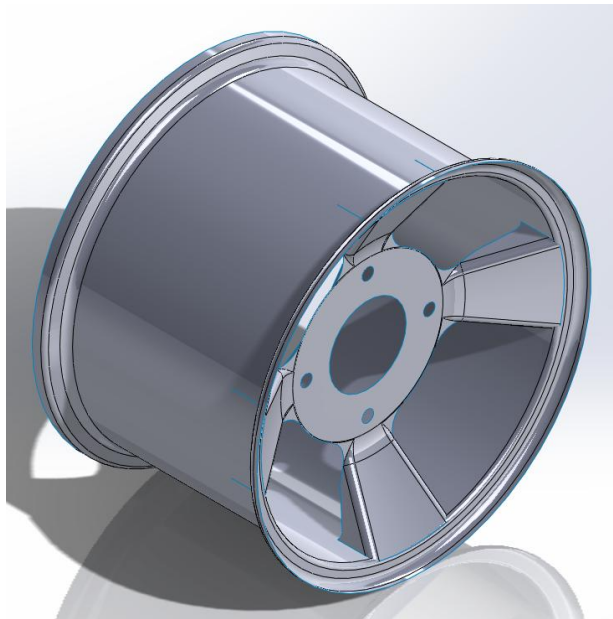


Figure 20: U Channel Wheel Design

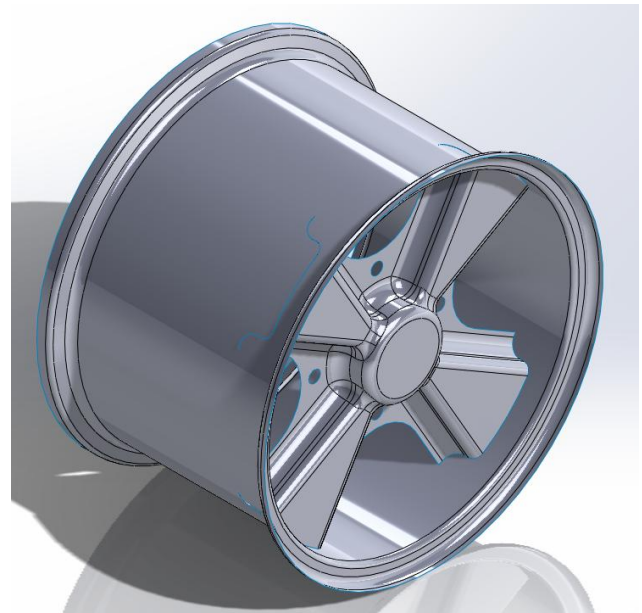


Figure 21: 911 Wheel v.3 Design

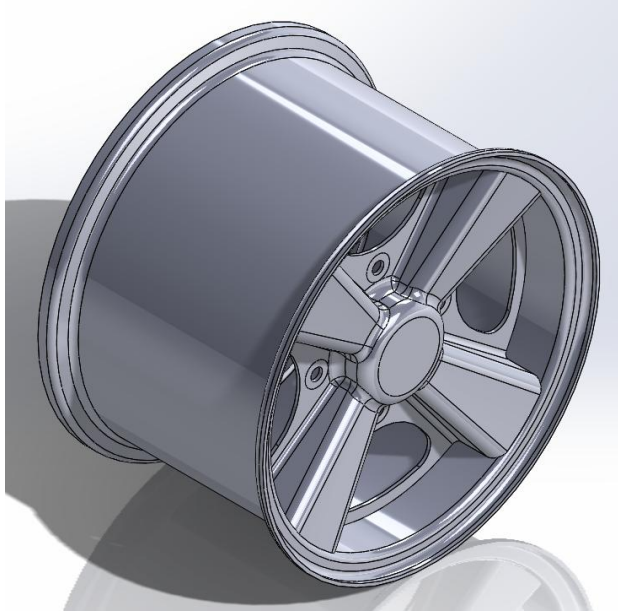


Figure 22: 911 Wheel v.2 Design

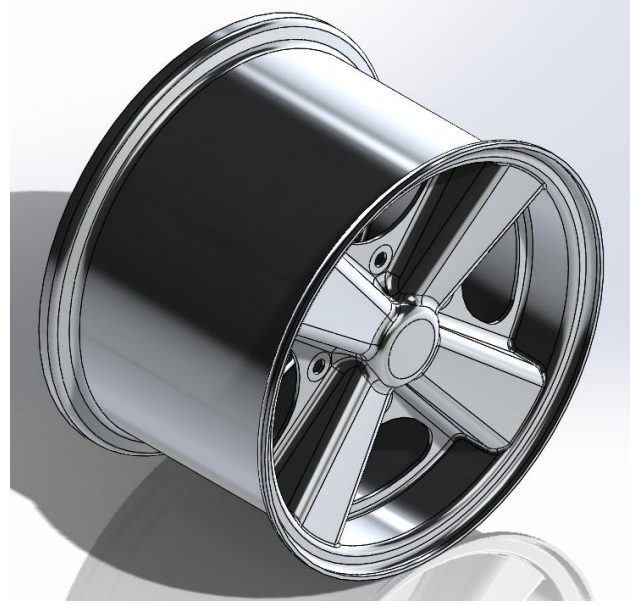


Figure 23: 911 Wheel v.4 Design



Figure 24: 911 Wheel v.5 Design

In every case, the limiting factor in terms of both stress and deformation proved to be the center of the wheel where the struts joined and bolted to the hub. No satisfactory solution for joining the U-channels at the center of the wheel was found. In every case, the U-channel wheels proved to be marginally heavier, more complex to layup, and less stiff than the simple wheel designs. While it may be possible to produce a wheel with U-channels that is superior to a simple wheel, it was concluded that the advantages of U-channel wheels were unproven and since U-channel wheels would be necessarily more difficult to manufacture, the U-channel designs were abandoned in favor of the simple wheel design.

Model name: Thickened 911 Wheel v4
Study name: Static Loading
Plot type: Static displacement Displacement1
Deformation scale: 30.3517

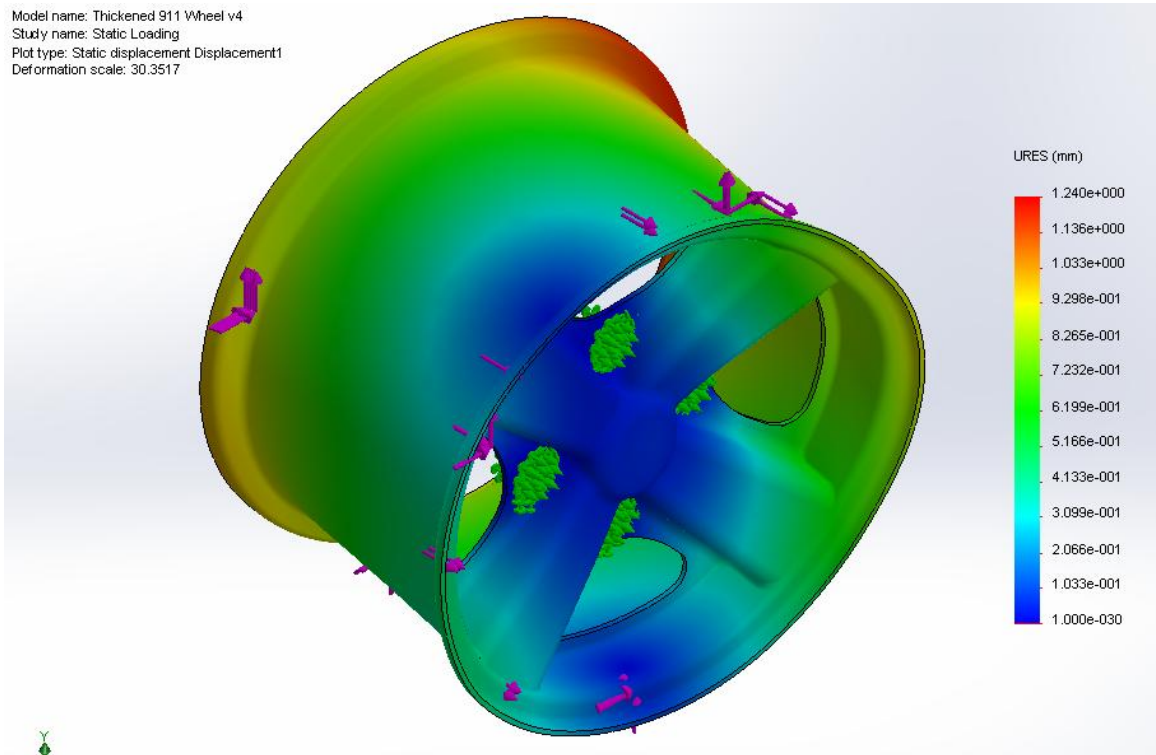


Figure 25: Displacement Results from Simplified Solidworks Simulation of Isotropic 911 Wheel v4

Model name: Thickened 911 Wheel v4
Study name: Static Loading
Plot type: Static strain Strain1
Deformation scale: 30.3517

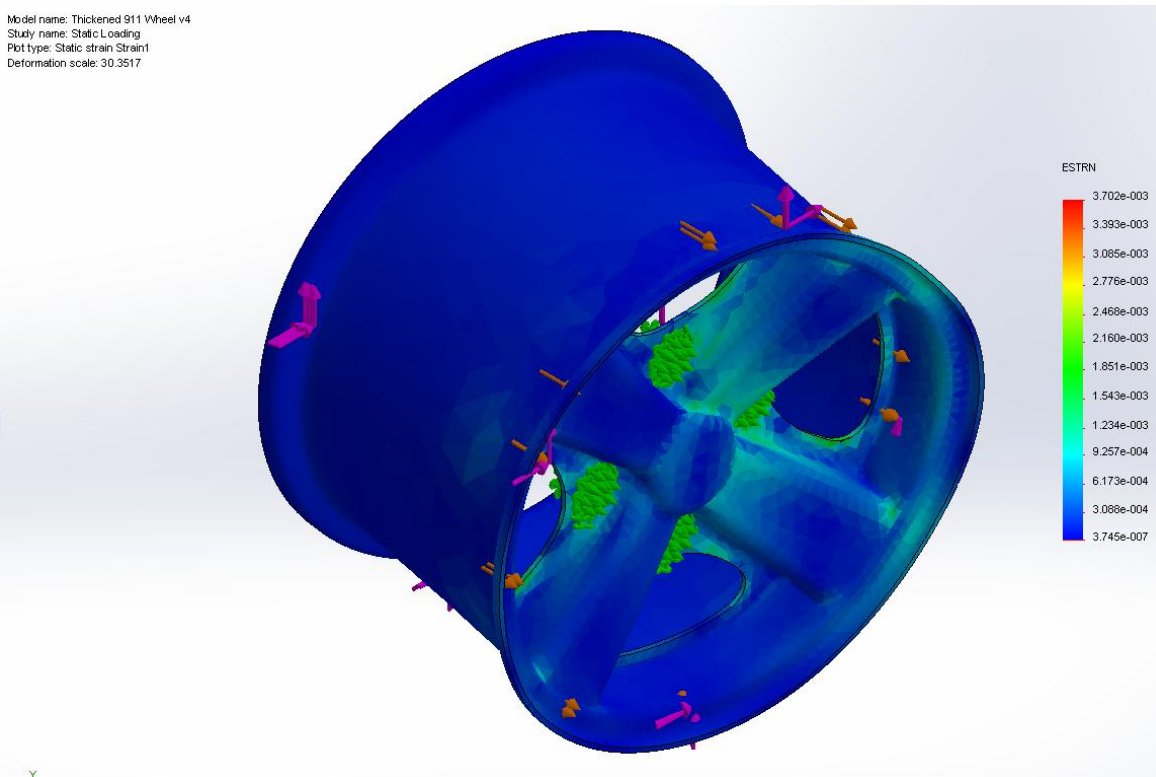


Figure 26: Strain Results from Simplified Solidworks Simulation of Isotropic 911 Wheel v4

Anisotropic Design

A anisotropic model of the wheel was developed in ANSYS Composite PrepPost in order to design and evaluate the layup schedule of the wheel. The "Design, Analysis, and Testing of an Automotive Carbon Fiber Monocoque Chassis" report provides an excellent walkthrough of setting up a ANSYS Composite PrepPost model (Wu, Badu and Tia 82-110).

The wheel was split into five regions: the inner (relative to the car) rim, outer (relative to the car) rim, center, conical spokes section, and main cylinder (see Figure 27). These sections were chosen in order to divide the wheel into regions of comparable stress states without making the layup excessively complex. These splits were implemented in the Solidworks model using parting lines. A zero-thickness Solidworks model of the wheel was then imported into ANSYS.

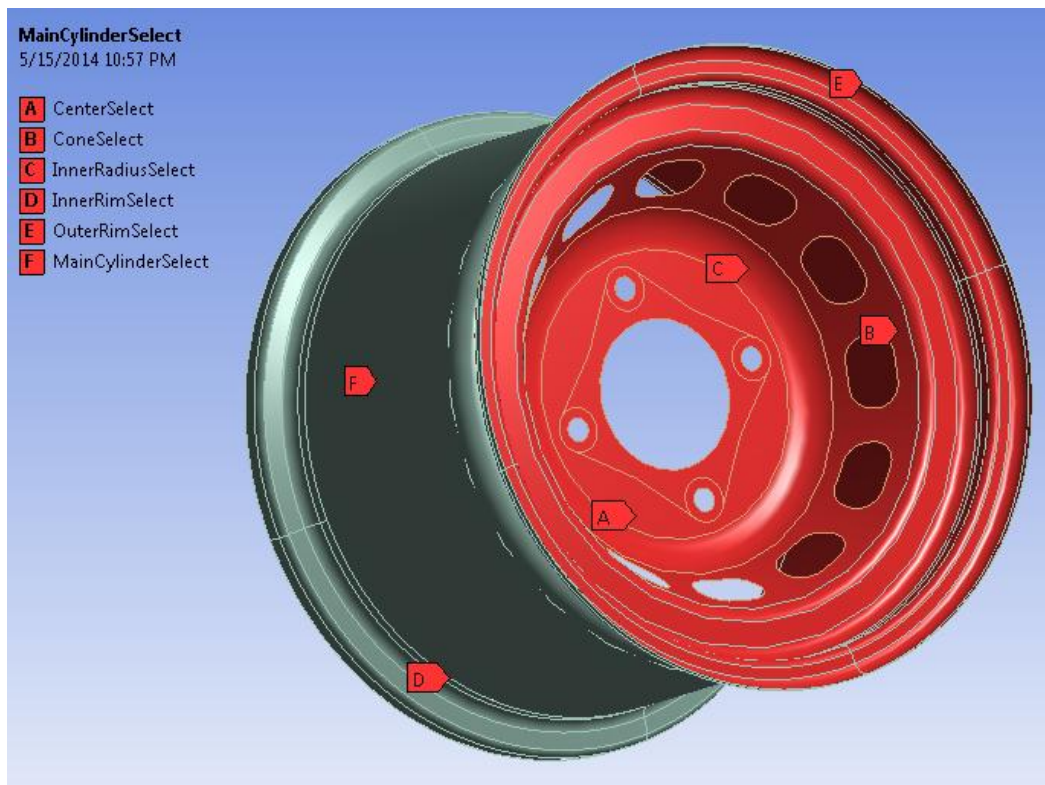


Figure 27: Wheel Layup Sections

Initial Model

Initially, all sections were simulated as symmetric layups of alternating 0 degree and 45 degree plies of T300 woven carbon fiber. This layup schedule was selected because it is specially orthotropic and quasi-isotropic (has equal in plane stiffness in all directions) (IIT Kanpur).

Maximum Load Simulation

To determine the necessary number of plies in each section, simulations of the combined worst case load scenario were run. The region immediately surrounding each lug was fixed and the combined worst case load scenario (see Table 2) was applied as shown in Figure 28.

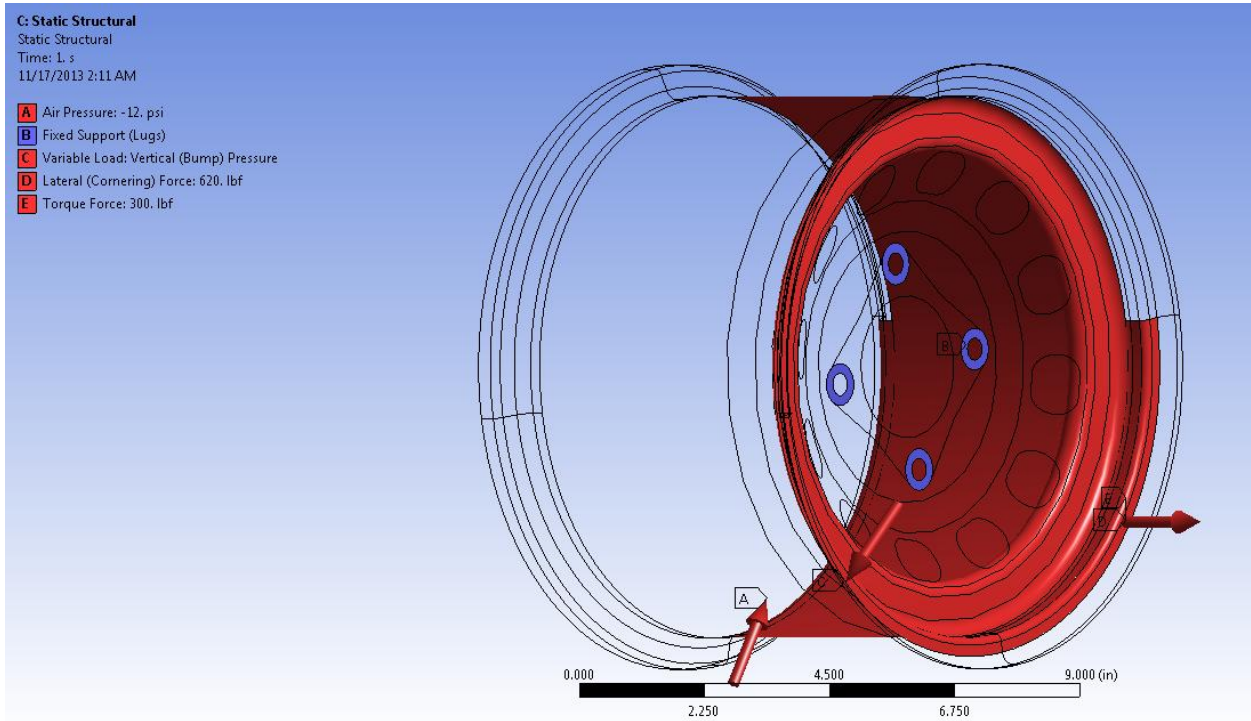


Figure 28: ANSYS Loading for Simultaneous Application of Max Loads

The wheel was meshed as shown in Figure 29.

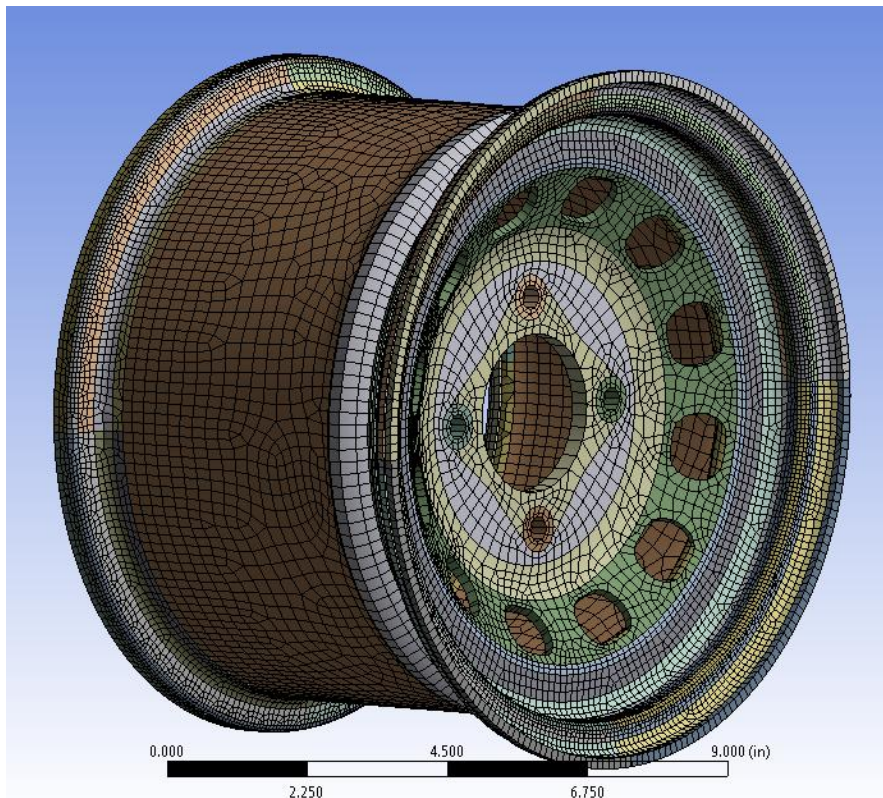


Figure 29: ANSYS Meshing

After each simulation, the number of plies was increased in each section and the simulation repeated until the wheel had a maximum Tsia-Wu failure criteria of less than 1/3 (a factor of safety of 3). A maximum Tsia-Wu failure criteria of less than 1/3 was reached when the number of plies in each section was as follows in Table 3:

Table 3: Initial Layup Schedule (Alternating Layers of 0 and 45 Degree T300 Woven Carbon)

Section	Number of Plies
Inner Rim	28
Outer Rim (including Drop Center)	40
Center	36
Conical Section	20
Main Cylinder	12

The simulation results for this layup schedule are shown below. As can be seen in Figure 30, the maximum Tsia-Wu failure criteria was found to be 0.556. This occurred on the edge of one of the fixed regions around one of the lugs and should not be assumed to be accurate. This region was therefore ignored. Outside of the area surrounding the lugs, the highest failure criteria was 0.278 and occurred on the bottom of the drop center. The vast majority of the wheel remained below 0.125.

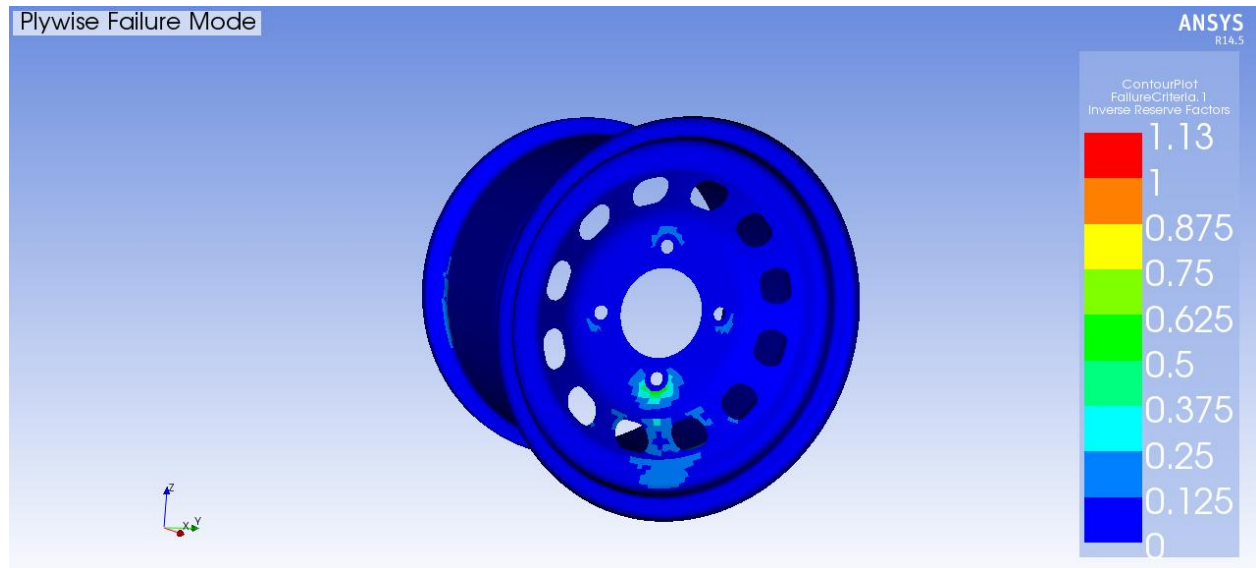


Figure 30: ANSYS Tsia-Wu Failure Criteria for Simulation of Simultaneously Applied Max Loads for Initial Layup

It should be noted that a maximum displacement of 0.089 inches was found to occur at the bottom of the inner rim.

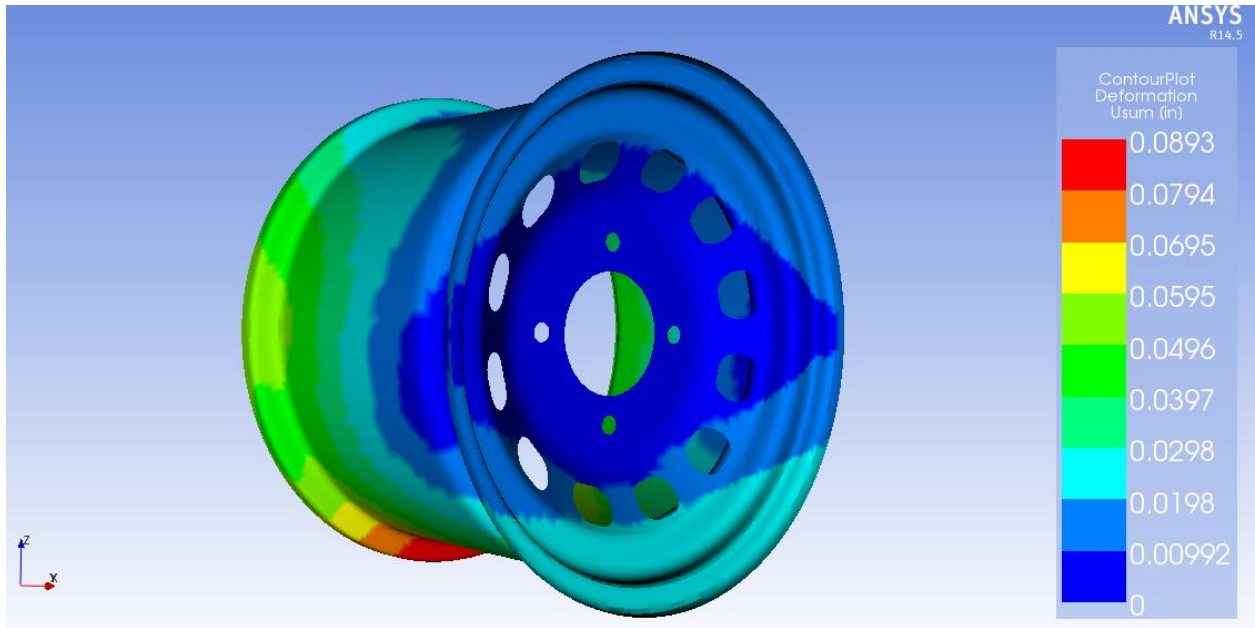


Figure 31: ANSYS Displacement Results for Simulation of Simultaneously Applied Max Loads for Initial Layout

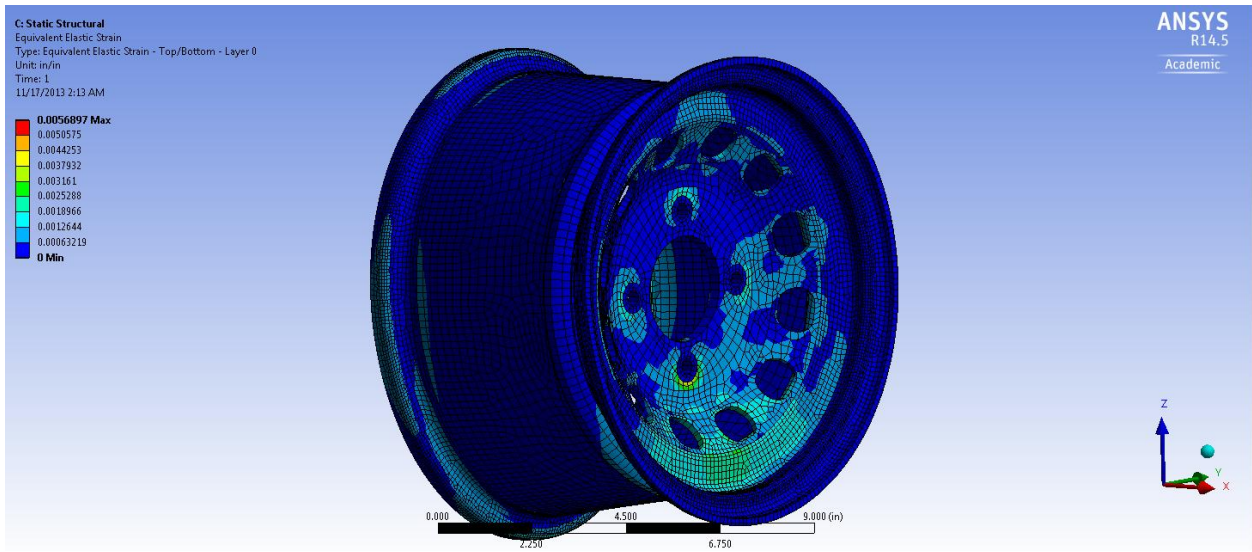


Figure 32: ANSYS Strain Results for Simulation of Simultaneously Applied Max Loads for Initial Layout

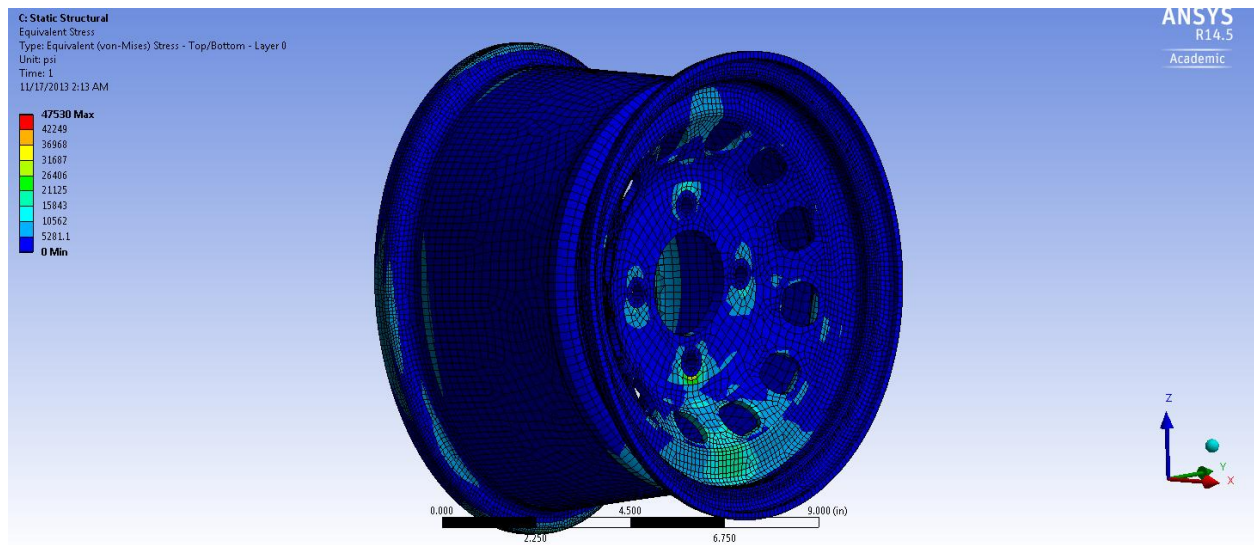


Figure 33: ANSYS Stress Results for Simulation of Simultaneously Applied Max Loads for Initial Layout

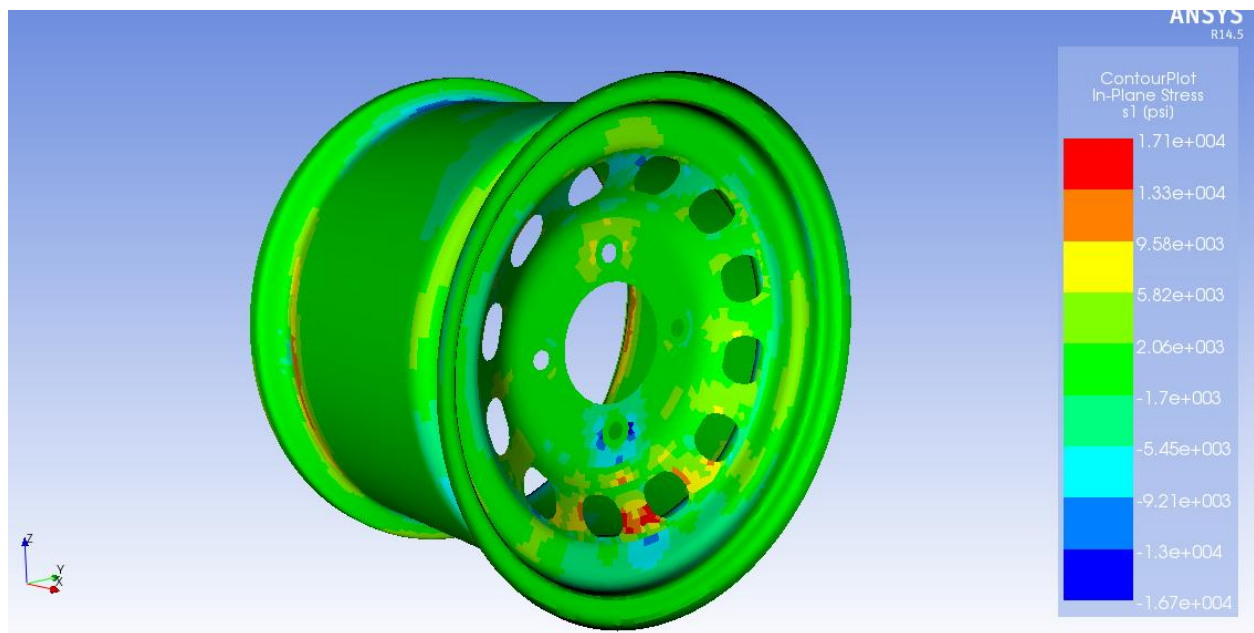


Figure 34: ANSYS In-Plane Stress Results for Simulation of Simultaneously Applied Max Loads for Initial Layout

Comparative Simulation

In order to evaluate the stiffness of this initial design, an ANSYS simulation of the wheel was configured to match experimental compliance testing that was done in 2010.

In the spring of 2010, an aluminum rim with a magnesium center and a carbon fiber rim with a magnesium center were tested. Up to 500 lbf of load were applied to one side of a tire mounted on the wheel to simulate cornering force while dial indicators were used to measure deflection. With 500lbf of load, the aluminum rim with a magnesium center deflected -0.029 inch on the loaded side and 0.022 inch on the opposite side. The carbon fiber rim with a magnesium center deflected -0.017 inch on the loaded

side and 0.010 inch on the opposite side. Information on the test procedure and the complete test results can be found in Appendix B: 2010 Wheel Compliance Testing.

In order to simulate the compliance testing, a 500 lbf of load was applied as shown below in ANSYS. This is an approximation of the load that was applied in testing.

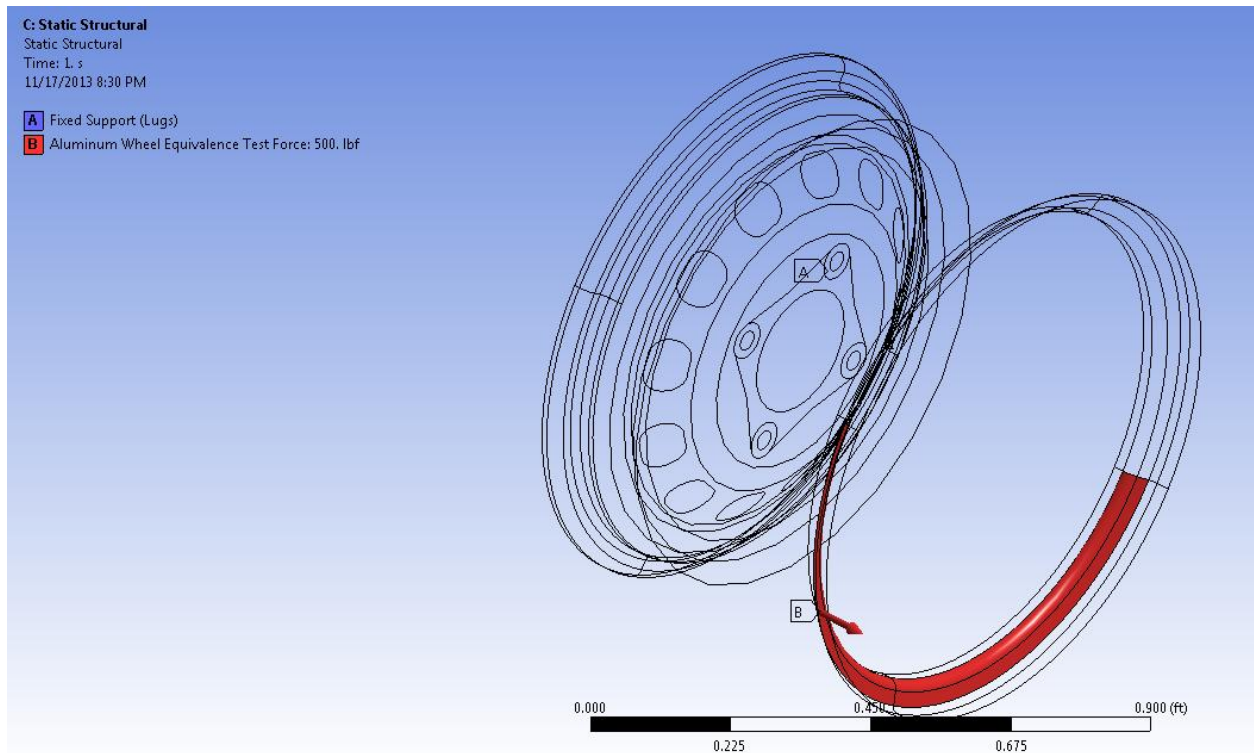


Figure 35: ANSYS Loading for Simulation of 2010 Wheel Compliance Testing

The resulting deformation is shown below. The maximum deflection was found to be 1.3 thousandths of an inch. In 2010, for comparison, 29 thousandths of an inch of deflection was measured on the aluminum rim and 17 thousandth of an inch of deflection was measured on the carbon rim. It should be noted that since in the 2010 testing, only a single point was measured, the maximum deflection during the 2010 tests may actually be higher than what was measured. It should also be noted that the 2010 wheels were of a larger diameter, so these wheels would be expected to deflect farther under load. Regardless, it was clear the initial 2014 single piece wheel design is significantly stiffer than the aluminum wheel and carbon wheel used in 2010.

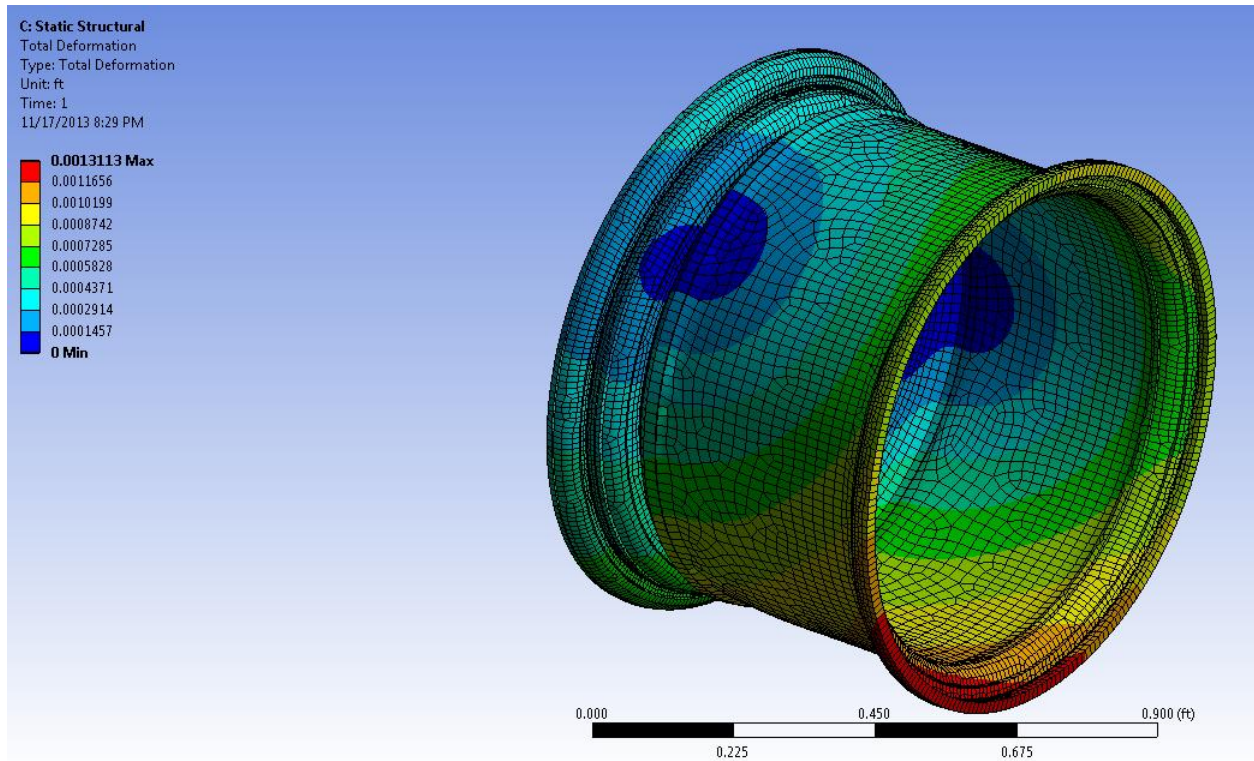


Figure 36: ANSYS Deformation Results for Simulation of 2010 Compliance Testing for Initial Layup

Layup Optimization

The first step to optimizing the layup was to select the prepreg(s) that would be used. Once the types of prepreg had been selected, the layup was iteratively optimized to minimize deflection in ANSYS. Once optimized for stiffness, the layup schedule was modified to adhere to design guides for fatigue, damage tolerance, and interlaminar stress. The modified layup was then simulated in ANSYS to determine the stiffness and factor of safety of the wheel.

Carbon Selection

The team's supply of carbon fiber consisted of several types of unidirectional tape and plain weave fabric. Unidirectional tape has the maximum possible stiffness and strength due to the fact that the fibers are not kinked (Niu 86). Since all of the fibers are aligned in the same direction, it is possible to customize the directional strength and stiffness of laminate through careful orientation of the layers of unidirectional tape, providing strength where needed and minimizing weight. However, unidirectional tape has poor drapability and can be difficult to work with. While uncorroborated, there are also potential concerns about the porosity of layups composed of unidirectional tape. While woven fabric has slightly lower stiffness and strength due to fiber kinking (Whitcomb and Tang), it has a number of important advantages. When a strand of fiber in woven fabric is cut or broken, the load is transferred to the surrounding fibers since the fibers are woven so as to be interlocking (Zipp Speed Weaponry). Therefore, at the edge of composite structure where the fabric has been trimmed, at edges or splices of plies in the layup, or in the event of damage the localized loss of ply strength will extend only one or two weave widths in distance (Zipp Speed Weaponry). In unidirectional composites, the fibers are not interlocking, so the load must be transferred through the composite matrix and the loss of strength is compromised along

the entire length of the fiber (Zipp Speed Weaponry). As a result of this property and others, woven fabric has higher fracture/impact toughness, damage tolerance, thickness uniformity, resistance to delamination, and drapability (Niu 90-91) (Zipp Speed Weaponry). Initially, constructing the wheels entirely out of unidirectional carbon was considered, however, due to the various pros and cons of unidirectional and woven carbon, it was decided to design the wheels to use primarily unidirectional carbon with outer layers of woven fabric.

Due to the quantities available, tensile moduli, and age of the available carbon, only the M46J unidirectional tape, T300 plain weave fabric, T800S unidirectional tape, and T800H plain weave fabric were considered for use. The T800 carbons used the same resin system and were intended to be autoclaved. The T800 carbons were eliminated from consideration due to concerns about using the carbon without an autoclave. See the Testing section for further discussion of the reasoning and testing that led to this decision. This left the M46J UNI and T300 weave as options. These both utilized OOA (Out of Autoclave) resin systems intended for use in VBO (Vacuum Bag Only) cure processes. As such, the M46J UNI and T300 weave were expected to have better resin distribution and lower void content than an autoclave prepreg such as the T800 (Gardiner). It was decided to use primarily M46J due to its high modulus with outer layers of T300. Despite the additional weight it adds, it was also decided to use surfacing film (which is specifically intended for enhancing surface finishes, but proved unavailable) or adhesive film as an outer layer to reduce surface porosity. This was done for the team's 2011 wheels and was reported to be effective. Both the T300 carbon and adhesive film utilize a different resin system than the M46J carbon. Discussions with Kostas Papathomas at i3 Electronics and Ryan Kennett at SpaceX (see Appendix G: Ryan Kennett Emails) confirmed that resin systems with similar chemistries and cure cycles should in theory be compatible, but that testing would be required to provide confirmation. The compatibility of M46J, T300, and adhesive film was confirmed through testing. A description of the test procedure and result can be found in the section Resin System Compatibility Testing.

Design for Stiffness

Once the types of carbon were selected, the wheel was optimized for stiffness. For the wheel center and spokes it was possible to select the laminate largely analytically with minimal use of ANSYS, because of the requirement that these regions be quasi-isotropic. The wheel rim, however, required that the ply schedule be customized to suit the directional loading it experiences. To design the laminate for the regions of the rim, the ply schedule for these regions was repeatedly adjusted and simulated in ANSYS using a manual iterative process guided by an understanding of composite mechanics.

Wheel Center and Spokes

There are a number of constraints and design guides which apply to the layup of the wheel center and spokes regions. Since the wheel rotates, these regions of the wheel must be designed to handle the application of load from all directions. For this reason, it is clear that these regions should have a quasi-isotropic layup with equal in-plane stiffness in all directions. Because of this specification, it is possible to design the laminate in these regions largely analytically before entering it into ANSYS.

To maximize stiffness, unidirectional M46J carbon was primarily used in these regions. For a layup composed of unidirectional fibers to be quasi-isotropic, the laminate must have at least three plies of

equal thickness and an angle of $\frac{\pi}{\text{Number of Plies}}$ between plies (IIT Kanpur). The combination of ply groupings that would be quasi-isotropic individually is also quasi-isotropic. This means that to design a quasi-isotropic laminate using a single type of unidirectional ply, it is only necessary to determine the number of plies necessary to provide the required stiffness and strength as well as the number of groupings. Like virtually all other laminates (excluding exotic specialized applications), the groupings should be symmetric across the mid-plane to eliminate bending-stretching-torsion coupling (Niu 438).

It is desirable to minimize the angle between adjacent plies in order to minimize interlaminar stresses (Niu 416, 440). In most applications, however, manufacturing concerns take precedence, and the number of ply orientations is limited. Most quasi-isotropic layups are achieved with a combination of ± 45 , 0, and 90 degree plies that form quasi-isotropic symmetric groupings, since minimizing the number of ply orientations greatly simplifies the cutting and orientation of plies during manufacturing. However, in the case of the wheel center and spokes, these regions are radially symmetric, so all plies have the same shape regardless of orientation. Because of this, it was acceptable to have a greater variety of orientations and not to limit this region to ± 45 , 0, and 90 degree plies.

Given these design constraints and guides, the obvious laminate is a symmetric spiral pattern in which the angle between adjacent plies is constant and equal to $\frac{\pi}{\text{Number of Plies}}$ (e.g. [0/30/60/90/-60/-30]). However, for the wheel center, due to the large number of plies required, this angle would be small enough to make orienting the plies during manufacturing excessively difficult. Furthermore, in the case of the spokes and wheel center, it was desirable to construct these regions using a combination of continuous plies extending across the entirety of both regions and build-up plies which only cover the higher-stress center region in order to maximize ply continuity. For these reasons, the laminate in the spokes region contained two duplicate symmetric groupings and the center region laminate contained four groupings. The inner spiral pattern extends only over the wheel center while the outer spiral pattern of layers extends over both the spokes and center regions.

To fully define the layup schedule in these regions, the only additional step was to use ANSYS to determine the required number of plies of M46J (while adjusting the angle between plies accordingly). The number of plies was determined by increasing the number of plies and repeating simulations until the Tsia-Wu failure criteria in these regions was adequately low. The simulation results showed that the center should be 24 layers thick and the spokes 12 layers thick with a 30° angle between adjacent layers. An outer layer of 0° and a layer of 45° T300 woven carbon were added on each side to increase the damage tolerance, fatigue resistance, and strength at free edges. The final layup schedule in these regions is shown in Table 4 and Appendix E: Layup Schedule Development, Wheel Layup Schedule v5. The 16 spokes plies covered both the center and spokes while an additional 12 plies covered only the center.

Table 4: Wheel Center and Spokes Layup Schedule

Section	Number of Plies	Thickness (in)	Laminate Code
Center	28	0.225	$[0_T/45_T/(0/30/60/90/-60/-30)_2]_s$
Spokes	16	0.129	$[0_T/45_T/0/30/60/90/-60/-30]_s$

Note: T= T300, else M46J

Rim

Unlike the spokes and wheel center, the rim of the wheel does not experience time-averaged uniformly oriented loading, so the optimal layup schedule is not quasi-isotropic. This meant that a more involved iterative process was required to determine the optimal layup for the rim. Repeated ANSYS simulations were run to find the stiffest laminate. As before, only specially orthotropic symmetric laminates were considered. To reduce manufacturing complexity, only ± 45 , 0, and 90 degree plies were considered. For woven plies, only +45 and 0 degree plies were considered because a +45° woven ply is the same as -45° and 0° is identical to 90°. It should be noted that 0° is typically defined as the principal loading direction and in this case as parallel to the central axis of the wheel.

Given this restriction, for a given unidirectional ply, there are only four orientations, while for a woven ply, there are two. This means that for a 24 ply laminate, for instance, there would be 144 possible ply schedules. The symmetry requirement reduces this number to 72. It would be enormously time consuming to simulate every possible combination, particularly given that the rim is divided into three sections, each with its own laminate schedule. Fortunately, it is not necessary to do so. Given an understanding of the mechanics at play, it is possible to iterate in a deliberate fashion and 'evolve' the design, greatly reducing the necessary number of simulations

Unidirectional plies are both stiffer and stronger than equivalent woven plies, so for the factors considered in an ANSY simulation, the use of unidirectional plies is always preferable. Woven plies should be inserted to address other issues such as porosity, ease of manufacture, free edge effects, and damage tolerance, even though doing so will reduce the strength/stiffness to weight ratio of the layup. For the most part, it is possible to make the choice between unidirectional and woven plies without iterating, since this decision is largely driven by factors not considered by ANSY.

Adding a ply in any given direction will increase the in-plane stiffness, and bending stiffness of the laminate in that direction. In-plane stiffness is independent of the stacking sequence of the laminate (Herakovich 118). Bending stiffness, however, is not (Herakovich 119); the farther a ply is from the neutral plane of the laminate (the center plane for a symmetric laminate), the greater bending stiffness it adds to the laminate. Given an understanding of these two effects, it is possible to see trends in simulation results and tweak the laminate accordingly. If orientating a greater fraction of the plies in a given direction reduces the deflection of the wheel, that adding more plies in this direction or shifting more of these plies towards the outer surfaces of the laminate may help further. By taking these trends into account, it is possible to greatly reduce the required number of simulations. This is, in effect, a manual version of the heuristic algorithm developed by Megan Rotondo in 2011 (Rotondo, ARG11 Fall Technical Report). Given the number of simulations required, it is likely quicker to iterate manually rather than attempt to implement an automatic process as Megan did.

Prior to the decision to use T300 and M46J carbon, a layup of the wheel consisting of T800H and T800S carbon was optimized for stiffness in ANSYS. The wheel was assigned a uniform thickness of twelve plies and limited to specially orthotropic symmetric angle-ply laminates. See IIT Kanpur's concise Laminate Constitutive Relations Lecture (IIT Kanpur) or chapter five of *Mechanics of Fibrous Composites* (Herakovich) for more information on the definitions and characteristics of specially orthotropic, symmetric, and angle-ply laminates. Sixteen different layup schedules were simulated and the maximum

deflection, weight per square inch, and deflection times weight per square inch (which was used to rank layup schedules) was recorded. The results can be seen in Appendix D: ANSYS Layup Optimization Results, Maximum Wheel Deflection using T800H and T800S Carbon Fiber.

Once the decision to use M46J had been made, the wheel was again optimized, this time using M46J. This time, different ply schedules were specified for the inner rim, outer rim, and main cylinder sections. Ten iterations of the main cylinder were tested. The best of these iterations was then specified as the layup for the main cylinder and ten iterations of the inner rim ply schedule were simulated. This process was repeated for the outer rim, for which only four iterations were simulated. The results can be seen in Appendix D: ANSYS Layup Optimization Results, Maximum Wheel Deflection using M46J Carbon.

The final layup added outer layers of T300 to the entire rim and replaced the entirety of the inner rims and outer rims with T300. Some of these changes were made after the layup was begun because it became apparent that applying the unidirectional M46J to the tight radii of the rims was impossible (see the Rim Layup section). The outer layers were added to increase damage tolerances and reduce porosity. T300 was substituted for M46J throughout the inner and outer rims because it became apparent that it would be nearly impossible to layup these regions using the unidirectional M46J due to their tight compound curvature. The results of this optimization process can be seen in Appendix D: ANSYS Layup Optimization Results, Maximum Wheel Deflection using M46J Carbon and T300 Carbon.

Design Guide Adherence

Once the layup schedule of the rim had been optimized for stiffness, its layup was modified slightly to conform to available design guides. Attempts were made to follow the following recommendations:

- Adjacent plies should not be orientated more than 60° apart (Niu 440)
- Avoid having a 0° ply adjacent to a 90° ply (Niu 442)
- If possible, use a homogenous stacking order (Niu 440)
- Avoid grouping plies of the same orientation (Niu 440)
- Avoid clustering 90° plies (Niu 440)
- Surface plies should be continuous and $\pm 45^\circ$ to the principal loading direction (Niu 440)
- A woven fabric should be used as the outermost layers (Vermont Composites)
- Use at least one +45/90/-45 group of unidirectional plies at the surface (Niu 440)
- 0°, +45°, -45°, and 90° plies should each compose at least 10% of a laminate (Niu 440)

Many of these recommendations apply only to unidirectional plies and some are redundant. The final layup schedule for the rim is shown below in Table 5. As can be seen, while some of these recommendations were followed, some were not relevant due to the use of woven plies and some were ignored because they would have excessively limited stiffness.

Table 5: Wheel Rim Layup Schedule

Section	Number of Plies	Thickness (in)	Laminate Code
Inner Rim	22	0.187	$[(45_T/0_T/0_T)_3/45_T/0_T]_s$
Outer Rim	34	0.289	$[(45_T/0_T/0_T)_5/45_T/0_T]_s$
Main Cylinder	14	0.113	$[45_T/0/45/90/0/90/-45]_s$

Note: T= T300, else M46J

With the exception of the recommendations to limit the angle between adjacent plies and use weave as an outer layer, none of the previously described suggestions were relevant for the wheel center and spokes because these areas are radially symmetric and the selection of a coordinate system orientation is therefore arbitrary.

Final Layup Schedule

The final layup incorporated 94 individual plies of carbon. This was roughly estimated to require 53 ft² of prepreg. ANSYS calculated a weight of 1.51 kg (3.33 lb). This weight estimate was expected to be overly optimistic, particularly because the adhesive film was not accounted of in the ANSYS model. The maximum deflection for combined worst case loading scenario for this design was 0.0294 in and was located at the bottom edge of the inner rim (see Figure 37). The maximum Tsia-Wu failure criteria for the wheel was less than 1/6 (see Figure 38).

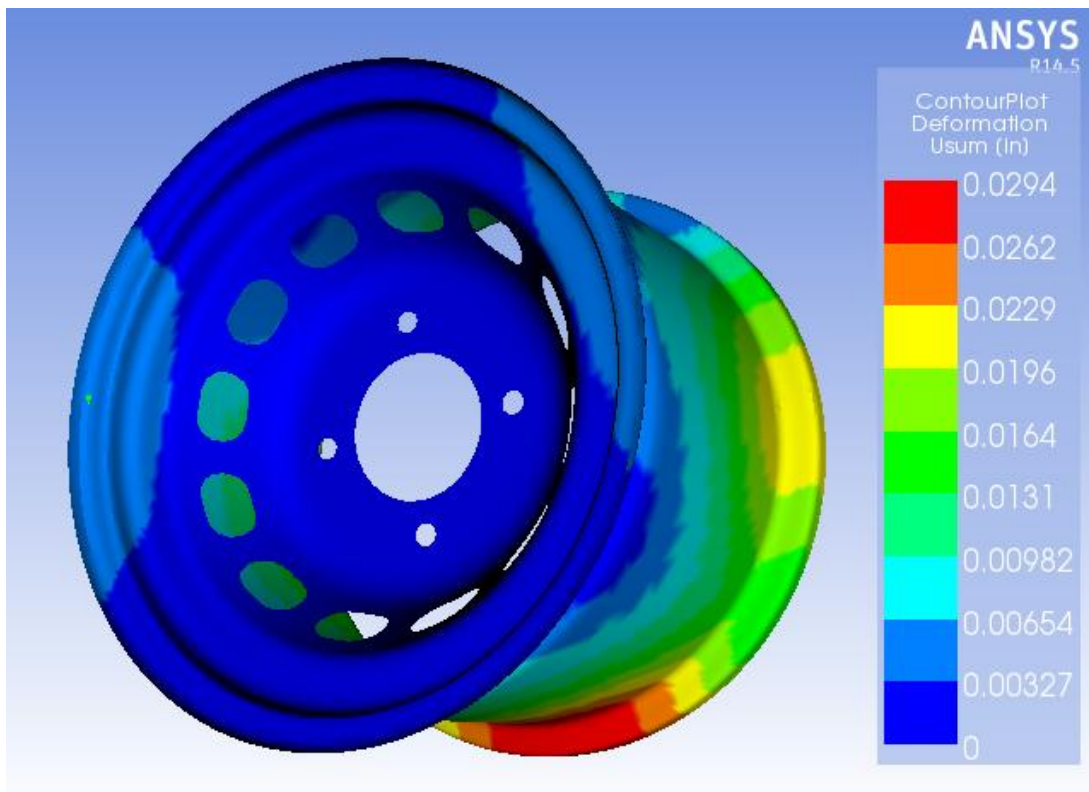


Figure 37: ANSYS Deformation Results for Simulation of Simultaneously Applied Max Loads for Final Layup

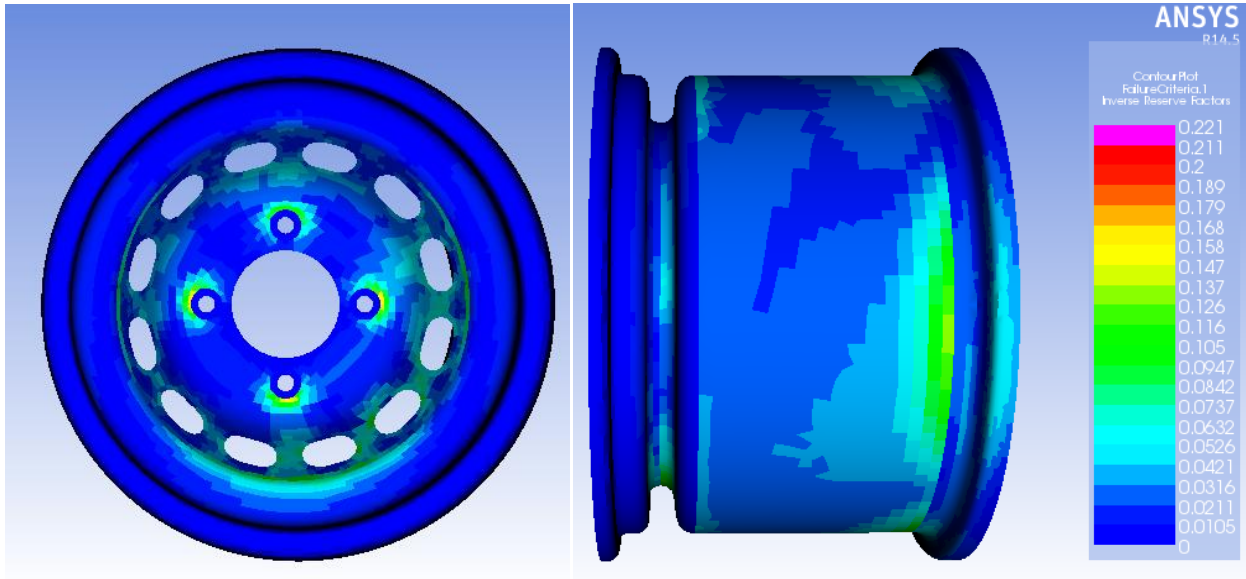


Figure 38: ANSYS Tsia-Wu Failure Criteria Results for Simulation of Simultaneously Applied Max Loads for Final Layup

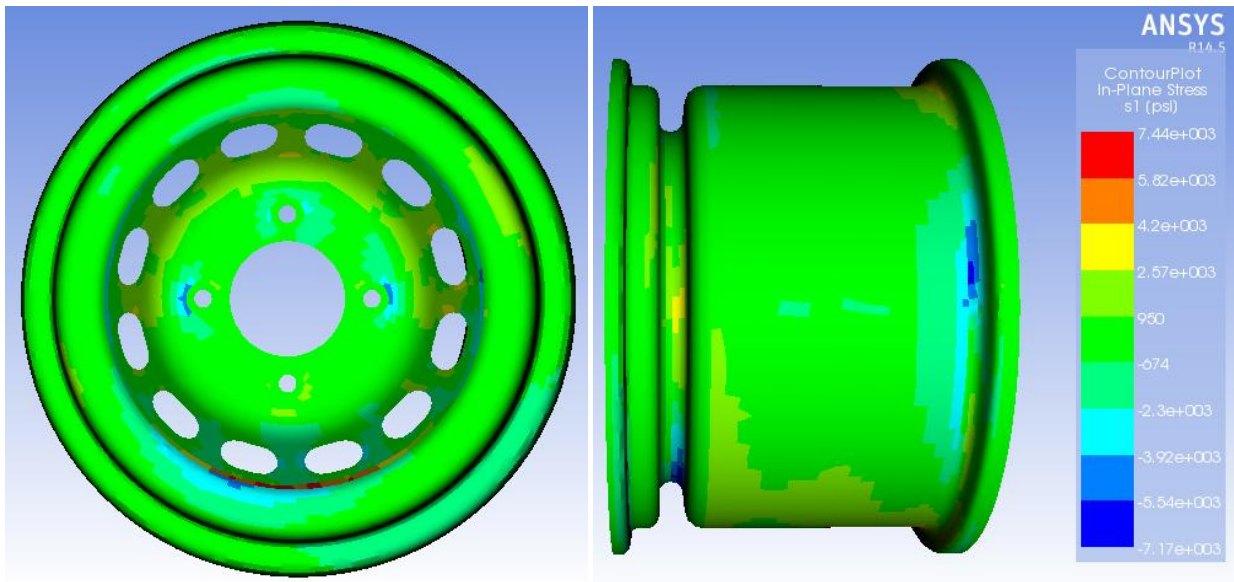


Figure 39: ANSYS In-Plane Stress Results for Simulation of Simultaneously Applied Max Loads for Final Layup

The extent and location of ply types can be seen in Figure 40. A chart showing the order of application of each individual ply is shown in Appendix F: Final Layup Checklist.

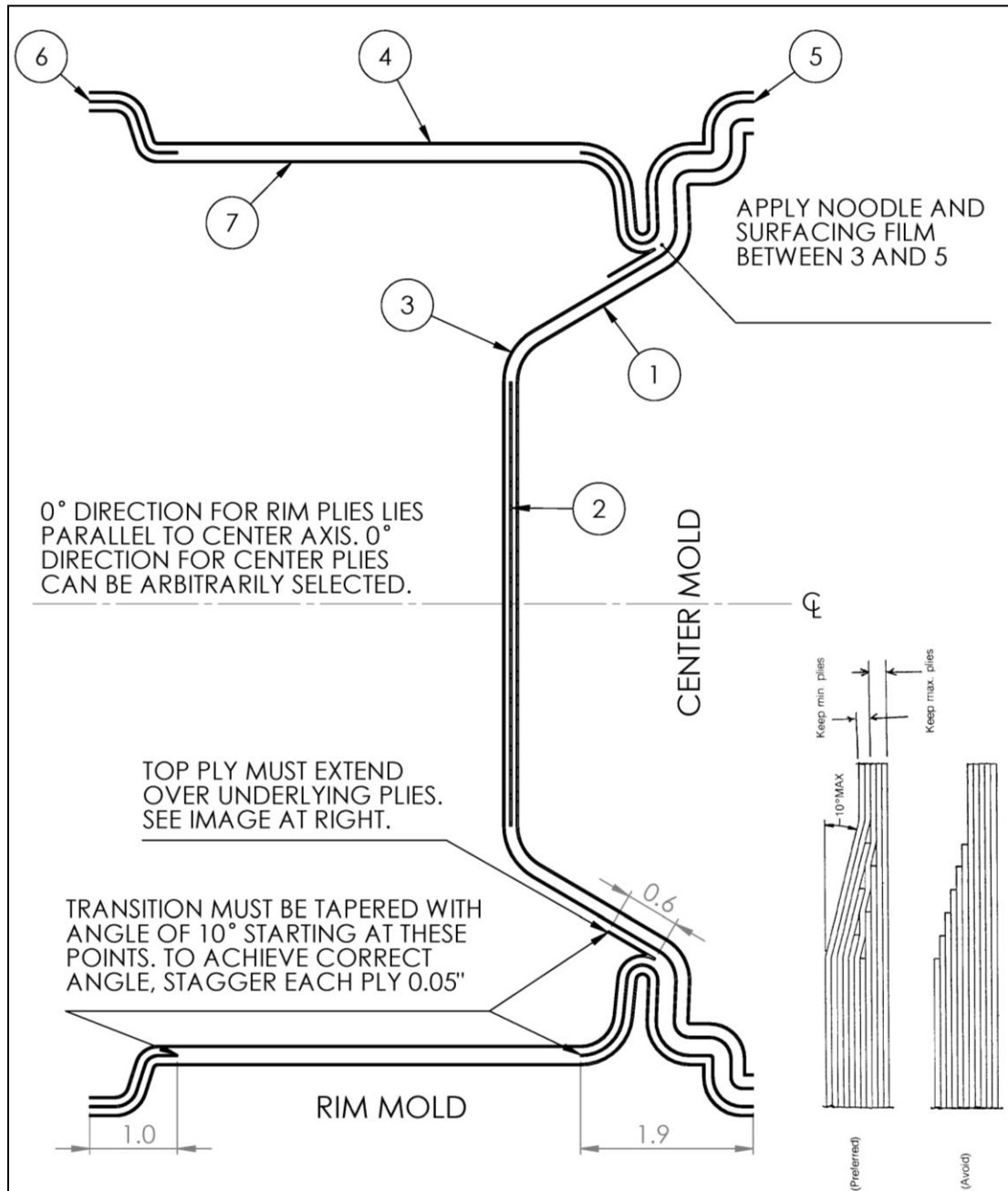


Figure 40: Laminate Ply Diagram and Instructions

At transitions between regions of different thickness, it is necessary to stagger the plies to allow for a transition angle of less than 10° to avoid fatigue delamination (Niu 440) (Peters 56). A continuous ply should cover these transition regions (Niu 440) (Vermont Composites). A model of the wheel that accounts for the varying thickness and staggered transitions between sections is shown in Figure 41 and the cross sections of this model is shown in Figure 42.

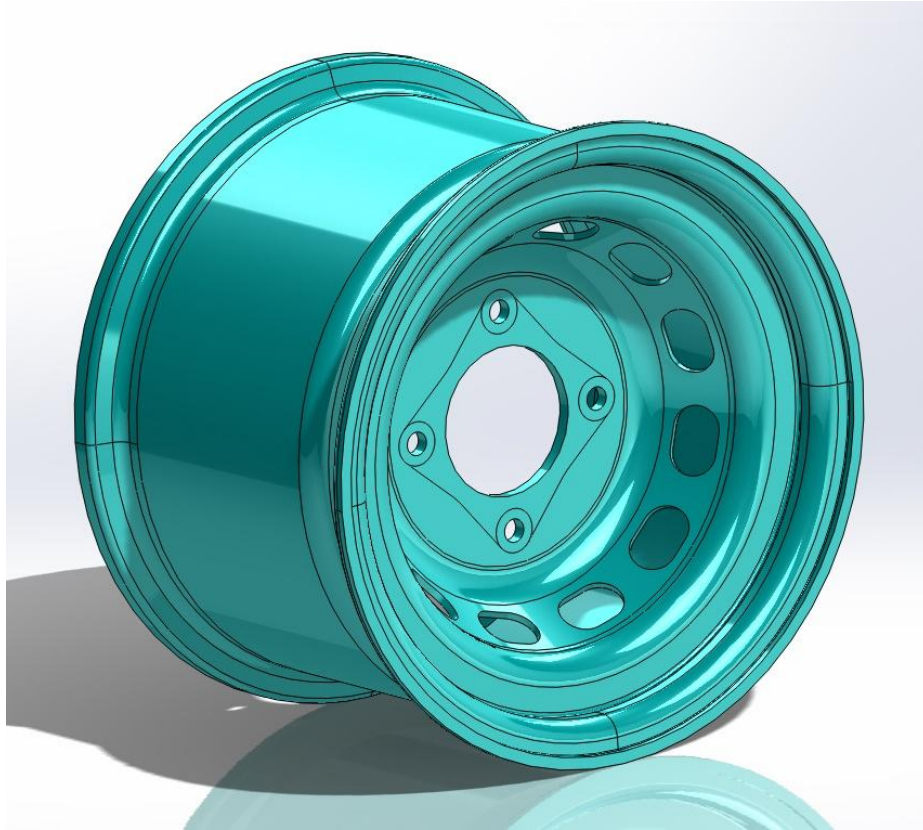


Figure 41: Solidworks Model of Wheel Showing Projected Laminate Thickness

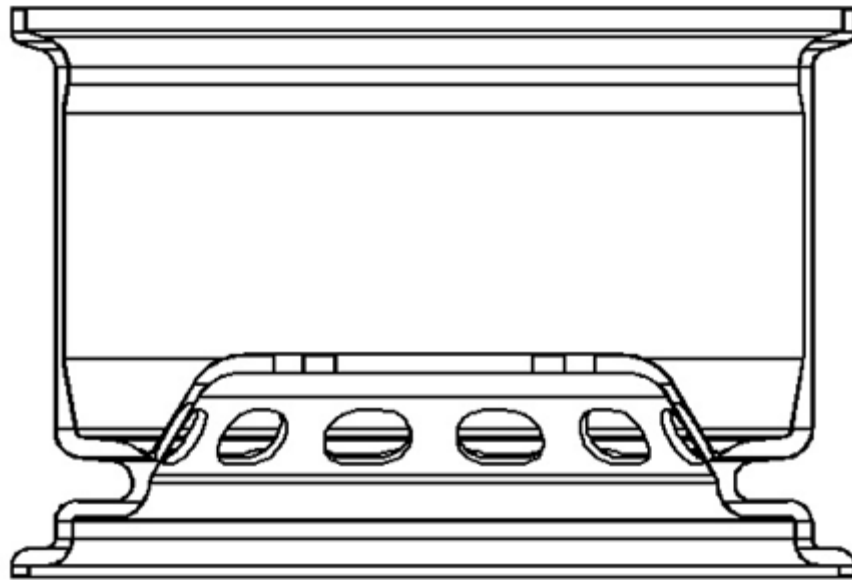


Figure 42: Cross Section of Wheel Showing Projected Laminate Thickness

Lug Attachment Design

Particular attention was directed toward the design of the lug attachment points in the wheel. Mechanical fastening of composites can be challenging and the loads carried by the wheel lugs are large

and high cycle. Discussions with Ryan Kennett (Cornell Racing alumni now working for SpaceX) confirmed that FEM simulations are not considered reliable enough to be used in industry for composite mechanical fastening design (see Appendix G: Ryan Kennett Emails). Finding a simple analytical approximation for fastener load distributions or load capacities also proved impossible. It is possible to generate generalized load capacity approximations for specific layups, but doing so requires extensive testing regimens that vastly exceed the team's capabilities (Niu 290-300). Therefore, the only way for the team to design mechanical joints in composite parts is simply to use approximate FEM or hand calculations and then experimentally verify the approximations experimentally. This was confirmed by Ryan Kennett.

In the case of the wheels, this process was simplified by the fact that the lugs and hub design was already fixed, so the only variables were the number of plies and layup schedule at the area surrounding the lugs. The required number of plies in the wheel center region was determined using ANSYS. The lugs were modeled simply by fixing the region that would be under the head of the lug. This is, of course, a *very rough* approximation of a bolt.

The wheel lugs are self centering and designed to fit into a conical, countersunk hole. Countersinking such a hole in carbon and then loading it seemed almost certain to result in delamination and failure, either during the countersinking of the holes or during the application of load. In addition, the act of torquing down the lugs seemed likely to result in damage to the composite. The 2011 wheels, for instance, experienced cracking around bolt holes when the flanges were tightened together (Rotondo, ARG11 Spring 2011 Technical Report 6). For these reasons it was decided to machine metallic 'washers' which would help distribute the load and eliminate the need to countersink the carbon.

A washer was designed for this application. The washers have a conical face and central hole designed to match the geometry of the wheel lugs. The washers are a full inch in diameter to distribute the fastener preload and applied tensile load. It was decided to extend a thin section of the washer through the carbon to prevent the lug threads from abrading the carbon and help distribute the bearing load. This cylindrical section was deliberately designed to be slightly shorter than the thickness of the carbon to ensure that the lug clamping load was applied through the carbon, rather than the washer. The geometry of the washer can be seen below in Figure 43.

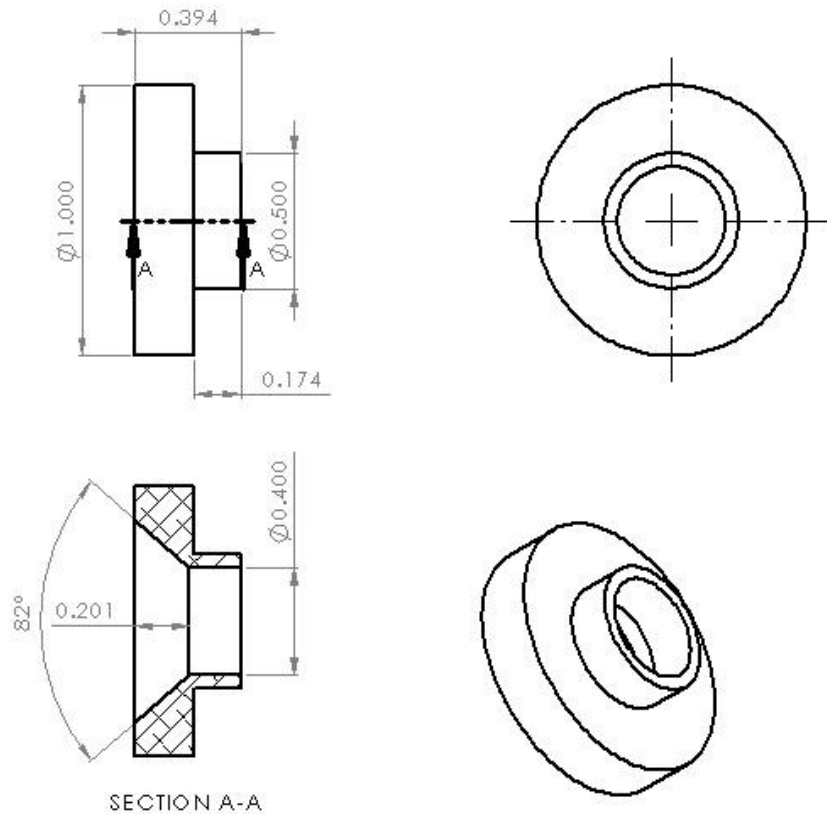


Figure 43: Wheel Lug Washer Design

Throughout the design of the wheel, the use of secondary bonding was deliberately not considered. The wheel washers were specifically designed to function without bonding. However, it was decided that the use of adhesive to bond the washers to the carbon wheel center could only increase the strength and resistance to damage of the lug attachment. The use of adhesive bonding was judged to be acceptable in this instance because due to the nature of the design of the washer; in the event of bond failure mechanical fastening would be maintained and catastrophic failure would not occur. Adhesive was expected to help to distribute the load from the washer to the carbon by filling any gaps, prevent delamination by binding the free edges of the carbon together, and eliminate any wear that would occur between the washer and carbon.

The team had a large supply of Hysol E-40HT structural epoxy available. While perhaps not the absolute best Hysol product for this application, Hysol E-40HT is a high strength toughened epoxy that is suitable and was expected to be more than adequate for bonding the washers (Loctite Structural Adhesives Selector Guide). Due to its ready availability, Hysol E-40HT was selected for use.

Since the ARG14 lugs are aluminum, the obvious material for the washers is also aluminum. However, aluminum produces a large galvanic potential when in contact with carbon fiber, resulting in galvanic corrosion (David Banis) (Peters). For this reason, unless aluminum is isolated from carbon fiber using a layer of fiberglass or an impenetrable layer of paint, it is not suitable for use (Peters). Given the

high stresses the washers experience and the fact that it would be impossible to inspect the underside of the washers, the use of aluminum was judged to be unacceptable for this application.

Titanium and many stainless steels are more cathodic and thus are compatible with carbon fiber (David Banis). Titanium is the lighter and thus preferable option, however it is substantially more expensive. Grade 2 titanium and 316 stainless steel were considered for use. For the 16 washers necessary for a set of four wheels, the weight difference between titanium and stainless steel would be about 1/3 lb. However, the necessary titanium stock would cost \$80 while the stainless steel would only cost about \$20. Due to the experimental nature of the first wheel, it was decided to use 316 stainless steel for the washers of the first wheel.

Laminate Testing and Validation

Several types of experimental testing were conducted to ensure that the ANSYS simulation of the wheel would accurately reflect the performance of the finished wheel. Laminate coupons were subjected to three point bending tests to ensure the compatibility of the T300 carbon, M46J, and adhesive film. A single lug attachment point was manufactured and subjected to cyclic loading to verify the load capacity of the wheel center.

Resin System Compatibility Testing

The flexural strength of samples composed entirely of 0° M46J UNI carbon fiber as well as samples with outer layers of green FM200-U adhesive film or 0° T300 woven carbon fiber was tested (see Table 6). A three-point bending test was used because while "flexural strength is not considered an intrinsic property" it is a simple test to run and it "is considered a good quality control test" (Niu 475). While a variety of complex tests would be required to fully quantify the properties of these laminates, a three-point bending test provides a simple test of bending strength and, indirectly, the propensity of the layup to delaminate. In this case, the flexural testing was intended to verify that the materials bonded as intended and would not delaminate under load at the transition between dissimilar materials.

Sample Preparation and Test Process

All samples were laid up on a metal plate, vacuum bagged, and then cured according to the recommended cure cycle for the M46J prepreg. When inspected, the samples did not have any visible defects and the adhesive film appeared to seal the surface of the carbon as intended.

Table 6: Flexural Test Sample Layup Schedules

Test Name Material	Layup Schedule
M46 UNI #1	[0 ₅] _s
M46 UNI #2	[0 ₅] _s
M46 UNI+Green Surfacing Film	[SF/0 ₄] _s
M46 UNI+T300 Weave	[0 _T /0 ₄] _s

As shown in Figure 136, samples were loaded to failure in a 3-point bending test. A materials science department Instron was used for this testing.

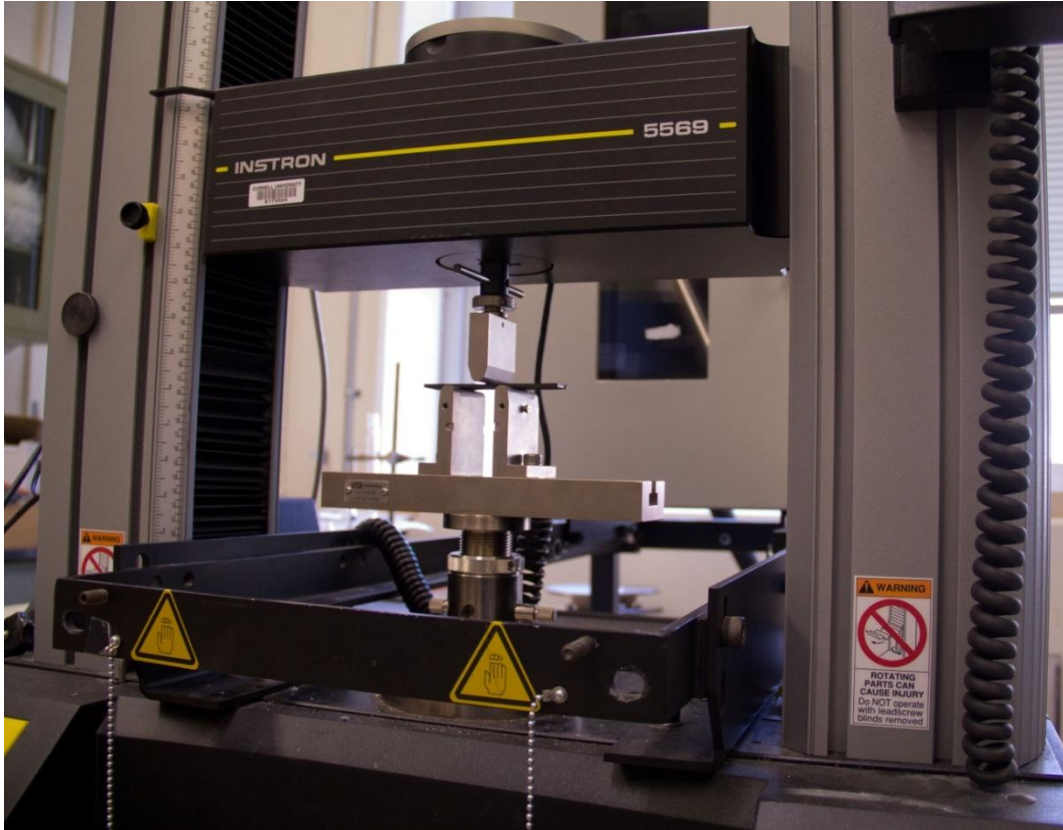


Figure 44: Flexural Bending Test Setup

Test Results

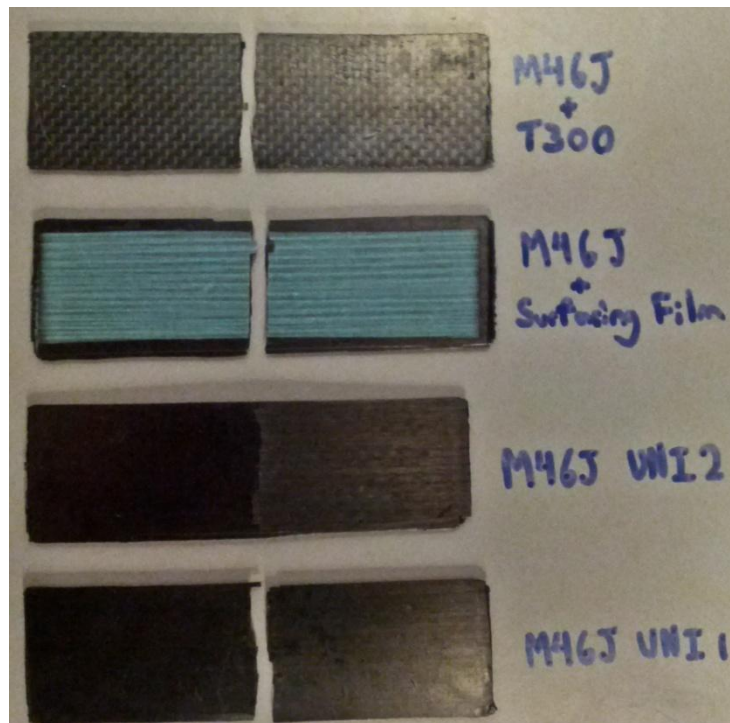


Figure 45: Broken Resin Compatibility Test Coupons

The calculated flexural strengths of the samples are shown in Figure 46. Additional test data can be found in Appendix C: Flexural Bending Testing. As can be seen in Figure 46, the two samples composed entirely of ten layers of M46J had the greatest strength. The variation in strength between these two ostensibly identical samples illustrates the variability of composite structural properties. As expected, the sample with eight layers of M46J with a layer of adhesive film on each side was significantly weaker. This was anticipated since this sample had fewer layers of carbon and the adhesive film was expected to add minimal strength to the sample. The sample composed of eight layers of M46J with a layer of T300 carbon on each side had a strength between that of the adhesive film and pure M46J tests. While the T300 added flexural strength, and was thicker than the M46J, it is lower modulus and strength than the M46J. The sample composed of T300 and M46J was weaker than the samples composed entirely of M46J. Notably, no sample experienced notable delamination between the transitions between different materials.

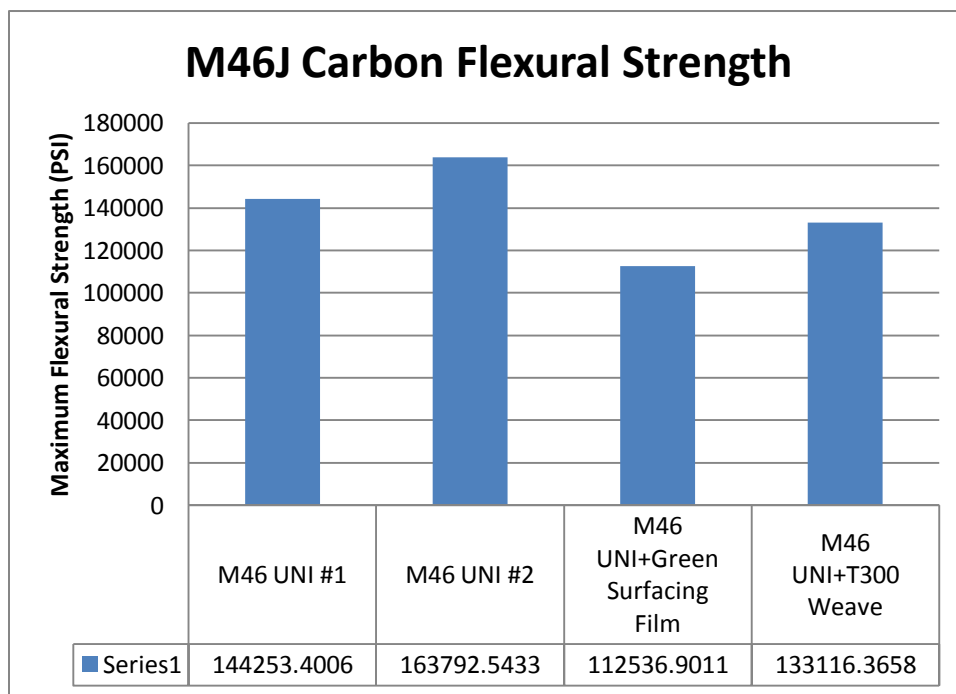


Figure 46: M46J Carbon Fiber Flexural Strength Test Results

Lug Attachment Design Testing

As noted previously in the Lug Attachment Design section, it was necessary to experimentally test the selected lug attachment method to verify its strength.

Test Panel Preparation

Carbon panels of roughly one square foot in size and a ply schedule identical to that of the wheel center were laid up and cured according the proscribed procedures for M46J. Carbide drill bits were used to drill the necessary hole in the center of the plate for the washer and the mounting holes along the periphery of the plate. A aluminum washer was machined and adhered to the carbon plate using Hysol E-40HT epoxy. Aluminum was used because it was available, it is easily machined, and long term corrosion was not a concern for this test. Special care was taken to ensure that the surfaces were properly prepared for bonding. For surface preparation guidelines, see (Hysol Surface Preparation Guide). The carbon panel

was sanded smooth where the washer would be bonded and cleaned with acetone. The aluminum washer was subjected to the same preparation process used in MAE classes to prepare aluminum for the attachment of strain gauges. The surfaces of the washer that needed to be prepared were cleaned with degreaser, sanded in a phosphoric acid solution, and cleaned with a neutralizer solution immediately prior to bonding. Gloves were worn during this process and efforts were made to avoid contamination. Once prepared, the Hysol was applied and washer bonded per the manufacturer's instructions (Hysol E-40HT). Due to time constraints, the cure rate was accelerated by baking the panel for several hours at 200° F (as allowed per the manufacturer instructions). The completed panel is shown in Figure 47.



Figure 47: Prepared Lug Attachment Test Panel

Load Calculations

The components of the load at each lug are shown can be roughly approximated as:

$$F_{x_{lug}} = \frac{\text{tire radius} \times F_{x_{wheel}}}{\text{lug distance from center} \times \text{lugs/wheel}} = \frac{9 \text{ inch} \times 300 \text{ lbf}}{1.875 \text{ inch} \times 4 \text{ lugs/wheel}} = 360 \text{ lbf}$$

$$F_{y_{lug}} = \frac{F_{y_{wheel}}}{\text{lugs/wheel}} = \frac{620 \text{ lbf}}{4 \text{ lugs/wheel}} = 155 \text{ lbf}$$

$$F_{z_{lug}} = \frac{F_{z_{wheel}}}{\text{lugs/wheel}} = \frac{1260 \text{ lbf}}{4 \text{ lugs/wheel}} = 315 \text{ lbf}$$

The in-plane load at each lug attachment point can be calculated as follows:

$$F_{inplane} = \sqrt{F_{x_{lug}}^2 + F_{z_{lug}}^2} = \sqrt{(360 \text{ lbf})^2 + (315 \text{ lbf})^2} = 478 \text{ lbf}$$

The normal load is simply:

$$F_{normal} = Fy_{lug} = 155 \text{ lbf}$$

The magnitude of the load is:

$$F_{total} = \sqrt{F_{inplane}^2 + F_{normal}^2} = \sqrt{(478 \text{ lbf})^2 + (155 \text{ lbf})^2} = 503 \text{ lbf}$$

The angle of the load from the surface of the wheel center is:

$$\theta = \tan^{-1}\left(\frac{F_{normal}}{F_{inplane}}\right) = \tan^{-1}\left(\frac{155 \text{ lbf}}{478 \text{ lbf}}\right) = 18^\circ$$

This means that the maximum combined worst case load for a single lug is a 503 lbf load orientated 18° away from the surface of the wheel center.

Test Setup

The existing blue panel test frame was used to support the panel. Two welded steel triangles composed of scrap steel tubing were manufactured and bolted to the blue test frame to support it at the appropriate angle vertical. For reasons that are unclear, the triangles were manufactured so as to position the carbon plate at an angle of 7°, rather than 18°, from vertical. Still, this angle was close enough for the purposes of this test.

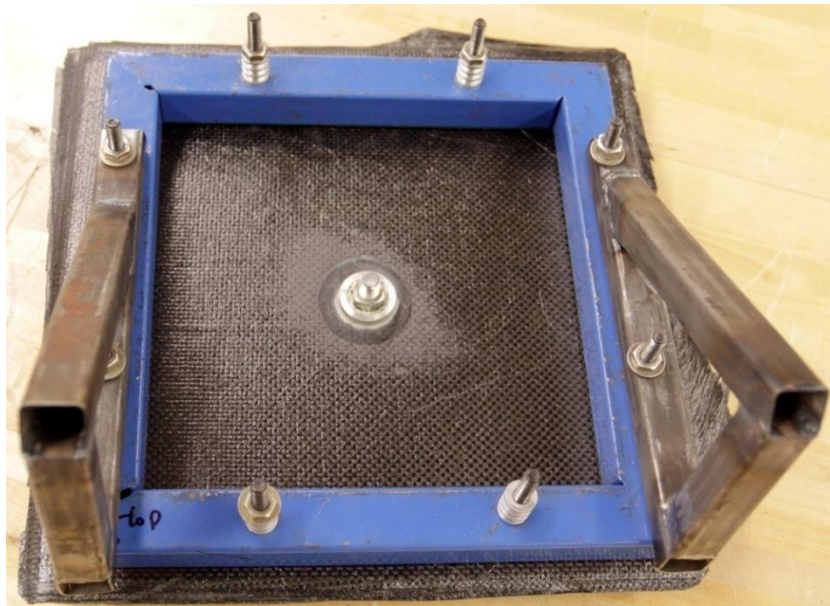


Figure 48: Lug Attachment Test Setup Assembly

A clevis was machined from scrap steel tubing to allow the lug to be attached to a rod end protruding from the Instron (Figure 49). The lug bolted through a holes in the clevis, the carbon panel, and the aluminum washer. Another hole in the clevis was positioned so as to allow the rod end to be connected in line with the center of the top surface of the hole in the carbon plate, so as to avoid

producing a moment around the lug. The fully assembled test setup can be seen in Figure 51. A finite element model of the clevis was simulated using Solidworks Simulation to determine its strength. It was found that with an applied load of 1400 lbf, the clevis had a minimum factor of safety of 1.45 (see Figure 50).

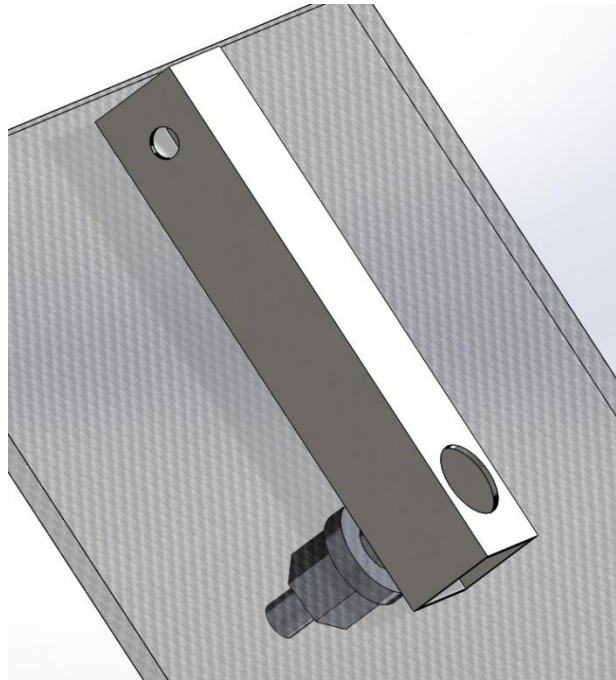


Figure 49: Lug Test Clevis Design

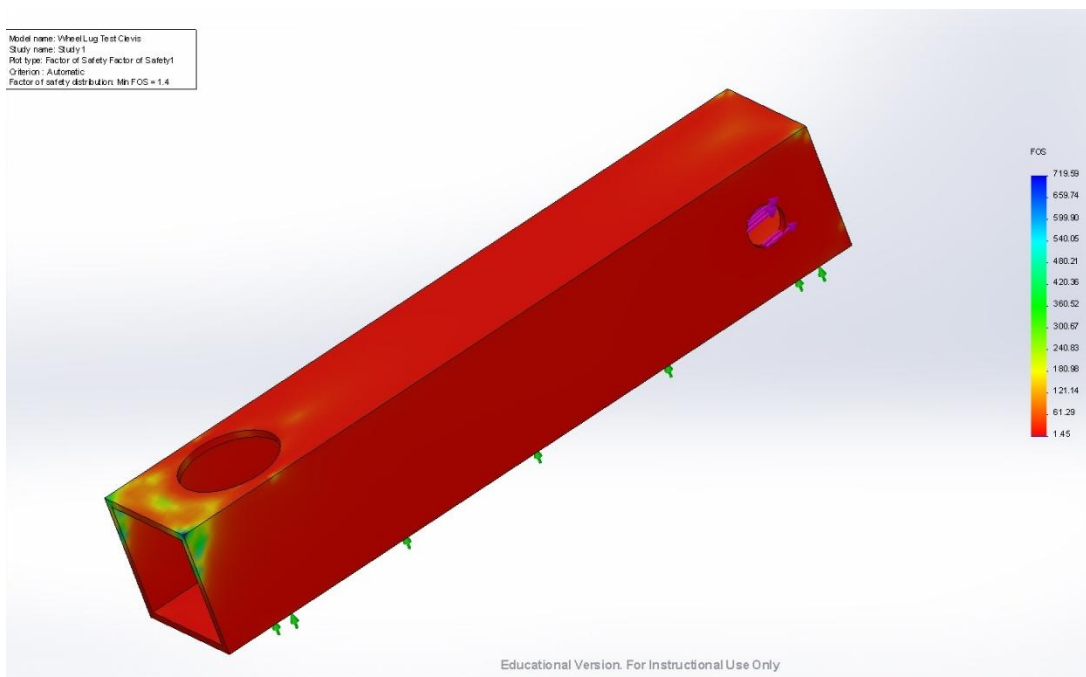


Figure 50: Lug Test Clevis Simulation Factor of Safety

Test and Results

Over 1000 cycles of ~1400 lbf of tension *and* compression were applied to the lug using an Instron machine 7 degrees away from parallel with the sheet. This load reflects close to three times the combined worst case load scenario tested in ANSYS (combined maximum bump, braking, and lateral loads per lug) and is vastly more extreme than anything the wheel is expected to encounter. A 1Hz sine curve was utilized to apply the load. This loading is equivalent to 2000 cycles. The number of cycles was limited by the extremely limited availability of the Instron. While it would have been desirable to test the lug attachment to failure, the test setup was not adequately strong for this to be possible.



Figure 51: Wheel Lug Attachment Test

It should be noted that the test varied from the actual wheel for following reasons:

- A aluminum washer was used instead a stainless steel washer
- The countersink angle was 90° rather than 82°
- An aluminum surface preparation procedure was used that differs from that used for stainless steel
- Holes were drilled with a carbide drill bit, rather than cut with a waterjet
- The Hysol was cured at an elevated temperature, rather than room temperature

- The testing was conducted after the Hysol had cured for less than 24 hours
- A standard nut, rather than a lug nut was used, because the lug nuts had not arrived
- The contact patch of the clevis differed in shape from that of the wheel hub

With the exception of damage to the aluminum washer resulting from the use of a standard nut which, unlike a lug nut, lacks a conical face, no visible damage to the aluminum washer, Hysol epoxy, or carbon panel resulted from the testing. The test was therefore considered to have demonstrated the reliability of the lug attachment method. The test also served to further validate the use of a combination of M46J UNI and T300 weave carbon (which use different resin systems).

Manufacturing Process Selection and Design

Prepreg laminates require both a mold and means of applying pressure. Typically the team uses either fiberglass or foam molds in combination with vacuum bags to manufacture parts. Due to the complex geometry of the wheel, alternative means of applying pressure and various unusual designs were considered and evaluated. Ultimately, a four piece mold consisting of three carbon fiber mold sections for the rim and a single high density foam mold for the wheel center was chosen and produced. Despite serious consideration and testing of other means of applying pressure during the cure cycle, in the end it was decided to simply vacuum bag the wheel.

Methods of Pressure Application

Adequate pressure must be applied to a prepreg layup during the cure cycle. Typically this is done by means of a vacuum bag. However, in cases where pressures higher than atmospheric are necessary or where pressure must be applied to the internal surfaces of a part, other methods may be necessary. A variety of these methods were considered for the wheel due to its geometry, the desire to minimize porosity, and the consideration of using the T800 series carbon which is intended to be autoclaved.

Autoclave

The first and most common of these alternate methods is the use of an autoclave. An autoclave is in essence a pressurized oven. To use an autoclave, a part is first vacuum bagged and then placed in the autoclave which is pressurized, increasing the pressure against the surface of the part well above the 14 PSI provided by atmospheric pressure. The use of an autoclave reduces laminate void content and allows the use of higher temperature higher viscosity resin systems (GMT Composites). The structural advantages of using an autoclave are minimal and there have been studies that have found that autoclaved composites are actually less damage resistant than equivalent oven cured composites (GMT Composites).

Due to a desire to reduce voids and porosity as well as the consideration of using the T800 prepreg which is intended to be autoclaved, the use of an autoclave was considered for the ARG14 composite wheels. Using an autoclave would have no substantial drawbacks, were an autoclave readily available for use by the team. Unfortunately, the nearest autoclave known to be potentially available to the team is located at Boeing's Philadelphia facility. Driving four hours each way to Philadelphia might be acceptable if only one wheel were being made, but the plan was to produce an absolute minimum of four wheels, using this autoclave would either require unacceptable amounts of travel or the manufacture of duplicate molds. Purchasing an autoclave is entirely out of the question due to the costs involved. In 2006,

the team manufactured a custom autoclave intended to be used to produce composite wheels (Rotondo, ARG11 Fall Technical Report 8). It appears the autoclave worked, but by all accounts it was sketchy and potentially dangerous to operate. Due to the pressures involved and catastrophic ramifications of failure, manufacturing an autoclave that is adequately safe, while possible, would be a yearlong project in and of itself. For these reasons, the use of an autoclave for the ARG14 wheels was ruled out.

Silicone Pressure Intensifier

Theory and Process

A more exotic means of applying pressure to a composite part is the use of silicone pressure intensifier(s). Silicone has a substantially higher coefficient of thermal expansion (CTE) than conventional mold materials. This means that if a block of silicone is placed against or within a composite part and then confined with rigid material, when the part is cured, the silicone will expand, pressing against the part, providing pressure. Silicone pressure intensifiers are particularly well suited to providing pressure in hollow parts (such as hollow wheel spokes), can provide pressure in excess of the 14 PSI limit of a vacuum bag, and leave a semi-tooled surface on the part (Crouchen 4-5).

To make a pressure intensifier, RTV silicone is molded to the proper shape. An undersized mold specifically intended for the silicone can be manufactured or the part mold can be thickened using a sheet of wax to provide clearance for the thickness of the carbon (Crouchen 6). The silicone is degassed using a vacuum chamber to remove air bubbles, poured into the mold, and allowed to cure (Crouchen 6). Mold release (must not be silicone based) or a non-stick surface must be used to prevent the silicone from bonding to the mold (Mosites Rubber Company, Inc.). Additional instructions for casting RTV silicone can be found on the website of Mosites (Mosites Rubber Company, Inc.).

After a part as been laid up (or in applications where the silicone is being used to fill a void in the part, during the layup) the silicone should be wrapped in release film to prevent silicone contamination of the part and ease post-cure removal (Mosites Rubber Company, Inc.) (Strong 148). The silicone must be rigidly enclosed for pressure to be applied. The part is then cured with the silicone in place. After the part has been removed from the oven, the silicone can be removed and reused. For a walkthrough of the use of silicone pressure intensifiers, see: (Sloan, High-speed press cure for high-speed racers).

Silicone pressure intensifiers can provide in excess of 100 PSI of pressure (Crouchen 5). More is not necessarily better; excessive pressure will result in a resin-starved laminate. It is therefore necessary to design the pressure intensifier to provide the correct amount of pressure (dependant on the type of prepreg). An equation to estimate the volume of silicone required to achieve a certain pressure is shown below:

$$V_1^R = \frac{(V_1^P - V_1^L)}{\left(\alpha^R - \alpha^M - \frac{P_2}{K_2} \alpha^R\right) \Delta T - \frac{P_2}{K_2}}$$

(Su and Wu 2)

This equation is based on the volume of the carbon fiber, the coefficients of thermal expansion of the mold and silicone and the bulk modulus of the silicone. Any gaps between the pressure intensifier and the

part must be accounted for when calculating the thickness/volume of the pressure intensifier. For further discussion of these calculations, see: (Su and Wu) and (Cremens).

Potential Use for Wheels

The use of a silicone pressure intensifier was considered for the wheels. A pressure intensifier would have been manufactured to serve as the male portion of the wheel mold within the main cylinder and inner rim of the wheel. This silicone pressure intensifier would likely have utilized a solid core of a lower CTE material to reduce the applied pressure and required quantity of silicone.

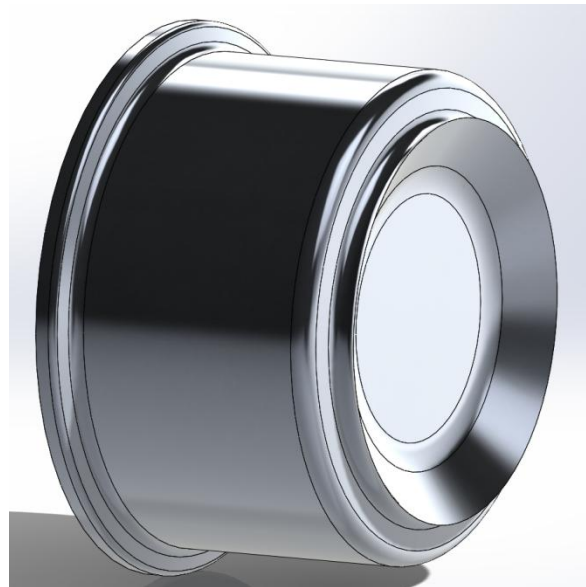


Figure 52: Wheel Silicone Pressure Intensifier Shape

This pressure intensifier would have applied a pressure greater than that possible with a vacuum bag, reducing the void content of the wheel and potentially allowing the use of the T800 carbon (which specified the use of an autoclave). In addition, the silicone would have provided the interior of the wheel with a semi-tooled surface. The use of silicone along the interior of the outer rim was also considered since this region required a double-sided mold and the use of silicone would have eliminated the need for the molds to as precisely account for the thickness of the carbon in this region.

Testing

A series of tests were conducted to evaluate the suitability of silicone pressure intensifiers and gain experience in their use. Three different molds were used, the "Shallow Mold" (see Figure 53), "Ring Mold" (see Figure 54), and "Bread Pan Mold" (see Figure 55). The shallow mold and ring mold were machined out of high density foam using a CNC router. The shallow mold was sanded and sealed with Duratec primer while the ring mold was simply wrapped with film release. The bread pan mold was simply a non-stick loaf pan that received no further finishing. For one of the two bread pan tests, a high density foam core wrapped in film release was used to reduce the necessary volume of silicone. These molds were intended to test different geometries and produce CFRP laminate samples for Intron testing.



Figure 53: "Shallow Mold" Layup Prior to Curing

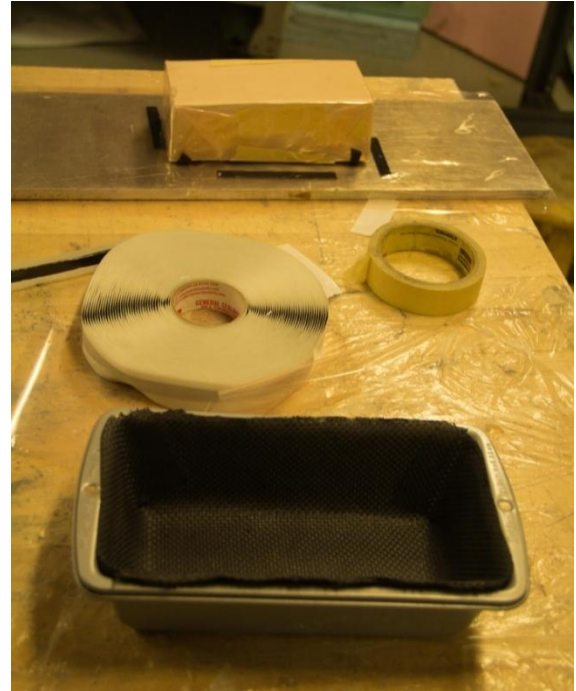


Figure 55: "Bread Pan" Layup with Cap in Background

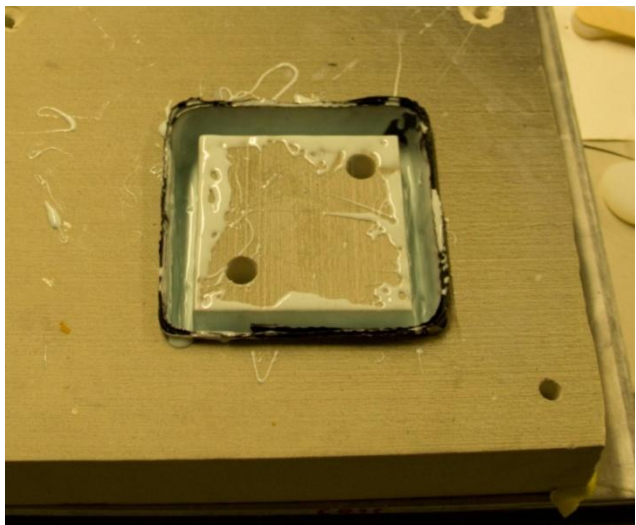


Figure 54: "Ring Mold" Layup During Silicone Pouring

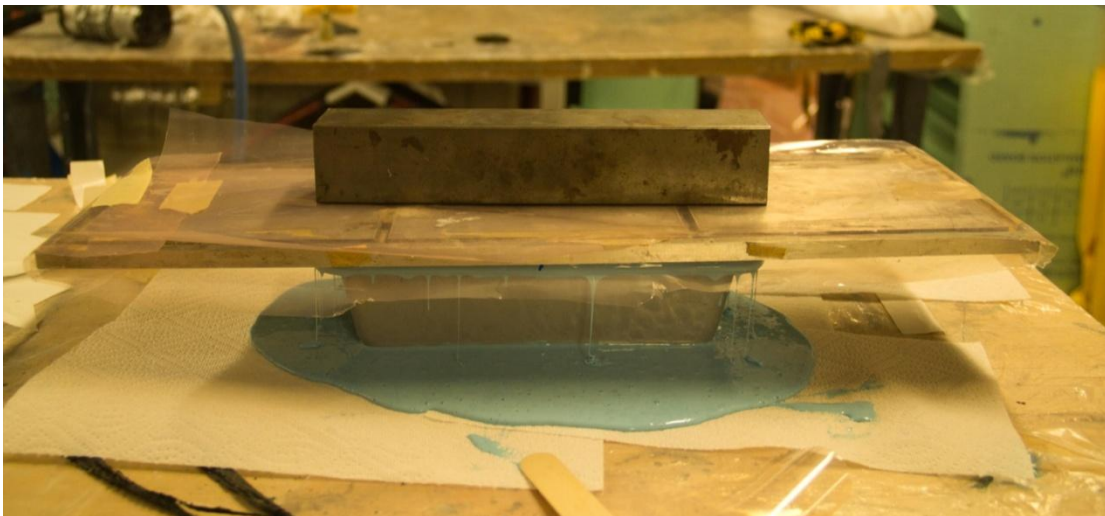


Figure 56: Cap Insertion into "Bread Pan" Layup During Silicone Pour

Ten layers of T800H carbon was used for each of the layups. After the carbon was laid up and debulked, the silicone was prepared. Silpak Inc. R-2264 RTV Silicone was mixed and placed in a 5 gallon bucket hooked up to a vacuum pump to allow the silicone to be degassed. The degassed silicone was then poured into the mold and allowed to cure overnight. A thick metal plate was then clamped over the mold and the mold was placed in the oven for curing. The T800H cure cycle was used to cure the carbon.



Figure 57: Cured "Bread Pan" Layup Showing Foam Portion of Cap in the Center

The intention of the testing was for the first layup to merely serve as a spacer to ensure that the silicone was cast to the proper size and shape. It was expected that curing the silicone in place would allow the silicone to provide pressure during the first layup, but no sources discussed using the silicone in such a manner, so it was unclear if this would work. The hardened silicone would then be removed and reused after the carbon was cured. Samples of the cured carbon would then be cut and subjected to a three-point bending test to evaluate the effectiveness of the silicone in apply pressure.

In reality, technical difficulties and time limitations prevented the implementation of a conclusive test program. The first five tests were invalidated by either not degassing the silicone or using inadequate hardener (see Table 7). The silicone in these tests either never cured or was filled with bubbles. Only a single test used properly degassed and mixed silicone. The silicone in this test adhered to the carbon resulting in its destruction during the removal process (see Figure 58). No test was ever conducted using an already cured block of silicone, despite the fact that not a single source suggests the use of un-cured silicone as a pressure intensifier.

Table 7: Silicone Pressure Intensifier Test Results

Test	Silicone Cure	Carbon Cure	Conclusion
Shallow Mold (A)	Complete. Lots of bubbles.	Minimal apparent problems	Silicone must be placed in a vacuum to degas before use
Shallow Mold (B)	Little to none	Extreme delamination	Inadequate hardener
Shallow Mold (C)	Partial	Extreme delamination	Inadequate hardener – difference between different mix ratios readily apparent
Ring	Partial	Destroyed during removal from mold	Inadequate hardener
Uncapped Bread Pan, Solid Core	Partial	Extreme delamination	Inadequate hardener – difference between different mix ratios readily apparent. Silicone not expected to provide pressure without cap.
Capped Bread Pan, Solid Core	Complete	Extreme delamination	Unqualified failure. Test procedure had no obvious flaws.



Figure 58: Laboriously Removing the Silicone from the "Bread Pan" Layup

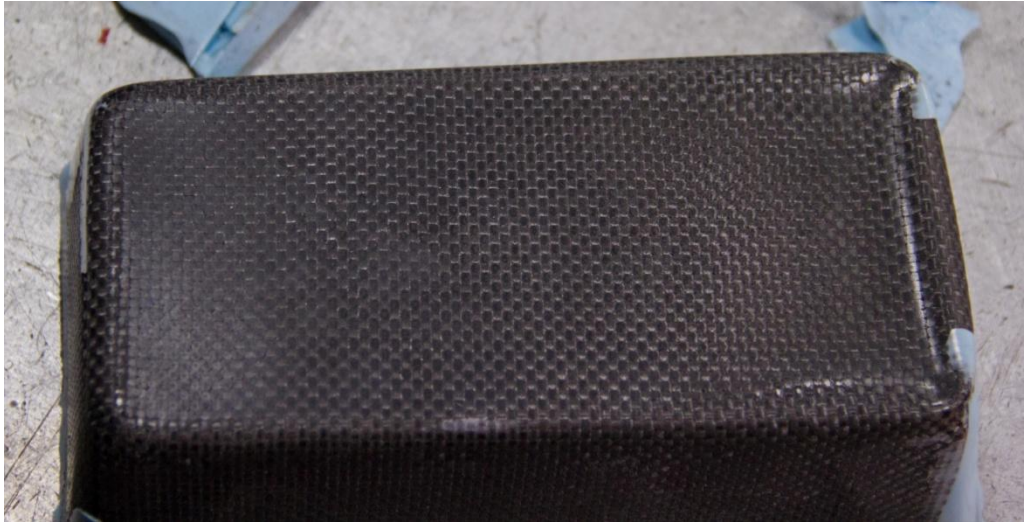


Figure 59: Underside of the "Bread Pan" Layup Showing Clear Evidence of Inadequate Applied Pressure



Figure 60: Test Samples from "Shallow Mold" Layups

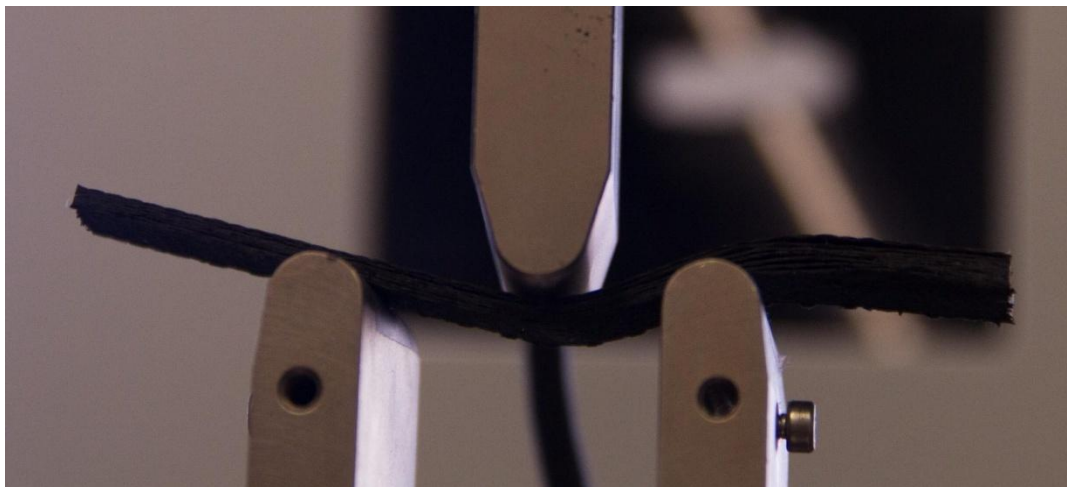


Figure 61: 3 Point Bending Test of a Silicone Mold Test Sample Showing Unacceptable Delamination

The consolidation and void content of the carbon ranged from marginal to utterly unacceptable (see Table 7). Bridging was generally visible in part corners (see Figure 59). Some flat sections were not obviously flawed, while others were so poorly consolidated that the application of even mild pressure by hand would result in delimitation. Samples were cut from all of the tests using a diamond grit bandsaw (see Figure 60) and subjected to a three-point bending test using an Instron (see Figure 61). The testing clearly showed that all samples delaminated excessively. Because the samples so clearly failed testing, the quantitative results of the Instron testing have not been consolidated and included in this report.

Lessons Learned

The silicone pressure intensifier testing was inadequate to evaluate the effectiveness of the use of silicone as a pressure intensifier. Some lessons were learned however:

- Adequate hardener must be used. Err on the side of caution and use more hardener than is required.
- The silicone must be degassed using a vacuum chamber.
- The silicone will adhere to and contaminate surfaces that are not non-stick or treated with mold release. The silicone should be isolated from the prepreg using film release. Prepreg should not be used as a spacer when initially casting the silicone.
- The silicone must be cast in advance before attempting to use it as a pressure intensifier in a layup.
- Shortcuts should not be taken during testing of silicone.

Silicone Vacuum Bag

A sample of uncured silicone sheet was obtained free of charge from Tim Schwarz at the Mosites Rubber Company. Uncured silicone sheet can be used to mold reusable custom vacuum bags that perfectly conform to the part (Mosites Rubber Company, Inc.). These bags are thicker and more elastic than conventional vacuum bags, making them more resistant to damage. Silicone bags are typically used in applications where multiple parts are being produced using the same mold.

Testing

Two tests were run to experiment with producing silicone vacuum bags. Instructions for working with uncured silicone sheet can be found here: (Mosites Rubber Company, Inc.). The silicone was formed to an old aluminum steering wheel mold and then cured in a oven using the recommended cure cycle.



Figure 62: Silicone Vacuum Bag Test After Cure

A single layer of silicone was used for the first test. For the second test, two layers were used. The results of the tests are shown in Table 8.

Table 8: Silicone Vacuum Bag Test Results

Test	Conclusions
1 Layer of Silicone Applied Directly to Mold and Vacuum Bagged With Film Release and Breather on Top	Became dangerously thin at sharp corners. Did not reliably fill narrow channels
2 Layers of Silicone Applied on Top of Breather and Film Release. Vacuum Bagged With Film Release and Two Layers of Breather on Top	Appears successful

Lessons Learned

The finished bag was never tested, but there is no reason to believe that it would not work as intended. Silicone bags potentially could aid in bagging parts with complicated geometry, particularly if multiple copies are being made.

Bladders

Another means of applying pressure to a mold internally is to use a bladder. Typically an elastomeric bladder is inserted into a part and then inflated with compressed air. Bladders can provide pressures greater than atmospheric and can be used in situations where the opening into the part is smaller than the cavity within. While a bladder could have been used in place of a pressure intensifier,

bladders were not seriously considered for use this year due to the potential difficulty of producing reliable custom bladders.

Mold Design

Splits

It was decided to use a female mold to form the rim of the wheel to guarantee the smoothness and geometric tolerances of the bead seats. There are no critical dimensions on the interior of the rim. Due to the required geometry of the rim, it is impossible to produce a one-piece rim mold (female or male) that does not have substantial negative draft. For this reason, it was necessary to use at least two molds to produce the rim. For a female mold, the rim molds must be split by a plane parallel and coincident with the central axis of the wheel. A two piece female mold would have approached zero draft at the intersection between the mold halves, so a three piece rim mold was designed in order to limit the minimum draft angle.

To form the wheel center and spokes, only a single mold is necessary. This mold could have been located on either the inner or outer (relative to the car) faces of the wheel center and spokes. The inner face of the wheel center is bolted against the wheel hub and is therefore its dimensions are critical. Despite this, it was decided to located the spokes and center mold on the outer face of the wheel to minimize the extent of the wheel which would have a mold on opposing surfaces. Alternatively, the center mold could simply have been terminated where it reached the rim, but it seemed unlikely that the resulting transition between mold and vacuum bag would function as intended.

Design, Materials, and Manufacturing Process Selection

Rim Mold

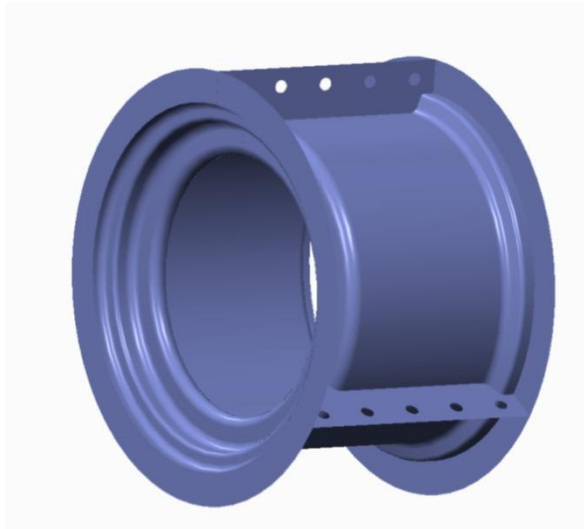


Figure 63: Draft Shell Model of the Three Rim Molds

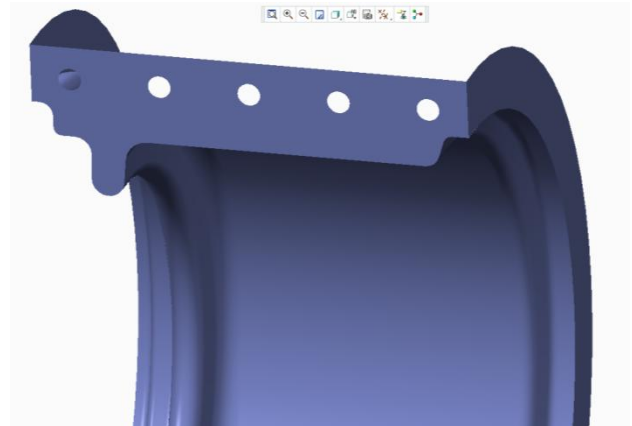


Figure 64: Draft Close-up Showing an Endplate of a Single Rim Mold

The rim mold was designed to consist of three identical molds which would be bolted together during the layup. The mold sections each consisted of a third of the rim with an end plate on three sides to allow the sections to be bolted together and to the center mold (see Figure 63 and Figure 64). Due to the fact that three identical molds would be required, it made manufacturing sense to make a single plug which would then be used to produce the three composite molds.

Normally the team uses orange tooling gel coat, chopped strand fiberglass mat, and vinyl ester resin to produce molds. As was vividly demonstrated by the failed first cure of the ARG14 monocoque face sheets, fiberglass has a different CTE than carbon fiber. Therefore, when heated during the cure cycle, a fiberglass mold will expand and contract at a different rate than the carbon fiber part. Carbon fiber also has the added advantage of being stiffer. Since maintaining the dimensional tolerances and, in particular, the cylindricity of the wheel was extremely important, it was decided to produce a heavily reinforced carbon fiber mold. The sole disadvantage of using carbon fiber instead of fiberglass is, of course, cost. In this case, the added cost was deemed justified. Since the weight of the mold was irrelevant and the surface finish was critical, it was decided to manufacture the molds using a wet layup. The team's supply of plain-weave carbon fiber was used as the reinforcement. Epoxy was used as the resin due to its superior strength and temperature resistance. Normally epoxy would not be used because chopped strand mat uses a fiber binder which dissolves in polyester resins, but not epoxy. In addition, epoxy is more expensive than polyester resin. The orange tooling gel coat was not used because it is polyester based and thus incompatible with epoxy.

It was decided to machine the plug out of high density foam. Aluminum would have been preferable, but the hundreds of dollars required to purchase aluminum stock of the necessary size could not be justified at the time. Turning a plug with a CNC lathe and then install end plates on the cylindrical plug to leave one third of the cylinder exposed was considered. However, while the team had easy access to CNC routers, a CNC lathe that could be used to machine foam was not so easily accessible. For this reason, the plug was designed to be machined with a CNC router (see Figure 65). Unlike a CNC mill, it is not possible to accurately zero a CNC router. Because of this, tool changes introduce non-negligible inaccuracies. The bulk of the rim plug was suited to being machined with a 1/4" end mill. However, the intersection of rim surface with the endplates required near-zero curvature. A smaller end mill would have required an unacceptable amount of machining time. This left two choices: accepting a 1/4" radius at these edges or machining the endplates separately and accepting the reduction in dimensional tolerances when the pieces were bonded together. The latter option was selected. The inner rim endplate was omitted, so the final mold consisted of four pieces of high density foam bonded together.

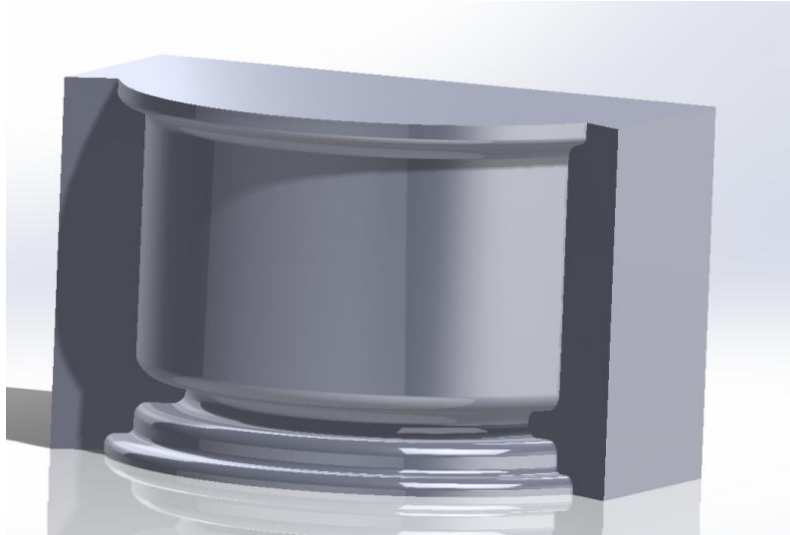


Figure 65: Rim Mold Plug Model Without Outer End Plate Installed

Center Mold

The center mold consisted of only a single piece. There was no obvious advantage to first machining a plug and using it to produce a composite mold, so a mold was simply machined out of a block of foam and then sanded and sealed. The geometry of the center mold design is shown below in Figure 66 and Figure 67. Note the bolt ring used to attach the assembled rim mold to the center mold.



Figure 66: Wheel Center Mold

(CNC ROUTER PART)
SEE: FSAE_WHEEL_CENTER_MOLD.IGS

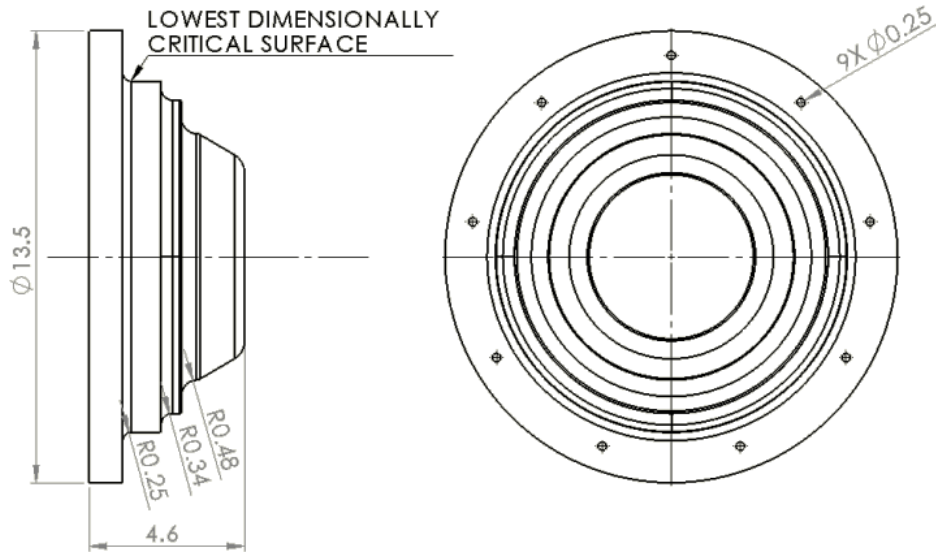


Figure 67: Wheel Center Mold Major Dimensions

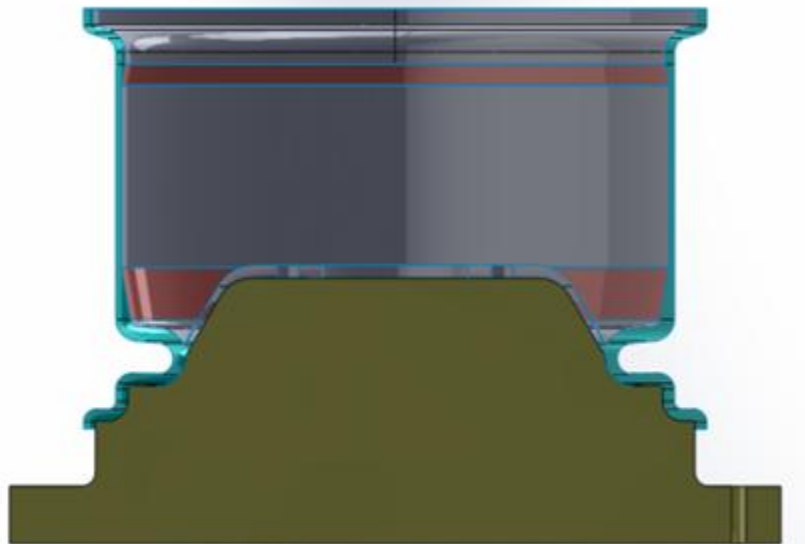


Figure 68: Cross Section of Center Mold and Wheel

Since the wheel has a non-zero thickness, when modeling the center mold, the surface of the center mold was offset from the surface of the rim mold. The center mold, rather than the rim mold, was offset because, with the exception of the wheel offset, its dimensions were not critical to the function of

the wheel. A Solidworks model accounting for the thickness of the different sections of the wheel was created (see Figure 68). The thickness of each region was calculated by multiplying the ply thickness value in the team's pre-preg inventory Google Doc by the number of plies. A 10° transition was used between areas of different thickness (shown as red in the image above). The center mold (shown as yellow) was modeled using the resulting surface of the wheel model.

ARG14 Wheel Manufacture

Mold Manufacture

To manufacture the molds, a foam center mold and foam rim plug were machined. Both were sanded and sealed. The rim plug was used to layup three identical carbon fiber rim mold sections. The mold was then clamped together, measured, and adjusted. Bolts and dowel pins were installed to connect and align the mold sections. A minor geometry problem was corrected with a layer of Duratec primer. Imperfections were then filled and the mold was sanded to prepare it for use.

Foam Machining and Assembly

The rim plug and center mold were machined from 40lb/ft³ high temperature foam. The molds were machined using one of the Architecture Department's CNC routers located in Rand Hall. One of Rand Hall's two CNT Motion CNC routers was used because these routers are larger, vastly more powerful, and more reliable than the MAXNC router in the Emerson Shop. In addition, these routers have automatic tool changing. IGES files were provided to the shop staff at Rand Hall who converted the files into g-code using RhinoCAM and then helped run the router.



Figure 69: The Start of the Rim Plug Finishing Passes

Separate end plates for the rim plug were machined using the Emerson Machine Shop router (see Figure 71). The end plates were cut from a thin sheet of foam to simplify the machining process. The end

plates were then bonded to the rim plug. An additional end plate was cut from a sheet of foam by hand and then bonded to the outer rim (see Figure 72 and Figure 73 for pictures of the assembled rim plug).

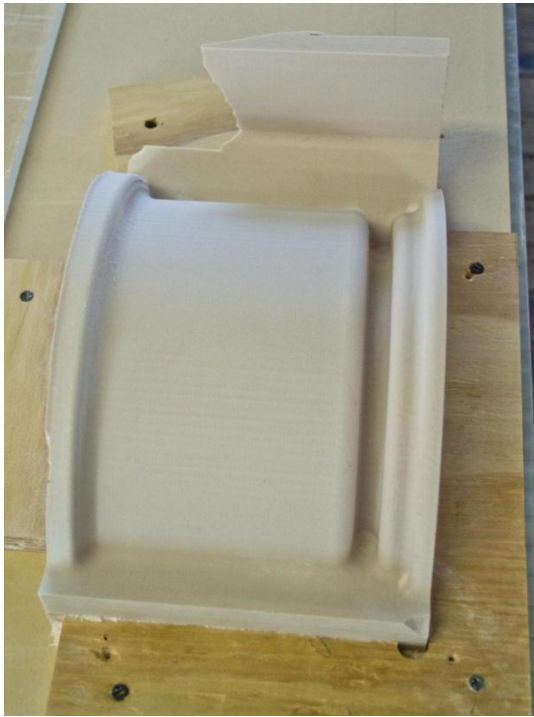


Figure 70: The Machined Rim Plug



Figure 71: Machining the Rim Plug End Plates

The center mold was also machined at Rand Hall. No piece of foam large enough to machine the entire mold was available. For this reason, a foam piece large enough to include all of the mold surfaces, but only part of the bolt flange was used. Separate blocks of foam were both glued and screwed to the main block to extend the undersized portions of the bolt flange. Rand Hall lacked a 0.25" drill bit of adequate length to fully drill the bolt holes, so these holes were partly drilled by the CNC router and then completed with a hand drill. The holes that were not located within the confines of the large machined section were located using a paper template and then drilled by hand (see Figure 74 for a picture of the assembled center mold).

Foam Surface Preparation

The foam plug and mold were sanded and Dolphin Glaze was used to fill large imperfections. A coat of Duratec Primer was then applied using a gel coat spray gun. Once dry, the surface was sanded and then another coat of primer was applied. This process was repeated until a smooth surface had been achieved. For the final coat, successively finer grits of sandpaper, all the way up to 1000 grit were used, followed by buffing compound. When sanding and applying Duratec, attempts were made to minimize the degree to which the dimensions of the plug and mold were altered. Great care was taken to ensure that surfaces of the mold and plug that would contact the wheel were free of imperfections. In particular, attention was paid to smoothing the drop center due to the steep draft angle in this region. Less attention was paid to the bolt flange and endplates of the plug and mold. To eliminate the need to finely finish the edges of the plug, packing tape was wrapped around these roughly sanded areas (see Figure 73). Packing

tape readily serves as a easily applied non-stick surface in low temperature applications in regions where the surface finish is unimportant. Packing tape was not used on the center mold since the center mold would eventually be baked in the oven.



Figure 72: Sanding the Duretec Coat on the Rim Plug



Figure 73: The Completed Rim Plug



Figure 74: A Freshly Sprayed Coat of Duratec Primer on the Center Mold

Rim Mold Layups

The three rim mold sections were laid up using the rim plug. In order to ensure that the mold was extremely stiff, ten layers of plain weave carbon fiber was used for each section. Twill, or another more conformable weave of carbon fiber would have been preferable, but only plain weave carbon was available. West System 105 resin and 207 special clear hardener were used as the resin system. 207 hardener was chosen because it was on hand, but 206 slow hardener would have worked equally well and is less expensive. A faster hardener, however, would not have provided adequate working time.

Since these parts were to be used as molds, ensuring that the inner surface of the mold was perfectly smooth was a priority. This is typically achieved through use of a tooling gel coat which is applied as a first layer, preventing 'print-through' and surface voids. Polyester gel coats are generally not fully compatible with epoxy resin systems, so the team's orange tooling gel coat could not be used. Commercial epoxy tooling gel coats are available, but none had been obtained in advance, so improvisation was required.

A search of online forums found that epoxy gelcoat could be made by adding powdered graphite and colloidal silica to regular epoxy. These are both sold by West System and other companies as standard epoxy additives. The graphite serves to make the surface lower friction, aiding part removal after the cure. Colloidal silica increases the viscosity of the resin and also the toughness of the cured surface. It should be noted that glass micro balloons, while similar in appearance to colloidal silica, cannot be substituted because micro balloons will produce a highly porous surface and make the surface less abrasion resistant. Colloidal silica was not available locally, but graphite is sold by hardware stores as a lubricant. Several small tubes of graphite were obtained from Lowes and used in the first layer of epoxy. It became apparent that the hardware store variety of graphite was more roughly ground than that sold as an epoxy additive. It was used regardless under the belief that it might still help and was unlikely to cause problems. Ultimately, while it did give the surface of the mold a sparkly appearance (see Figure 79), it is not clear if the use of graphite had any impact on the functionality of the mold.

Since colloidal silica or another usable thickener was not available, the epoxy used for the first layer was allowed to sit and 'gel' in a cup for roughly a half hour after being mixed. Since the curing of epoxy is exothermic, large quantities kept in a cup will 'gel' and cure much faster than if the epoxy is spread out over a surface. Once the epoxy had adequately thickened, it was painted onto the mold so as to cover the entire surface of the mold (see Figure 75).

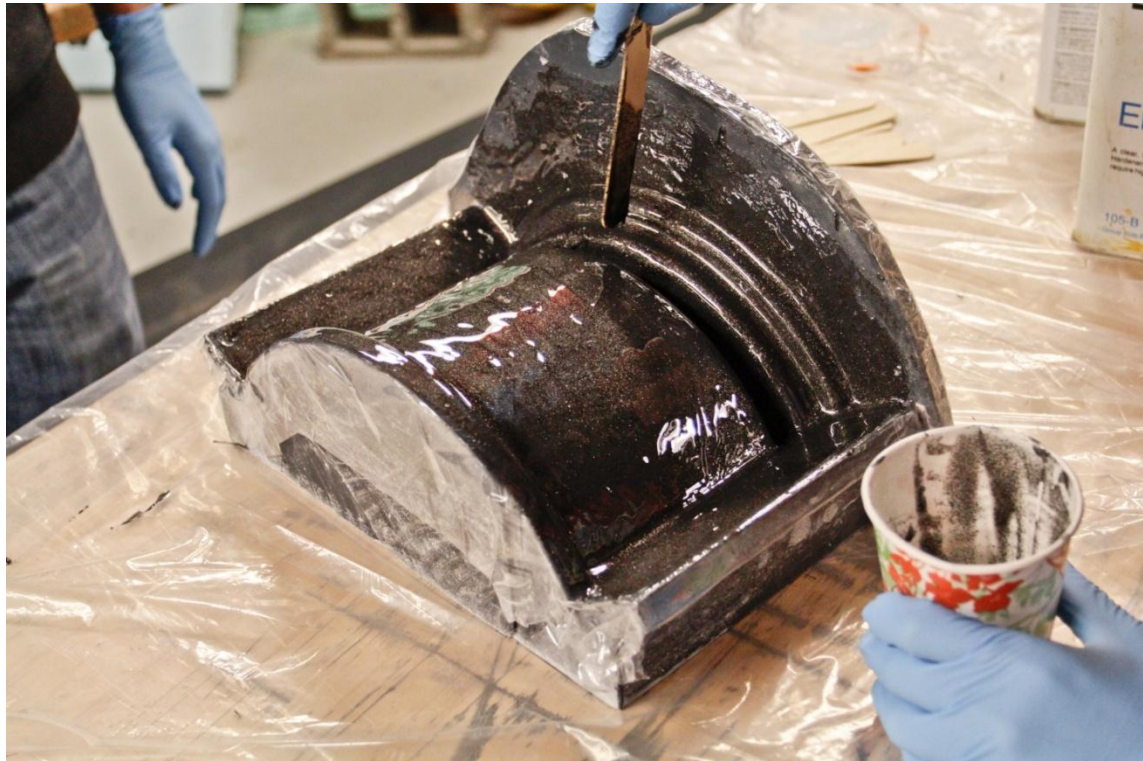


Figure 75: Applying Gelled Epoxy During a Rim Mold Layup

Freshly mixed epoxy was then applied along with layers of carbon fiber. The carbon fiber was all cut in advance and heavily spliced to allow for it to conform to the complicated mold geometry (see Figure 76). Prior to the application of each additional layer of carbon, a layer of epoxy was applied by hand. The carbon was then pressed down to ensure that it fully saturated and no voids were present. If needed, additional epoxy was applied to saturate any visible dry regions. No effort was made to saturate carbon fiber extending off of the surface of the mold. This process was repeated until all ten layers had been applied.



Figure 76: Carbon Fiber Cut for a Rim Mold Section Layup

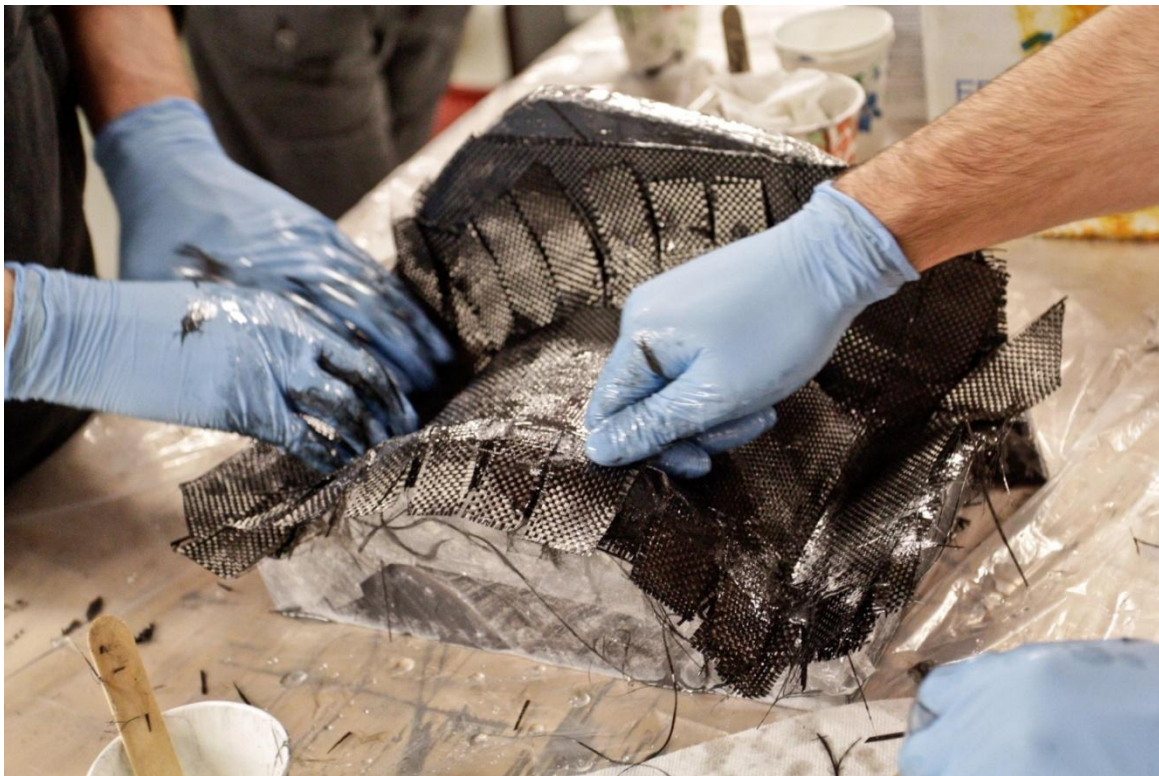


Figure 77: Rim Mold Layup

Wet layups are to some degree an art form, particularly when complicated by mold geometry or the use of stiff fabric. Fortunately, in the case of the molds, weight is irrelevant, so an extremely resin-rich layup can be used, which greatly eases the layup process. Once laid up, the molds were simply allowed to cure overnight without the use of a vacuum bag. Vacuum bagging was deemed unnecessary in this case since there was no benefit to drawing out excess resin.



Figure 78: Working on the Drop Center of the Rim Mold Layup

Once the rim sections cured, they were removed from the plug. This was achieved by clamping the foam plug in a large vise, prying up the edges, and then giving the part a few firm tugs. In every case, after some pulling, the mold popped right off of the plug. The mold sections were then trimmed by hand using a Dremel.



Figure 79: A Cured Rim Mold Section Prior to Trimming



Figure 80: Trimmed Rim Mold Sections

Alignment and Evaluation of Dimensional Tolerances

The mold surfaces of the rim molds are largely devoid of straight or cylindrical faces which could be easily utilized when aligning the sections. The end plates, while flat, were known to have questionable tolerances. The corners of the molds between the mold surfaces and end plates were too rounded to allow reliable alignment. No good indicating features were available to align the parts. An attempt by other members of the team to align the parts using an indicator on a mill proved utterly unsuccessful.

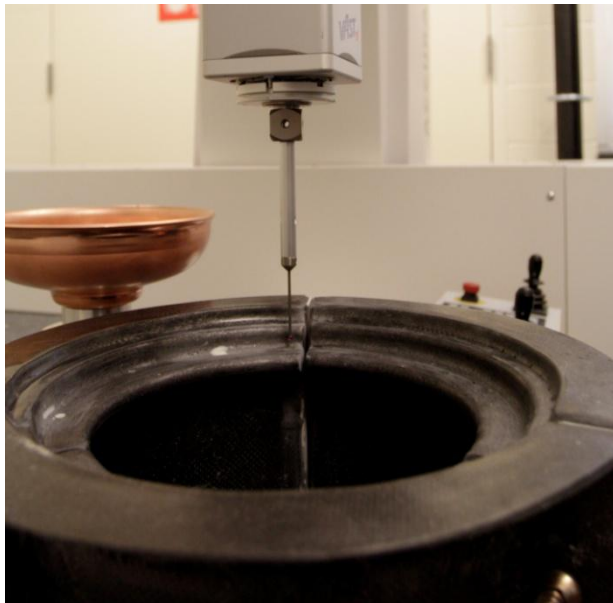


Figure 81: Measuring the Rim Mold with a CMM



Figure 82: Rim Mold CMM Measurement Setup

To align the mold sections, cylindrical foam pieces with the diameter of the insides of the main cylinder of the wheel were cut out using the Emerson Machine Shop CNC router. Thin sheet metal shims were cut and inserted between the endplates of the rim mold sections in order to properly space the mold sections. The sections were then clamped together using C-clamps.

At this point, it was difficult to obtain a sense of how round the mold was and what its tolerances were. For this reason, with the help of Joe Conway, an FSAE alum, the dimensions of the mold were evaluated using the LEPP CMM (Coordinate Measuring Machine). The alignment of the sections was adjusted slightly to compensate for apparent misalignment and the mold was re-measured. A summary of the final results is shown below. The complete results can be found in Appendix H: Wheel Rim Mold CMM Results.

Specifications (The Tire and Rim Association)

Diameter: 9.968

Diameter Tolerance +/-0.015 (e.g. 9.953-9.983)

Axial Tolerance: +/-0.063

Outer Rim Bead Seat CMM Results

Diameter: 9.9221 (0.0309 below specified range)

Upper Tolerance: 0.0100

Lower Tolerance: -0.0100

Axial Deviation: 0.0340

Inner Rim Bead Seat CMM Results

Diameter: 9.9124 (0.0406 below specified range)

Upper Tolerance: 0.0079

Lower Tolerance: -0.0079

Note: All units inches. The bead seats are conical so the measured diameter is dependent upon the height at which measurements are taken. The actual diameters (diameters at the point specified by the TRA) are likely slightly larger than recorded.

Rim Mold Post Processing and Assembly

At this point, while the rim remained clamped together, three 0.25" holes were drilled through each of the endplate pairs and sets of shims. The sections were then bolted together, locking their relative position in place. To ensure that the alignment could be maintained after the rim was disassembled, steel bushings were machined to match dowel pins. Two additional holes were drilled through each set of end plates, the dowel pin was inserted, and a bushing was slid over the dowel pin on each side. Five minute epoxy was used to bond the bushings to the end plates. After the five minute epoxy bonds repeatedly failed, the bushings were removed and re-bonded using West System epoxy mixed with copious quantities of glass micro-balloons (see Figure 84). This fixed the bonding problem, though wrapping fiberglass or carbon fiber around the bushings would likely have provided a more secure connection. The shims and sections were marked with a paint marker to ensure that it was obvious how to reassemble the mold.

To drill the holes for the bolt ring connecting the center mold to the rim mold, the rim mold was placed on top of the center mold. The conical shape of the spokes region served to align the molds relative to each other. Bolts were then inserted through the back side of the center mold and used to mark the position of the holes in the flange of the rim mold. The holes were drilled and the relative orientation of the rim and center mold was marked with a paint marker for future reference.

Unfortunately, after the rim mold was manufactured, it was realized that the mold did not include relief along the main cylinder section to allow the tire to be slid on during mounting. This feature was not incorporated into the team's CAD model of the aluminum Kiezer wheels, but was present on the actual wheels. While very slight, team members with experience mounting tires advised that the absence of relief would make manual tire mounting nearly impossible. To correct this omission, the rim mold was disassembled, masked off, and then sprayed with a very heavy coat of Duratec primer (see Figure 83). The masking tape was then removed and the edges of the Duratec were sanded to create a smooth transition between sections. The end results can best be seen in Figure 86.



Figure 83: Rim Sections Masked in Preparation for Spraying of Duratec

The rim sections were heavily sanded to remove any imperfections. Dolphin Glaze was used where needed to fill any depressions. The rim mold was then reassembled using the dowel pins for alignment. The gaps between rim sections required substantial filling. Dolphin Glaze was repeatedly applied and sanded until the gap was entirely smooth and a continuous surface had been formed. The end result can be seen in Figure 85.



Figure 84: The Outside of the Assembled Rim Mold



Figure 85: A Joint Between Sections of the Rim Mold

Once all surface imperfections had been filled, the rim mold was sanded with increasingly fine grits of sandpaper to smooth the surface. Buffing compound was used as a final abrasive. The fully prepared rim and center mold is shown below in Figure 86.



Figure 86: The Completed Rim and Center Mold

Lesson Learned

The plug was manufactured in several pieces which were then bonded together. This was done in order to create the sharpest possible corner at the edge connecting the rim endplates and main cylinder (see Rim Mold). In the end however, these corners ended up being fairly rounded due to the application of Duratec. The bonding of multiple pieces introduced inaccuracies into the plug dimensions. As a result, notable gaps were present between sections of the rim mold that needed to be filled with metal shims. In addition, the flanges could not be reliably used as reference surfaces when evaluating the geometry of the mold since the accuracy of these surfaces was known to be low. It is clear that machining the rim plug

as a single piece would have reduced manufacturing complexity, increased dimensional accuracy, and had minimal impact on the corner radius at the relevant edges.

Sanding and applying layers of Duratec to foam molds necessarily introduces a degree of inaccuracy and reduces mold tolerances. On most parts, the tolerances are low enough that this is not a concern. On composite wheels, this is in fact a problem. For this reason, despite the high cost and substantial machining time required, it is strongly recommended that future composite wheel plugs be machined out of aluminum. Since aluminum has a substantially different CTE than carbon fiber, caution should be exercised if aluminum is to be used as a mold for pre-preg parts. Machining aluminum plugs and then using room temperature wet layups to create mold sections bypasses the thermal expansion issues. Utilizing this approach would increase dimensional tolerances and eliminate many of the manufacturing headaches that were encountered.

The mold manufacturing process demonstrated the value of incorporating indicating and, ideally, aligning features into the mold sections. Aligning the molds was extremely difficult and could potentially have been more accurate. However, it should be noted that these features will only be as accurate as the machining process and materials used. Since foam molds were used, the use of such features was not seriously considered since the dimensional tolerances of the manufacturing process were not expected to be adequate. Were the plugs/molds to be machined out of aluminum, this would eliminate the tolerance problems and allow for the use of aligning features.

Layup Process

At the start of the layup, the mold was split into two sections: the rim and the center. Prior to the start of the layup, both mold sections were sealed and released using the team's standard mold preparation procedures. The mold sections were each laid up separately initially. Eventually, the two mold sections were then joined together and the layup was continued. See Appendix F: Final Layup Checklist for the order in which plies were applied. Throughout the layup process, extreme care was taken to minimize bridging and other imperfections. Roughly every four layers, the molds were debulked. Once laid up, the wheel was vacuum bagged and cured according to the cure cycle for the M46J carbon. The wheel was then removed from the mold and post-cured at a higher temperature, again per the instructions for M46J carbon.

Rim Layup

A layer of yellow FM-73 adhesive film was applied to the surface of the rim mold (see Figure 87). The FM-73 was intended to serve as a surface film which would reduce surface porosity and provide a smooth surface for the bead seats. The adhesive film also had the added advantage of serving as a tackier base layer which aided the application of the first layer of carbon to the mold. Despite the fact that the adhesive film was tackier than the carbon, adhering it to the non-stick surface of the mold proved difficult and required the frequent use of a heat gun. Eliminating bubbles also proved challenging. Pricking bubbles with a needle was found to be the most effective means of eliminating them. Since the adhesive film was non-structural, it was spliced as much as needed to allow it to conform.

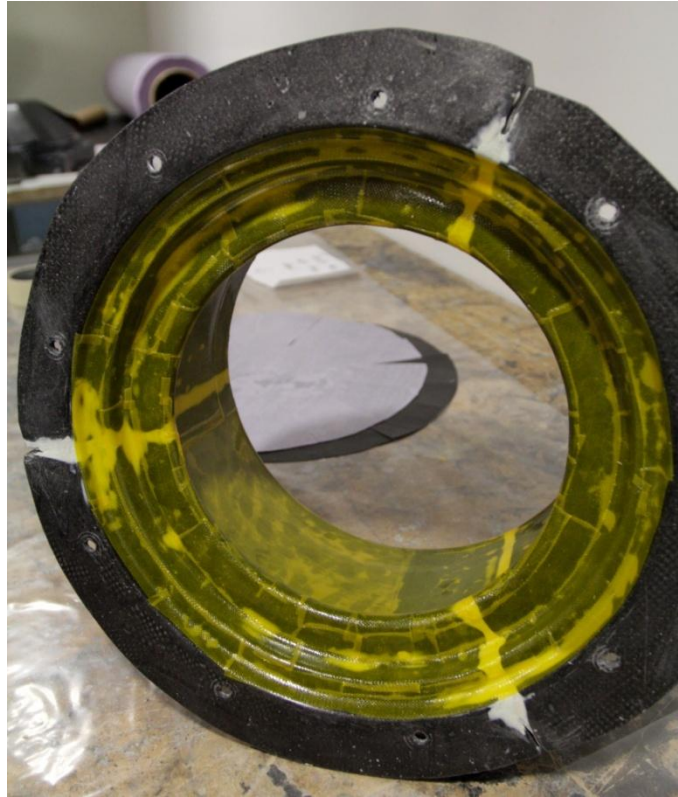


Figure 87: The Initial Layer of FM-73 Adhesive Film on the Rim Mold

Two layers of T300 woven prepreg were then applied (see Figure 88). These layers each covered the entirety of the rim mold. These layers were spliced at the rims and drop center to allow the carbon to conform.

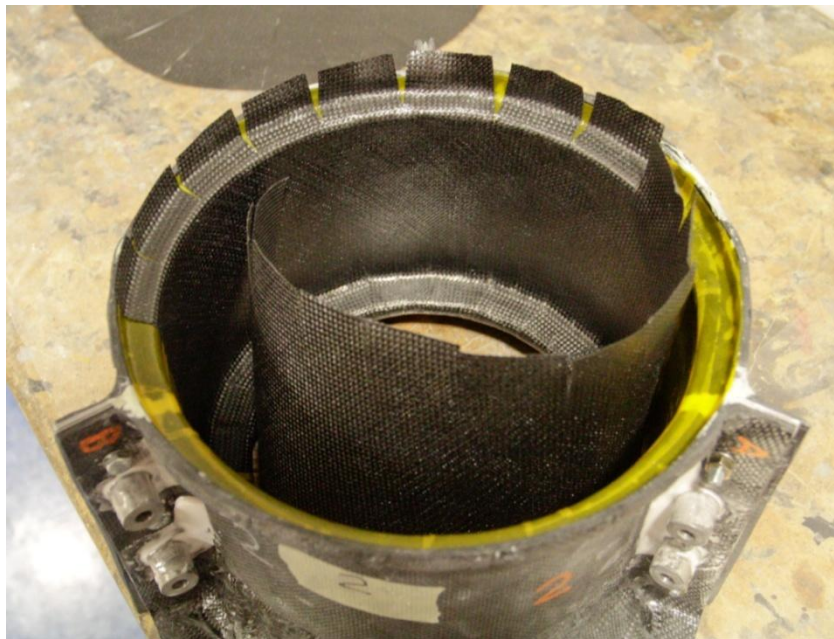


Figure 88: Application of the First Layer of T300 Carbon to the Rim Mold

Initially, excluding two outermost layer on each side, the entirety of the rim was to be composed of M46J unidirectional carbon. Several layers of M46J were applied, but it quickly became apparent that at the rims and dropcenter, applying 0° (axial direction) M46J was difficult, +/-45° M46J was nearly impossible, and 90° (circumferential direction) M46J was outright impossible. After the first few layers had been laid up and debulked, a decision was made to abandon the use of M46J in the rim and dropcenter regions. The layup was redesigned to account for this change (see Final Layup Schedule) and most of a day was spent laboriously peeling back the first several layers strand by strand.



Figure 89: The Drop Center and Outer Rim Following a Debulk Cycle

The rim layup was then continued using the updated and final layup schedule. Three types of pieces of carbon were used: woven sections covering the inner rim, woven sections covering both the outer rim and drop center, and unidirectional pieces covering the main cylinder. The woven pieces typically were half a circumference in length (so two pieces were required for each layer) and the unidirectional pieces were typically a third of a circumference in length (so three pieces were required for each layer). The rim pieces overlapped with the main cylinder section by roughly half an inch. The exact

amount of overlap was deliberately varied to obtain a gently sloped transition between sections. The inner rim pieces were spliced so that section overlapping the main cylinder was left uncut. Attempts were made to offset the location of the splices so that adjacent layers had splices in different locations. The larger outer rim and drop center pieces were spliced similarly. For these pieces, the section covering the tip of the drop center was left uncut and the pieces were spliced on both sides of this strip. 1/2" to a 1" of overlap was used for woven pieces composing a single layer. The location of this overlap was deliberately varied to minimize variation in rim thickness. The splicing and overlap of the unidirectional main cylinder pieces varied depending on the fiber orientation. For 0° and 45° plies, the edges were cut along the direction of the fibers. Since the fibers were nut cut, a butt joint with zero overlap was used for these pieces. The 0° and 45° plies were spliced exclusively along the fiber direction (see the splice faintly visible on the left side of Figure 90). This avoided cutting fibers and minimized the impact of splicing on the strength of the wheel. For the 90° plies, this was not possible, so a full inch of overlap was used. The 90° were spliced along the fiber direction and, when absolutely necessary, across the fiber direction.



Figure 90: The Inner Rim and Main Cylinder Following a Debulk Cycle

The rim was debulked every 3-4 layers. Prior to debulking, a razor blade was used to trim the carbon extending beyond the edge of the mold. Cutting several layers at a time in this manner using the edge of the mold was found to be very easy. The edges were trimmed prior to debulking to prevent the excess carbon from being crushed in the vacuum bag, distorting the carbon on the mold.

Once 2 full plies, 16 outer rim/drop center plies, 10 inner rim plies, and 6 main cylinder plies had been applied, the rim was ready to be joined with the center mold.

Center Layup



Figure 91: First Layer of the Center Layup

The center layup consisted of two types of plies: spokes plies and center plies. The 16 spokes plies, of which 9 were applied prior to the joining of the molds, consisted of large circular pieces that were spliced radially in a 'star shape' (see Figure 91 and Figure 92). The 12 center plies were smaller circles that were spliced around the edges as needed (see Figure 93 and Figure 94). The two outermost spokes layers on both sides of the laminate were T300 while the remainder of the plies were M46J.

The first eight plies were spokes pieces. Two T300 layers were applied, followed by six M46J layers. At 90° increments, splices in the spokes plies were cut all the way to the flat circular face at the center of the mold. For the T300 woven layers, additional splices were cut radially in 45° increments. For the M46J unidirectional layers, frequent additional splices were cut using a razor blade along the fiber direction every 1/2" to 1" as needed to allow the plies to conform. A protractor was used to maintain the 30° spacing between adjacent layers. The mold was debulked every 3-4 layers.

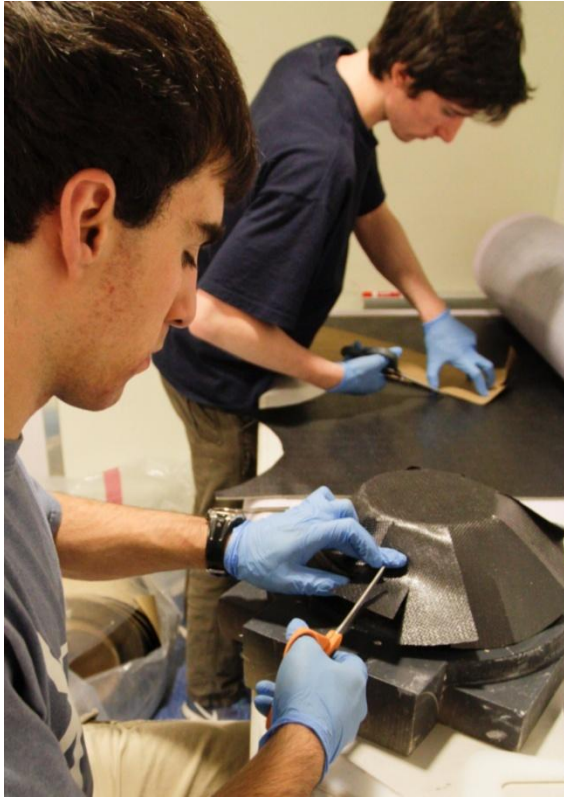


Figure 92: Splicing the First Layer of the Center Layup



Figure 93: Heating a Center Ply



Figure 94: The Prepared Stack of Center Plies

The 12 center plies were then applied. Since these plies only slightly extended beyond the flat central surface, minimal splicing and effort was required to apply these plies. The plies were stacked so that the ply diameter decreased slightly with the application of each additional layer (see Figure 94). This was achieved by cutting the smallest ply first and then using it as a template in conjunction with a thick Sharpie to mark the next. This process was repeated for each ply, ensuring a roughly 1/8" offset was maintained between the edges of adjacent plies and a gradual transition occurred. One last spokes layer was then applied before the mold sections were ready for joining. This layer was applied prior to joining to ensure that the center plies were encapsulated and held down.

Joining the Molds

Once the appropriate stage of the center mold and rim mold layups had been reached, the wheel was prepared for joining. A layer of red FM200-3M adhesive film was applied to the outer rim and drop center on the rim mold. This is not a standard procedure for a co-cured part, since the adhesive film layer has negligible fiber content and is therefore weaker than a carbon ply. The adhesive film was used in the hope that it would flow to fill any voids between the two wheel sections during the cure of the wheel. The potential for filling voids was believed to outweigh the drawbacks of increasing resin content in this region.



Figure 95: Applying Adhesive Film to the Rim Prior to Joining the Molds

The gap between molds was based upon an estimate of layup thickness that did not take into account curvature or the effects of splicing (see the Center Mold section). This was a known risk and the expectation during design was that any inaccuracy could be accounted for by modifying or remaking the center mold after the first wheel layup. During the joining process, it was found that this gap was far

larger than anticipated. The limiting factor was the inner diameter of the drop center which was roughly 7.4". This impinged on the conical spokes face of the center layup which had a base diameter of roughly 7.9". Due to the steep angle of this face, a roughly 1/4" gap was created between horizontal faces. The near vertical faces of the outer rim were impacted far less by this offset. The outer rim bead seat diameter of the rim was 9.6" while the corresponding surface of the center mold ranged from 9.6" at the sharp outside edge to 10.1" at the inside edge. Gaps were measured using small blocks of T300 carbon. The number of plies of the blocks was increased until the wheel sections seated firmly. This allowed the thickness of the gap and number of plies needed to fill it to be determined.



Figure 96: The Assembled Mold\

The gap was filled with over narrow plies of T300 carbon. 45° layers were mostly used since these proved far easier to apply. The existence of these shim plies and the reliance on 45° plies was far from ideal from a structural standpoint. Still, it was expected that, given the massive buildup of thickness in this region, the strength of the joint would be adequate.

Once the gap was filled, bolts were inserted through the holes in the center mold and the rim mold was positioned. Nuts and washers were installed and heavily torque-d down, locking the rim in place. Since the region between the two molds would not be exposed to the vacuum bag during the cure cycle, the bolt preload was relied upon for applying pressure in this region. The hope was that the high pressure in this region would displace the adhesive film when it liquefied during the cure cycle, forcing it into voids and minimizing the adhesive layer thickness elsewhere. Mold alignment was entirely reliant on

the radial symmetry of the layups. No surfaces which could possibly have been used as references remained exposed, so no measurement of the alignment of the relevant surfaces was possible. It was hoped that the deliberate randomization of splices and overlap regions throughout the layups would result in minimal imbalance. Ultimately, the main concern was that the face of the wheel center be perpendicular to the center axis of the bead seats.

Noodle Application



Figure 97: Noodle Installation

The joining process left a 'deltoid gap' at the joint that needed to be filled. This type of gap is commonly seen in composite I-beams or ribbed panels. While filling the deltoid gap is occasionally referenced in literature, determining the specifics of how to properly fill the gap proved quite challenging. Eventually, engineers and technicians at Boeing's Philadelphia facility were able to provide a walkthrough of the process (see Appendix I: Noodle Instructions).

M46J unidirectional carbon was cut along the fiber direction with a razor into roughly 1/8" strips. These strips were then pressed into the gap (see Figure 97). Effort was made to pack the resulting 'noodle' into the gap as tightly as possible. This proved to be an extremely frustrating process since the strips refused to compact and stay in place. If the M46J had been substantially tackier, the difficulty of forming the noodle would likely have been substantially alleviated. Ultimately, the gap was mostly filled and the layup was resumed.

Combined Layup

The layup of the combined mold incorporated elements of the previous layups of the separate center and rim molds. The main cylinder and inner rim plies remained unchanged. Spokes plies were similar, but smaller, extending only to the edge of the deltoid gap (see Figure 98). The drop center plies were reduced in size and overlapped with both the main cylinder and spokes plies by 1/2" to 1". In total, 5 spokes, 10 inner rim, and 16 drop center M46J plies were applied. These were followed by 2 T300 woven spokes layers and a final T300 layer which covered the entire rim from drop center to inner rim.



Figure 98: Application of a Spokes Ply During the Combined Layup



Figure 99: Final Layer of the Combined Layup

As a final step, the small triangular gaps present on the surface of inner rim (see Figure 99) were filled with tiny triangular sections of T300. This was done on the final layer to improve the surface finish and smoothness of the inner rim. This was not necessary on the drop center because the drop center plies overlapped at each splice, rather than forming gaps as occurred on the inner rim.

Curing

Initial Cure

In preparation for the initial cure, the wheel was vacuum bagged. The edges of the center mold and other sharp exposed features outside the mold were wrapped with numerous layers of peel ply to reduce the risk that these features would pop the vacuum bag. A layer of high temperature red film release was then applied to the exposed carbon. The film release was aggressively perforated using an awl to allow for resin to pass through the film release during the cure cycle. The film release was pleated to prevent it from bridging and was then held in place with high temperature flash breaker tape.



Figure 100: First Layer of Film Release and Protective Breather Applied

The area of greatest concern during vacuum bagging was the drop center. To ensure that bridging did not occur and that pressure was evenly applied in this region, pressure intensifier tape was used (see Figure 101). The instructions provided by Cytec were followed for this process; see: (Airtech International Inc.). Pressure intensifier tape is essentially a much thicker version of mastic tape that is packed into corners during a layup. It is isolated from the layup by film release. During the cure, it softens and fills corners, reducing the curvature the vacuum bag is forced to navigate and preventing bridging.



Figure 101: Pressure Intensifier Tape



Figure 102: Second Layer of Film Release

A smaller second layer of hand-perforated film release was applied over the pressure intensifier to isolate it from the breather. Several layers of breather were then used to cover the layup. A massive wad was packed into the center of the wheel and additional breather was used to wrap the outside of the mold. The huge quantity of breather was used out of an abundance of caution to prevent bridging, both preventing the vacuum bag from popping and ensuring consistent pressure distribution by the bag.



Figure 103: The Breather Wrapped Mold Prepared for Bagging

A high temperature bag was used. The bag was extensively pleated to prevent bridging of the bag. This would have been a good application for stretchy Stretchlon bag, but Stretchlon was not available for use at the time and the frequent debulking had provided ample experience with pleating nylon bags. The bag was sealed with mastic tape. A vacuum connector was used. It should be noted that the vacuum connector should not be placed in contact with the laminate because it will leave an imprint during the cure. Instead it should be placed on the outside of the mold and a path for airflow to the laminate should be formed with breather.

As per Cytec's specifications (Cytec Industrial/Aerospace Materials), the wheel was cured for four hours at 248° F with a 70 minute ramp up and ramp down. Once cured, the wheel was removed from its mold. The center mold was unbolted from the rim and popped off without any additional effort. The rim sections were unbolted. A mallet was then used to drive a plastic wedge between the end plates of the rim sections. This freed the rim sections without significant difficulty.



Figure 104: The Cured Wheel Prior to Removal from the Mold

The cured wheel is shown in Figure 105. Note the yellow color of the outer adhesive film and red color of the adhesive film barely protruding from the outer rim.



Figure 105: The Wheel Following its Initial Cure

Post-Cure

The M46J requires an additional free standing post-cure after the part has been removed from the mold. It should be noted that larger parts may need to be supported during the post-cure to prevent sagging as the part is heated. The wheel however, was not supported. The wheel was post-cured at 356° F for 2 hours with a 12 hour ramp up and 100 minute ramp down. Since the oven temperature controller was known to be inaccurate, a thermocouple was taped to each side of the wheel center. During the post-cure, the oven set point temperature was adjusted to maintain the desired thermocouple temperature.

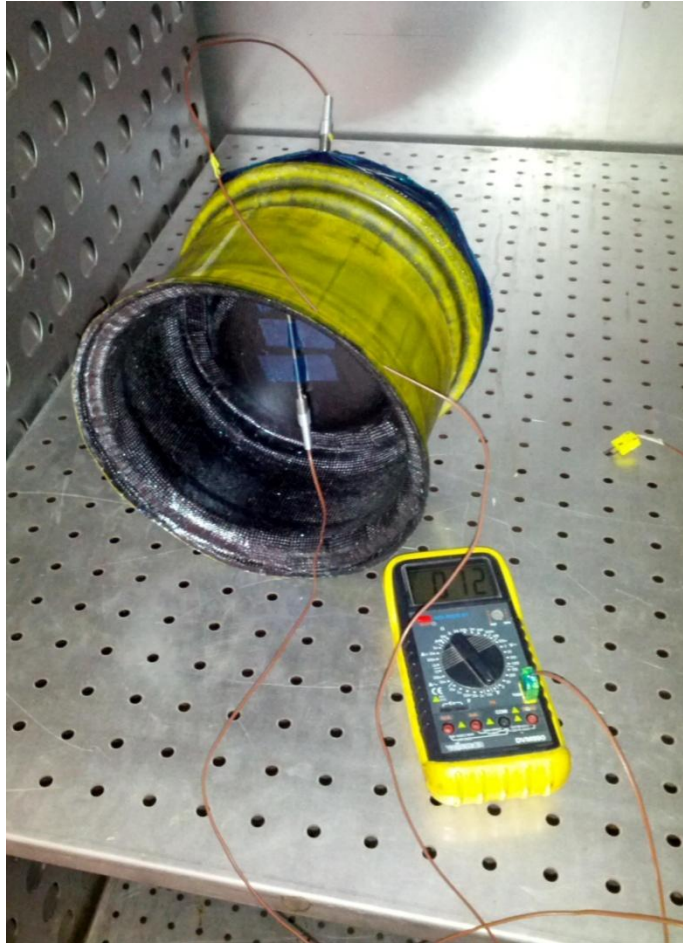


Figure 106: The Wheel Prepared with Thermocouples for the Post-Cure

Lessons Learned

Carbon Application Techniques

Splicing and Conformity

Due to the complex geometry of the wheel and intense loading it would experience, great care was required during the layup process. Voids in the cured laminate reduce strength and stiffness below that of the theoretical design. A void is equivalent to a delaminated region and can grow, leading to failure. Minimizing the void content of the layup is essential, particularly for a part as highly stressed as the wheel. In a part such as the wheel, any detectable bridging whatsoever is entirely unacceptable.

Making the carbon plies conform to the complex compound curvature of the wheel proved challenging. While prepreg will bend to conform to a relatively tight simple radii, prepreg has a limited ability to stretch and shear to conform to compound curves. For all intents and purposes during the layup prepreg is infinitely stiff in the fiber direction(s). Attempting to stretch prepreg along a fiber direction is futile. Prepreg does however have some degree of 'give' in other directions. For this reason, the ability of prepreg to conform to a given surface is highly dependent on the ply orientation. For the rim of the wheel

for instance, +/-45° woven fabric will conform far easier than 0/90° woven fabric. For unidirectional plies, the difficulty of obtaining good conformability increases as the ply angle diverges from 0°.

The conformity and drapability of a prepreg is dependent on its weave and thickness. Unidirectional tape tends to be minimally conformable. Plain weave (as opposed to twill, harness satin, etc.) is the least conformable of the standard fabric types. Thinner prepregs will of course be more flexible. It is possible and desirable to massage prepreg to stretch it in the out-of-fiber-direction, allowing it to conform compound curvature. There are limits, however, to what can be achieved by doing this.

When a ply will not otherwise conform, splicing will be required. Splicing, while necessary, results in cut fibers and a corresponding localized loss of strength. This effect is more pronounced for unidirectional prepreg than woven prepreg, but it is present in both. For unidirectional prepreg, it is extremely preferable to splice along the fiber direction. This can be done with a razor blade and avoids compromising the fiber strength. It is not always possible to avoid cutting fibers in unidirectional plies, but the number of cut fibers can be minimized by frequent splicing along the fiber direction. Woven fabrics have better drapability, but still will require splices. There is no particular technique for splicing woven fabrics, though it should be noted that the required frequency of splicing will be dependent on ply orientation. In areas with stress concentrations or where laminate thickness is critical, splicing should be avoided if possible.

Once spliced, plies can be forced in place using low friction plastic tools. Particularly in sharp corners, substantial pressure should be applied with the tools. If the surface feels soft or there is the sound of plies unsticking, the ply is bridging in that region. The ply should be aggressively forced into place until there is no evidence of bridging. Debulking will further minimize void content, but it is dangerous to rely on debulking to eliminate bridging in corners; the shear strength of the adhesion between plies generally prevents plies from sliding to fill corners during debulking.

Contamination

Cornell FSAE has historically done a poor job of avoiding contamination during layups. Contaminates - particulate, chemical, or otherwise - will reduce the strength of the completed part. Contaminates reduce interlaminar strength and should be avoided. Aerospace composite manufacturing often is conducted in a low-grade clean room. There are limits to what is possible for the team to do, but basic precautions can be taken. Leaving an entire razor blade in a laminate, for instance, is far from an ideal. Work and cutting should take place on clean surfaces. Airborne particulates and aerosols should be avoided. Prepreg should be isolated from ice and water. Technically, prepreg is supposed to be stored in a sealed bag for 4-6 hours after being removed from a freezer to prevent condensation from forming on the prepreg (Cytac Industrial Materials), but this may not be feasible for the team to do. The part should be covered when not actively worked on. Gloves should be worn when handling the part or prepreg both to protect hands from the resin and to protect the part from contamination.

Prepreg Life

Prepreg has a very limited usable life when out of the freezer. Typically resin systems have a 'tack life' and a 'shop life.' The tack life will be on the order of several days out of the freezer and the shop life on the order of several weeks. For best results, prepreg should be applied within its tack life and cured

before the end of its shop life. This is not always possible. The early plies of the wheel, for instance, were out of the freezer for months, due to the duration of the layup. The team already uses expired prepreg, so rigidly adhering to the manufacture life limits seems excessive, but efforts should be made to limit the time spent by prepreg out of the freezer.

Tack

The tackiness of prepreg is dependent on the resin system, resin content, and age of the prepreg. Expired prepreps such as the team generally uses, will generally be low-tack. This can make the layup process more challenging. It is often necessary to increase the tackiness of a ply to make it adhere to the previous layer. This is typically done with the application of heat using a heat gun. It should be noted that heating prepreg will reduce its usable life. It should also be noted, that heating prepreg to temperatures approaching the cure temperature of the resin system is highly undesirable. Vermont Composites, for instance, limits the temperature of their heat guns to 140° F. Using a heat gun set to 600°, for instance, is not advisable, particularly if done for an extended period. During the wheel layup, an inexpensive hairdryer was purchased and used. The hairdryer proved effective, though it heated a larger area than a heat gun.

Debulking

Debulking is essential for consolidating plies and minimizing void content. The part should be debulked every several layers for up to 30 minutes (Cytec Industrial Materials). The wheel will need to be debulked a many times. Creating a vacuum bag and set of film release that can be reused repeatedly will greatly speed the layup process. Care should be taken to protect the bag from sharp corners on the mold to prevent damage to the bag. Bridging will also damage the bag, so the bag should be extensively pleated to prevent bridging (and apply pressure evenly). For the wheel, this involved shoving most of a very oversized bag into the main cylinder of the wheel. If the bag is properly taken care of, it should last 5-10 uses.



Figure 107: The Rim Prepared for Debulking



Figure 108: Debulking the Rim



Figure 109: Debulking the Combined Mold

Using bag tube, reusable bag seals, and metallic vacuum connectors can entirely eliminate the need to use mastic tape every time the part is debulked. Reusable bag seals are sold by ACP Composites (see **Error! Reference source not found.**). These blue and white extruded plastic pieces lock over a bag producing a reliable removable seal. Unlike when working with mastic tape, it is not necessary to ensure that the bag is not crinkled or pleated in the area where it is sealed. The seals can be pressed into place by hand, but using a rubber mallet to tap the white cylinder in the blue pieces speeds the process. It should be noted that the seals should only be used at room temperature, so the seals cannot be used during the cure cycle. For debulking or wet layups however, these seals are an enormous time saver.

Time

The greatest single challenge when manufacturing the wheel was the time required for the layup. The layup was started during the last week of January and was not completed until the end of March. In total the layup required 2 1/2 months to complete. During the first two weeks, two people worked on the layup virtually around the clock, but the remainder of the layup was largely completed by one person. It is believed that the layup took in excess of 250 hours of work to complete. This vastly exceeded initial projections and in combination with the limited available manpower due to delays in the manufacturing of the ARG14 monocoque prevented the manufacturing of more than one wheel in 2014.

For comparison, it is reported that the ARG11 wheels required only 64 hours each to layup (Rotondo, ARG11 Fall Technical Report 30). The high standards maintained throughout the layup, complex geometry, use of prepreg with poor conformability, large number of plies, inexperience, and difficulty in joining the mold sections combined to make the layup incredibly time intensive. It is expected that were the layup to be repeated and worked on *extremely* efficiently, the time required would be closer to 150

hours (see Table 9). This could be further reduced by mitigating the clearance problems when joining the molds through remaking the center mold.

Table 9: Wheel Layup Time Estimate

Ply Type	Number	Minutes Per Ply*	Total Hours
Inner Rim	20	30	10
Outer Rim & Drop Center	16	60	16
Drop Center (Combined Mold)	16	45	12
Spokes (Center Mold)	9	60	9
Spokes (Combined Mold)	7	45	5.25
Center	12	15	3
Full Rim	2	90	3
Full Rim Adhesive Film	1	480	8
Joint Shim	1	1320	22
Noodle	1	360	6
Debulking	16	60	16
Final Layer Gap Filling	1	120	2
Total Estimated Hours:			110.25
Actual Hours:			>250

* Does not account for time required to cut plies and assumes plies are being applied efficiently.

Laminate Quality

The wheel was free of any notable voids or delamination. The edges of the outer rim were not properly laminated (see Figure 110), but this was expected and beyond the line at which the wheel would be trimmed. Primitive tap testing did not reveal any problems and the wheel resonated admirably.

The surface finish of the cured wheel was lower quality than was hoped. The goal had been to obtain a glossy non-porous surface. The end result was neither. As can be seen in Figure 110, the exposed carbon on the spokes of the wheel had some resin buildup at corners, a somewhat rough surface, and a faint brown tint. As can be seen in Figure 111, the adhesive film was pockmarked with bubbles, entirely defeating its intended purpose. Once the wheel was post-cured, the color of the adhesive film changed and the surface imperfections became even more apparent (see Figure 112). On the post-cured wheel, the region of the wheel that was cured against the Duratec covered portion of the mold was a distinctly different color. Most of the bubbles were also located in the Duratec contacted regions. This has led to speculation that the Duratec out-gassed during the cure cycle, forming bubbles between the mold and wheel as well as giving the surface of the wheel a slightly brown color. Duratec has a heat distortion temperature of 201° F, less than the cure temperature of the wheel (Hawkeye Industries Inc.). It should be noted that this remains speculation; the use of Duratec may not be at fault. However, high temperature testing should be conducted in advance if Duratec is to be used as a mold surface on future oven-cured parts.



Figure 110: Wheel Spokes After Initial Cure



Figure 111: Mold Removal



Figure 112: The Post-Cured and Trimmed Wheel

Mold Durability

One section of the rim bolt flange deflected under load (see Figure 113). This occurred at a single region where the flange was thin and nowhere else. The bolts attaching the flange to the center mold were heavily preloaded, so the flange was subjected to substantial loads. West System 105 resin with 207 hardener has a ASTM D-648 heat deflection temperature of 117° F and a Ultimate Tg of 116° F (West System). It should be noted that these temperatures do *not* represent the temperature at which the epoxy loses all structural strength; they are simply a standardized measures of the softening of epoxy when heated (Niederer). This was known in advance and the West Systems was expected to maintain adequate strength throughout the cure. Everywhere that the mold was the full intended thickness, this was the case. However, the effects of the softening of the epoxy are apparent in the one region that was both unusually thin and highly stressed. It appears that West Systems can be used at temperatures of up to 250° F if the laminate is of adequate thickness and is not excessively loaded. However, obtaining a laminating resin specifically intended for high temperature applications might be advisable in the future.



Figure 113: Damage to the Rim Mold Bolt Flange

The surface of the Duratec primer on the center mold cracked in several places. The cracks appear to be the result of the thermal expansion of the foam center mold. Interestingly, there was no evidence of these cracks on the surface of the wheel. This may mean that the cracks did not form until the cooling portion of the cure cycle. It would not be difficult to repair the cracks, but the cracks suggest that Duratec coated foam molds should not be used at high temperatures.

Post Processing

Once post-cured, a variety of additional post processing steps were necessary. The wheel was trimmed, sanded, sealed, holes were cut, a tire valve was installed, and lug washers were bonded.

Trimming

Manually

Both edges of the wheel needed to be trimmed. Since machining composites is banned in most machine shops and these edges could not be cut with a waterjet, this had to be done manually. Fortunately, the tolerances of these edges are not critical because they simply extend slightly beyond the tire.

The rims were roughly cut using a Dremel and a standard abrasive cutoff wheel. To ensure that the edges were cut evenly, a jig was constructed. The wheel was placed on a stack of partly machined wheel hubs which contacted the center of the wheel on top of a metal plate. This ensured that the wheel was aligned with the metal plate and allowed for it to be rotated. A Dremel was hose-clamped and duct-taped to a magnetic base which was attached to the metal plate. This setup held the Dremel in the

appropriate position. The Dremel was then turned on and the wheel was rotated, trimming off a section of the rim.

Any angular misalignment of the Dremel led to the cut line drifting over time and lateral forces being applied to the cutoff wheel. Frequent adjustments were required to maintain the accuracy of the cut and prevent the cutoff wheels from shattering. Still, lateral forces on the cutoff wheels led to frequent breakage. Cutting through thick carbon heavily loaded the Dremel and led to it becoming worryingly and painfully hot. On several occasions, cutting was paused to allow the Dremel to cool down. Once the first rim was trimmed, the wheel was flipped and the appropriate adjustments were made so the next side could be trimmed as well.

Some of the difficulty could have been alleviated through using the proper tools. Purchasing a tungsten carbide grit cutoff wheel (e.g. McMaster-Car part #1257A52) is a worthwhile investment and is recommended in the future. This would prevent breakage, reducing loading on the tool, and reduce heat buildup that could damage the part. Dremels are not powerful enough to cut thick composites properly and quickly succumb to the abrasive and conductive carbon dust that is generated. A high quality flex shaft tool has more power and locates the motor away from the damaging dust. Such a tool would also be a worthwhile investment and probably would pay for itself over time.



Figure 114: Grinding Down the Inner Rim



Figure 115: Closeup of Grinding Down the Inner Rim

The initial cuts were rough and the wheel was deliberately cut slightly oversize. To finish the edges, the edges were then ground down. For the inner edge, a Dremel was used with a grinding bit (see Figure 114). The Dremel was positioned in a manner similar to that used for the cutting and the edge was ground down until flat.

The outer rim required a more complicated grinding process. In order to remove the poorly laminated region of the edge, it was found to be necessary to grind down the outer rim at an angle to form a conical face. This edge would be over 1/2" thick, so the small Dremel grinding bits were too small. In addition, the large amount of material that needed to be removed would quickly have overheated the Dremel. For these reason a pneumatic grinding tool was used. The tool was again held in position using a magnetic base. Since the grinding wheel was angled, the position of the wheel relative to the grinder would determine the depth of the grinding. Two magnetic bases was installed on either side of the grinder to limit the movement of the wheel while still allowing it to be rotated (see Figure 116). The edge was ground down until a smooth conical face was achieved.



Figure 116: Grinding Down the Outer Rim

Waterjet

The lug holes and center hole were cut via means of a CNC waterjet cutter. A waterjet was used due to its ability to cleanly and precisely cut composite materials without creating thermal damage or delamination. It was originally planned to also operate the waterjet in a 3-dimensional mode to cut vent holes in the conical spokes face. This plan was abandoned because the roughly 1/4" of carbon that was used to shim the wheel sections when the molds were joined reduced the width of the inner side of the spokes face. As a result, it was not clear that the spokes holes could be cut without cutting the highly stressed drop center.

The waterjet cutting was completed with the help of Joe Conway using the LEPP OMAX waterjet cutter. A .STEP model of the wheel was provided and used to generate the necessary control program for

the waterjet. To ensure that the wheel was aligned relative to the cutter, a piece of high density foam was clamped to the table and a hole the diameter of the inner rim was cut. The wheel was then hammered into this hole (see Figure 117) ensuring that it was properly centered. The desired holes were then cut in the wheel. The cuts revealed virtually no voids, indicating an extremely low void content in this region. This was expected since the center face is flat and was thus easy to layup.



Figure 117: The Wheel Prepared for Waterjet Cutting

Sealing and Surface Preparation

The surface of the wheel was heavily sanded. The face of the wheel was sanded to smooth the surface and removed the excess resin that had built up at corners. The interior of the wheel was sanded to remove the 'wrinkles' of resin that resulted from the wrinkling of the film release layer during the cure. An orbital sander was used to flatten the inner center face of the wheel where the wheel would contact the hub. The heavily pockmarked adhesive film around the main cylinder of the wheel was removed since it served no purpose and added weight. A pneumatic tool with a wire brush was used to remove the adhesive film. The wire brush ground through the adhesive film, but minimally impacted the harder

carbon fiber below as intended. The adhesive film along the bead seats was left untouched since it was in better condition and the surface finish of the bead seats was essential. The outside of rim was then sanded by hand to further smooth it. All surfaces of the wheel were sanded using increasingly fine grits of sandpaper until 400 grit was reached.

Once the wheel had been sanded, it was cleaned with compressed air followed by acetone and isopropyl alcohol. Notable remaining voids and imperfections were then filled using West System 105 resin and 207 special clear hardener mixed with colloidal silica. The colloidal silica was added to enhance the strength, durability, and viscosity of the epoxy. The entire wheel was then brushed with an extremely thin coat of unadulterated epoxy using disposable lint free wipes. This was done to seal the wheel and enhance the aesthetics of the wheel. The appearance of the wheel after this step is visible in Figure 118.

As a final sealing step, the wheel was sealed with Microseal-AC. An exhaustive search of the web and literature was unable to identify sealants used to fill porosity in composite parts. Eventually, per the recommendation of Ti International, the company that manufactured the ARG14 carbon intake runners, Microseal sealant was used. Composites sealing is not a listed use of Microseal, but discussions with both Ti International and The Microseal Co. confirmed that it can be used for this purpose. The wheel was again cleaned with acetone and then brushed with several coats of Microseal. As per manufacturer instructions, the wheel was placed in a sealed plastic box as the sealant dried to prevent the sealant from becoming opaque (The Microseal Co.).

Washer Installation

Four 316 stainless steel washers were machined and installed on the wheels. Recommended surface preparation procedures for stainless steel involve degreasing and etching. The recommended processes vary, but involve carcinogens, contact poisons (e.g. hydrofluoric acid), highly corrosive chemicals, and strong acids (Ellsworth Adhesives) (Henkel Corporation Aerospace Group) (Smooth-On, Inc.). The required chemicals were not readily available and could not be used safely, so the etching process was skipped. The risk of skipping this step was judged to be acceptable since the bonds would not be critical to maintaining the structural integrity of the wheel. The washers were abraded using 220 grit sandpaper and cleaned using acetone. The surface of the wheel to which the washers would be bonded was abraded with 100 grit sandpaper to remove all sealants and surface layers and then cleaned with acetone and isopropyl alcohol.

A bead of Hysol E-40HT structural epoxy was applied around the base of each washer using an epoxy gun. The washers were then pressed into their respective holes by means of an arbor press. The washers were machined to give a slight interference fit, so significant force was required to insert the washers. Excess epoxy was then wiped off and the bonds were allowed to cure. The installed washers can be seen in Figure 118.

Tire Stem Installation



Figure 118: The Sealed Wheel with the Tire Valve Installed

In order to pressurize the tire, a tire stem valve needed to be installed. The valve needed to pass through the rim, be accessible for filling, not interfere with the bead seats, and not come in contact with any of the other unsprung components of the car. These requirements dictated that the valve be installed beyond the center face of the wheel that mounts against the hub and before the drop center (see Figure 119). Two holes were drilled, a 0.453" holes through the rim and a 21/32" holes through the spokes face. The larger holes allowed access to the valve from the front of the wheel.

The smaller holes was drilled using a carbide drill bit and the larger holes was drilled using a carbide drill bit followed by a larger high speed drill bit. The carbide bits proved effective and quickly drilled through the carbon in minutes. The high speed steel bit proved ineffective and over an hour was required to laboriously drill through the wheel using the steel bit, despite the presence of a smaller pre-drilled hole. Since the team does not have carbide bits larger than 1/2", it is recommended that in the future, holes larger than 1/2" be avoided or an appropriate carbide bit be obtained.

A Slime TR 418 tubeless tire valve was purchased from Autozone. Attempts were made to purchase a valve stem puller tool locally, but none were available. Making a valve stem pulling tool was

then investigated, but Schrader valves use a rare 0.305-32 thread, so the necessary tap was not available. After trying unsuccessfully trying to force the valve through the hole by hand, locking pliers were used. This slightly marred the surface of the valve, but was successful. It should be noted that due to the thickness of the wheel in this region, the rubber seal at the base of the valve did not extend fully through the wheel. This did not appear to impact the ability of the valve to seal against the hole. Silicone gasket was applied around both sides of the hole as an additional redundant seal. The installed valve can be seen in Figure 118.



Figure 119: Hole Drilled for the Tire Stem Valve Revealing the Extent of Laminate Void Content in this Region

Lessons Learned

The wheel post processing was generally successful, but some steps to improve the process in the future could be made. The tire required to prepare the surface of the wheel could be greatly reduced by taking steps to improve the poor surface finish of the laminate during the layup process. Constructing

more precise cutting and grinding setups would be advantageous during the trimming of the wheel. Purchasing the proper cutoff wheel and ideally a flex shaft tool would also be helpful. More thought should be put into chemically treating the metallic washers prior to bonding. Using titanium, rather than stainless steel, washers would likely greatly simplify the surface treatment process since the proscribed processes for treating titanium are simpler (Ellsworth Adhesives) (Henkel Corporation Aerospace Group) (Smooth-On, Inc.). Investigating whether lighter weight or otherwise improved tire valves are available may be worthwhile.

ARG14 Wheel Testing and Evaluation

A variety of tests were conducted to evaluate the suitability of the wheel for use on the FSAE. The dimensional tolerances of the wheel were checked, cases of interference with other unsprung components were identified, the ability to mount a tire was confirmed, the wheel was leak tested, the wheel was loaded to measure its stiffness, and the wheel was cyclically loaded to verify its capacity to handle all anticipated loads. These tests were necessary both to evaluate the performance characteristics of the wheel and demonstrate its ability to replace the existing alloy wheels on the FSAE car.

CMM Evaluation

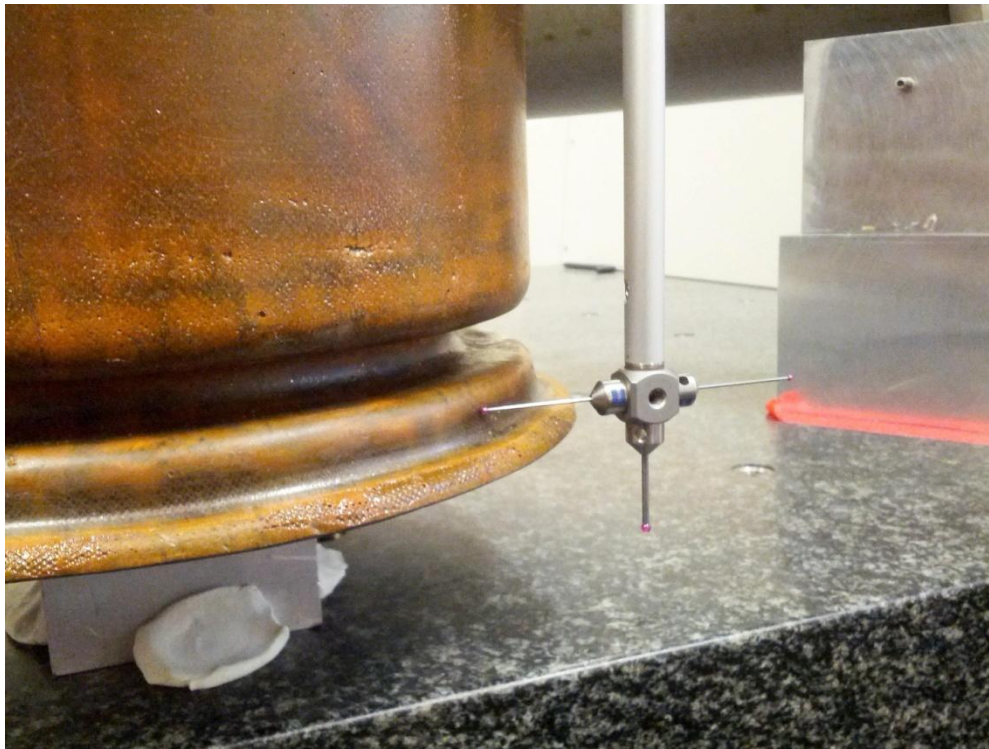


Figure 120: Measuring the Outer Bead Seat Tolerances Using a CMM

The cured wheel was evaluated using a CMM (Coordinate Measuring Machine) with the assistance of Joe Conway. The diameter of the bead seats and the alignment of the bead seats relative to the face of the wheel that mounts against the hub were measured. The measured diameters of the bead seats are shown in Table 10. The complete CMM results for the wheel can be found in Appendix J: Wheel CMM Results.

Table 10: Wheel Bead Seat Dimensions

	TRA Specified Diameter (inch)	CMM Measured Mold Diameter (inch)*	CMM Measured Wheel Diameter (inch)*
Inner Bead Seat	9.968 +/-0.015	9.3968	9.8741
Outer Bead Seat	9.968 +/-0.015	9.9221	9.9080

Note: *The bead seats are conical so the measured diameter is dependent upon the height at which measurements are taken. The height at which the wheel bead seats were measured may not match that of the mold measurements or the point specified by the TRA.*

The measured bead seat diameters are up to 0.0789" less than the range specified by the TRA (Tire and Rim Association). Due to the tight fit and stretchiness of the tires, this is not expected to pose a problem. Were the tires either to not seal or slip under hard braking or acceleration, this could likely be corrected through the application of an additional layer of epoxy to the bead seats.

The measured wheel diameters were slightly less than the measured mold diameters. This difference may simply be the result of the measurements being taken at different heights, but is likely to be at least partly the result of the sanding the bead seats received. It is also possible that this was impacted by the relative thermal expansion of the mold and wheel during the cure cycle or shrinkage of the wheel.

The bead seats were used to define a theoretical cylinder. The central axis of the cylinder was found to vary by 0.0310" from perpendicular relative to the face of the wheel that is bolted against the hub. This dimension represents a measure of the alignment of the beads relative to the hub and thus relative to the wheel's axis of rotation. Given that the center face was aligned relative to the rim simply by bolting the two mold sections together and relying on the radial consistency of the layup to align the molds, this is a shockingly good value. This is evidence that the randomization of splice locations and regions of overlap did result in a consistent layup thickness when averaged over enough plies. The accuracy of the inside of the center face, unlike that of the outside of the center face, was also dependant of the consistency of the layup of the center face. However, since no splicing was present in this region and the region is flat, it is not surprising that the center face would have a consistent thickness. It should be noted that this degree of alignment exceeds the radial run out limits specified by the TRA, but is within the ranges frequently described as acceptable in online automotive forums. Given that vibration and ride comfort is not a substantial concern for an FSAE car, this degree of accuracy is expected to be adequate.

Clearance Verification

The wheel was installed on both the front and rear of the car to verify that it did not come in contact with any fixed unsprung components. In the front of the car, it was found that the center face of the wheel contacted the brake calipers which unexpectedly extended slightly beyond the mounting face of the hub. Placing a roughly 1/8" spacer between the wheel and hub should allow the installation of the wheel at the front of the car. In the back of the car, the wheel contacted the oversized shims between the uprights and clevises. These shims could simply be ground down or possibly just realigned. This would allow the wheel to be installed at the rear of the car.

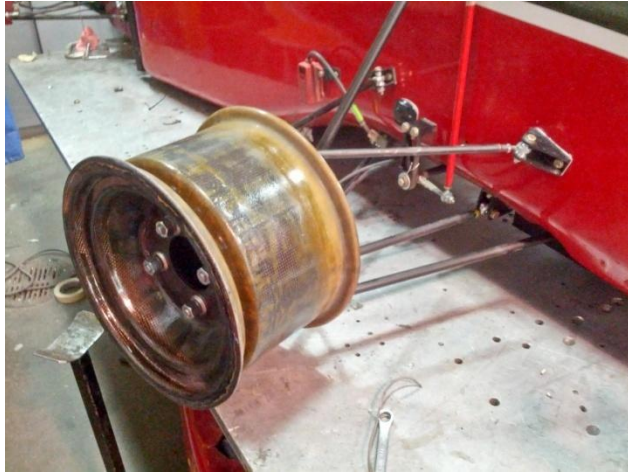


Figure 121: Wheel Installed at the Front of the Car



Figure 122: Internal Component Clearance of the Wheel when Installed at the Front of the Car

Tire Mounting



Figure 123: The Wheel with a Tire Mounted

It was known that the team's typical method of mounting tires using a tire iron had damaged past carbon wheels. For this reason, the wheel was taken to Ithaca Recreational Sports to have the tire mounted professionally. Ithaca Recreational Sports was the only local shop that was found that was familiar with composite wheels, small diameter wheels, and no-touch tire installation. Ithaca Recreational Sports stated that they typically would not be willing to work with composite motorcycle wheels due to the high liability if the surface finish was marred, but they were willing to work with this wheel. They

stated that they have the ability to do a no-touch tire installation, though the arms of the tire changer sometimes come in contact with the wheel. However, when presented with the wheel, they ended up installing the tire by hand. They mentioned using soapy water as lubricant and tire spoons to aid the installation. They stated that they did not need to use the drop center when mounting the tire, but it is not entirely clear that question was communicated correctly. The wheel was not in any way damaged during the installation. The cost of the mounting was \$16. It is suggested that Ithaca Recreational Sports be contacted in the future to learn their method for mounting tires so that the team can replicate it.

Leak Testing

Once the tire was mounted, it was pressurized to 13 PSI (1 PSI greater than is typical for the team). After 48 hours at rest, the tire pressure had dropped by less than 0.5 PSI. The pressure gauge used was not accurate enough to determine the rate of pressure loss with any greater specificity. This rate of pressure loss is more than adequate for the team and is a vast improvement over the ARG11 composite wheels. According to the recollections of Masaki Endo, the ARG11 wheels would unacceptably deflate in under 10 minutes. It appears that the porosity and leakage problems experienced in 2011 are no longer a concern.

Weighing

The wheel was weighed after the trimming of the rim, but before the other post processing steps and found to weigh 4.25 lb. As expected, this was greater than the ANSYS estimate of 3.33 lb. The use of adhesive film, the substantial shimming between the center and rim layups, and the fact that none of the holes (including the planned spokes holes) had been cut all undoubtedly contributed to difference. Unfortunately, the wheel was not weighed again before the tire was installed. After the tire was installed, the wheel was found to weigh roughly 1 lb less than a Kiezer wheel with a tire mounted. If extrapolated to four wheels, this would translate to a weight reduction of 4 lbs of unsprung rotating mass and a roughly 1% reduction in the mass of the entire car. This is approximately equivalent to a 6.5 lb reduction in static mass elsewhere on the car and therefore a 1.5% decrease in car weight (Mason). More accurate measurements will have to wait until the tire is next removed.

Load Testing

Prior to testing the wheel on the car, it is necessary to conduct static load testing to verify the capacity of the wheel to withstand all anticipated loads and quantify the wheel stiffness. To do so, a test procedure and test rig was developed to simulate vehicle loads using an Instron or equivalent load frame. The necessary test rig was manufactured and all other needed preparations were completed, however, at the time of writing, the testing has been indefinitely postponed because the only Instron with the required specifications on Cornell's campus currently requires a new controller before it can be operated again. Attempts were made to use Professor Miller's MTS load frame, however after setting up the testing, it was concluded that the test posed a risk of damage to the machine due to the high torque applied to the machine, so testing was discontinued.

The radial (Z-axis) and lateral (Y-axis) components of the combined worst case load scenario will be applied to a tire mounted on the wheel while the wheel is bolted to a fixed simulated hub. The use of a tire will ensure that the load was realistically distributed through the bead seats of the wheel. The load

will be repeatedly applied to the wheel in order to check for load cycle fatigue damage stemming from manufacturing defects or layup design flaws. This process would be repeated as the rotational position of the wheel is varied in 45° increments to confirm that the wheel is axisymmetric in terms of both load capacity and stiffness.

The combined worst case load scenario will be approximated by pressing the wheel at an angle against a flat plate. To eliminate the need for the plate to be angled relative to the axis of motion of the Instron, the tangential component (X-axis) of the combined load scenario will be omitted. At 300 lbf, this load component represents only a small fraction of the total load, so it was neglected to reduce the complexity of the required test rig. This left a 1260 lbf radial and 616 lbf lateral load component. As shown below, this requires that 1403 lbf of load be applied at an angle 26° from vertical.

$$\text{Load Angle} = \tan^{-1} \left(\frac{\text{lateral load}}{\text{radial load}} \right) = \tan^{-1} \left(\frac{616 \text{ lbf}}{1260 \text{ lbf}} \right) = 26^\circ$$

$$\text{Total Load} = \sqrt{\text{lateral load}^2 + \text{radial load}^2} = \sqrt{(616 \text{ lbf})^2 + (1260 \text{ lbf})^2} = 1403 \text{ lbf}$$

This load will be applied both statically to allow the wheel stiffness to be quantified and cyclically to confirm that the wheel can survive the repeated application of the design loads. The cyclic tested is intended to reveal any manufacturing defects that may be present and lead to low cycle fatigue failure as cracks or delamination propagates. High cycle fatigue testing is not being conducted because doing so may require an unfeasible amount of testing time and would render the wheel unusable. In addition, the information necessary to determine the spectrum of loads the wheel would encounter during use is not available. It should be noted that the design load is a worst case scenario; the loads normally experienced by the wheel during use should be far less. As such, one load cycle is roughly equivalent to one operating anomaly (such as running over a traffic cone), rather than one typical revolution of the wheel.

Test Rig Design

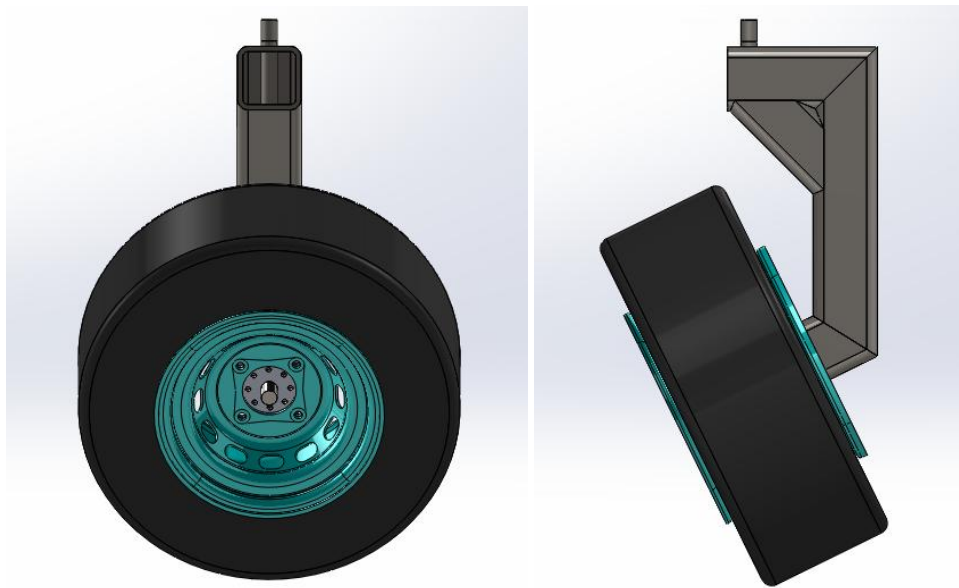


Figure 124: Wheel Load Test Rig CAD Model

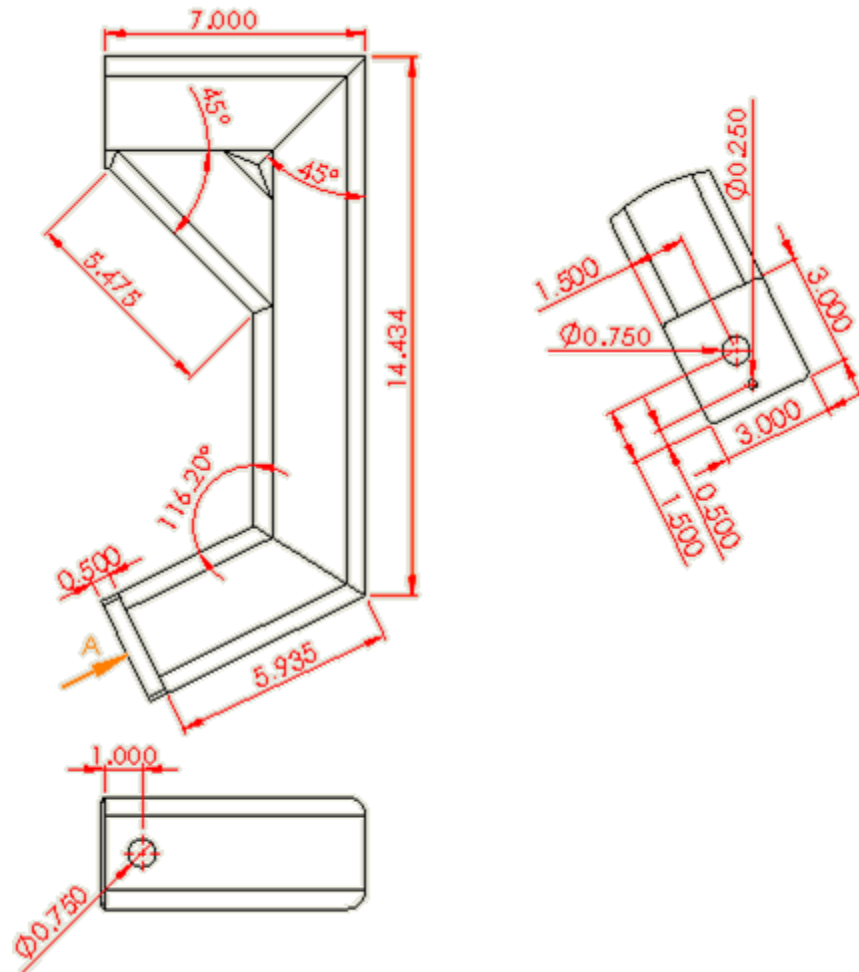


Figure 125: Wheel Load Test Rig Welded Arm

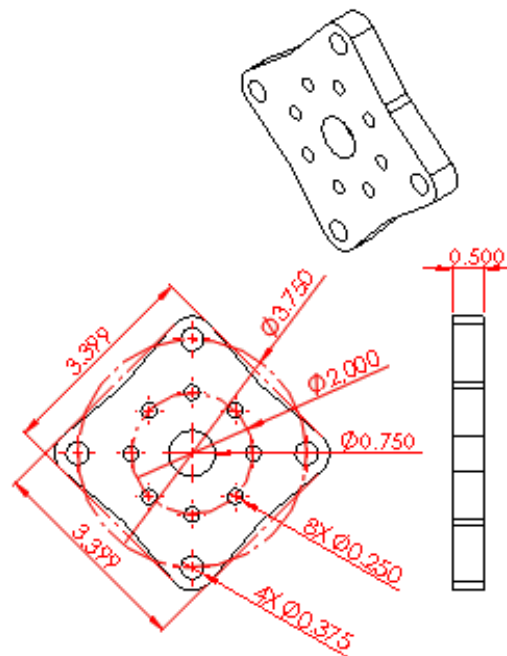


Figure 126: Wheel Load Test Mounting Plate

To allow the necessary load to be applied at the required angle, a test rig assembly was designed and manufactured. The test rig is designed to be attached to the actuator of a Instron or equivalent machine and apply a load to the wheel with an attachment plate and lugs that simulate the hub design on the 2014 Cornell FSAE car. The mounting plate is designed so that it can be rotated and locked into position in increments of 45°. The test rig is dimensioned so that the load is applied to the tire roughly inline with the Instron actuator, to minimize the bending moment acting upon the test machine.

Due to the high loads and bending moments that the test rig will be required to withstand, it was designed as a welded steel structure. The general geometry was specified and then Solidworks Simulation FEM analysis of the structure was conducted with different types of steel tubing. 0.25" thick 3"x3" tubing was found to be the bare minimum that would withstand the applied loads. A length of 1"-14 threaded rod was incorporated into the top of the design to allow it to be screwed into the Instron. A 1/2" thick steel end plate was included on the far end to allow the rotating attachment plate to be attached. A plot of factor of safety for the final design is shown in Figure 127. It can be seen that despite the use of heavy duty components, a factor of safety (FOS) of roughly 1 is maintained. This excludes the area around the end plate hole which was found to have a FOS of 0.28, but is not accurately simulated. Thicker tubing was not used increase the FOS of the part due to concerns about the team's ability to weld it and because the failure of the test rig would not be catastrophic.

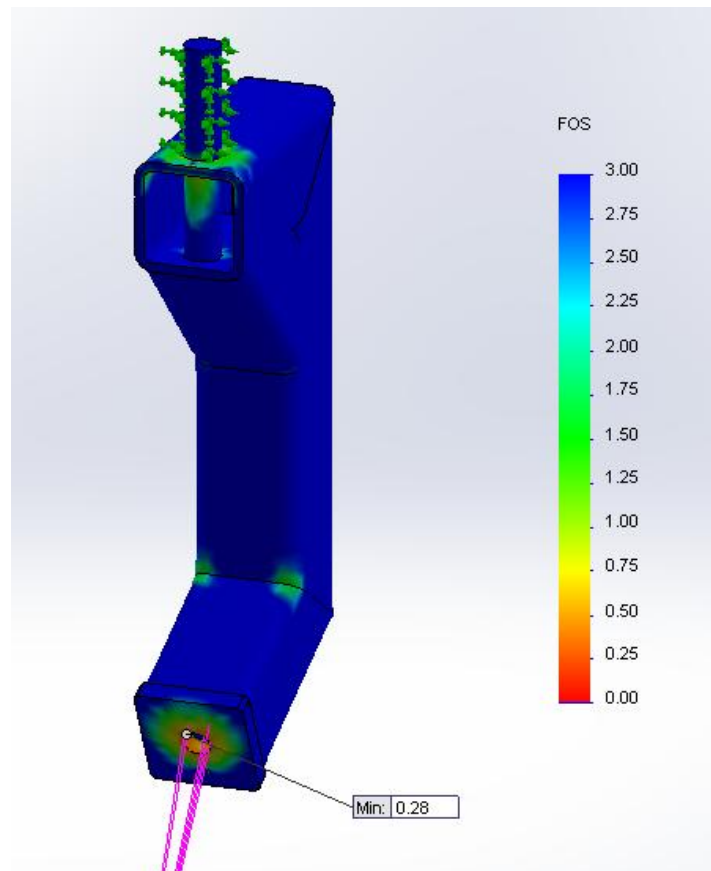


Figure 127: Factor of Safety Plot for Wheel Load Test Rig Welded Arm

A mounting plate was designed to match the mounting face of the 2014 wheel hubs. Its outer perimeter matches that of the hubs. Holes for wheel lugs, a 3/4" bolt for mounting, and a ring of holes for a quick-release pin to allow the rotational angle of the wheel to be locked in different positions were included (see Figure 126).

Test Rig Manufacture



Figure 128: Assembled Wheel Load Test Rig



Figure 129: Wheel Load Test Rig with Wheel Installed

The necessary steel was inexpensively obtained locally from Ben Weitsman & Son Inc. The tubing was cut with a horizontal bandsaw. The cut pieces were then chamfered with a bench grinder to allow for full weld penetration. The tubing and threaded rods were wire brushed to remove surface scale, cleaned, and TIG welded. The welded structure is shown below in Figure 128. The mounting plate and a spacer washer were cut out using the LEPP waterjet cutter. Wheel lugs were installed into the mounting plate holes using an arbor press.

Test Setup and Procedure

To test the wheel, the test rig should first be screwed into the actuator of the Instron and the wheel (with a mounted tire) should then be mounted on the rig. The lug-nuts should be torqued to 35 ft*lb and the tire inflated to 12 PSI. Tire pressure should then be measured to serve as a reference.



Figure 130: Side View of Test Rig Setup on Prof. Miller's MST Load Frame

Initially, the wheel stiffness should be evaluated. To do so, a lever-action dial indicator can be mounted to the steel test rig using a magnetic base and used to measure the deflection of the bottom of the inner edge of the wheel relative to the wheel hub. This is the point predicted by ANSYS to deflect the most. The measured deflection can therefore be compared to the maximum deflection predicted by ANSYS to evaluate the accuracy of the ANSYS simulations. Care should be taken to account for any deflection of the test rig between the wheel and where the indicator is mounted. A second dial indicator may be required to measure test rig deflection. 1500 lbf of load should then be applied to the wheel by pressing it against the bottom plate of the Instron. Deflection should be measured and this process should be

repeated at each of the eight angle increments. Comparing the deflection at each angle should allow for the radial symmetry of the wheel stiffness to be evaluated. During one of these tests, the tire pressure can be measured while the load is being applied to allow for the maximum pressure to be more accurately simulated in ANSYS in the future.

If it is considered desirable to compare the carbon wheel stiffness to the existing alloy wheels, the deflection should also be measured at a lower load, such as 600 lbf, at a representative angle. This same test should then be conducted after mounting an alloy wheel on the test rig. The lower load should be used because the load capacity of the alloy wheels is unknown and the full 1500 lbf of load could potentially damage the alloy wheels.

Once the wheel stiffness had been measured, the dial indicator should be removed and cyclic load testing can be conducted. 1000 cycles of 1500 lbf of load should be applied sinusoidally at the maximum possible frequency (likely on the order of 1 Hz) at each angle increment. After each angle increment had been tested, the wheel would be visually inspected for damage and the tire pressure would be measured and recorded. In particular, the drop center and intersection between the face and rim the of the wheel would be closely inspected. If damage is visible, testing should be discontinued. If leakage occurs, the tire should be re-pressurized and testing continued. After the cyclic loading is complete, the stiffness of the wheel should be measured as done previously to confirm that its stiffness remains unchanged. Any substantial difference in wheel stiffness may indicate the presence of damage which may not be externally visible.

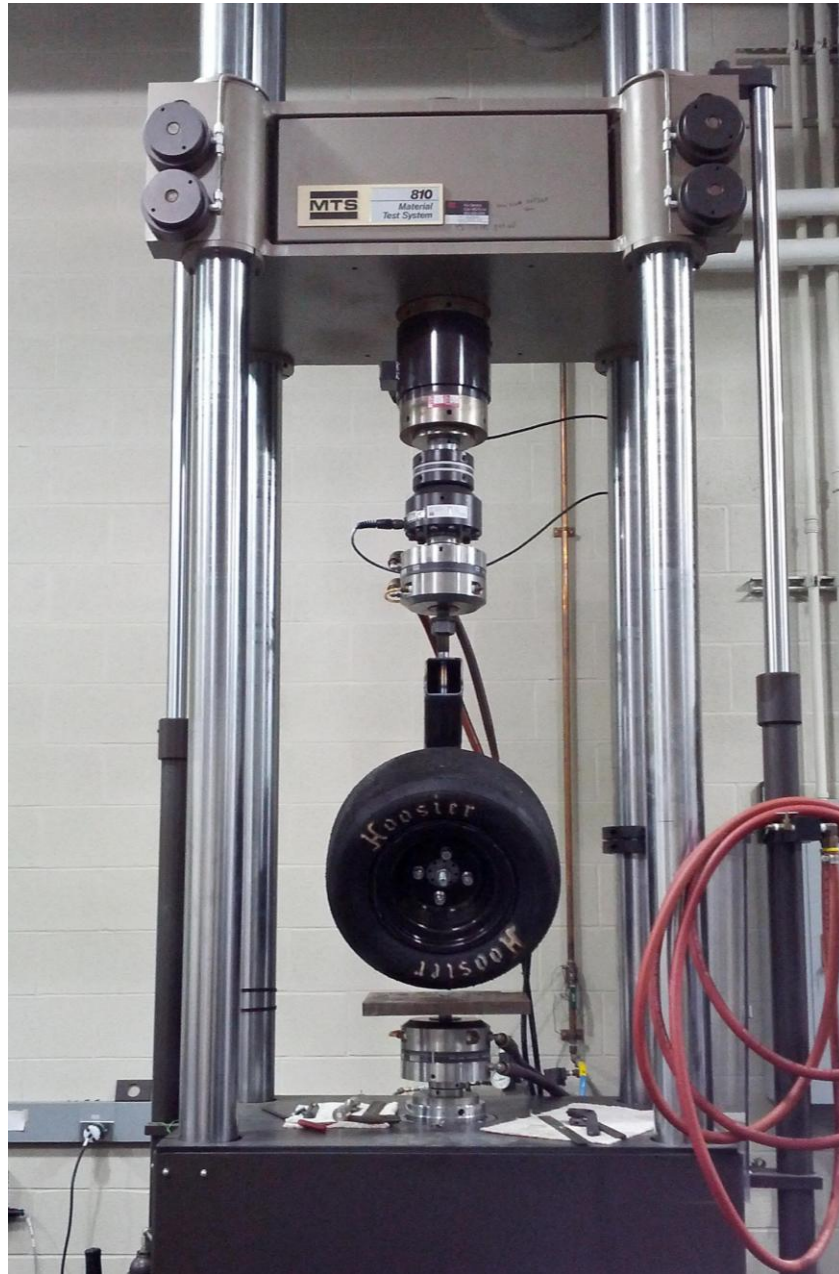


Figure 131: Wheel Load Test Setup on Prof. Miller's MST Load Frame

Conclusion

During the 2013-2014 school year, a single-piece proof of concept composite wheel was designed and manufactured. At the time of writing, it appears, though it has yet to be confirmed, that a fully functional monolithic CFRP FSAE wheel was successfully designed and manufactured. This would represent the first time that Cornell FSAE has successfully produced a composite wheel and would make Cornell one of a handful of FSAE teams which have succeeded in developing single-piece composite wheels.

The wheel weighs 1 lb less than the existing Kiezer alloy wheels. If multiplied across the four wheels of the car, this represents a 4 lb reduction in unsprung rotating mass that would be equivalent to 1.5% reduction in the static mass of the car. The wheel was found to meet all design requirements that could be tested, however testing of the wheel stiffness and load capacity was delayed due to the unavailability of the required Instron machine. Once the Instron again becomes operational, the necessary testing can be conducted. If, as expected, the wheel has greater stiffness than the existing alloy wheels and withstands the applied loads, it will then be ready for the final validating test: testing on the FSAE car.

Lessons Learned

A variety of lessons were learned during the development of the wheel that can be applied to future wheels. The recommendations listed below likely apply to any composite wheel and should be taken into consideration during the development of the team's next generation of CFRP wheels.

Molds

The consistency of the layup thickness was found to be high and required dimensional tolerances of the bead seats were found to be lower than specified by the TRA. Because of this, it may be possible to switch to using male molds and still maintain adequate bead seat tolerances. This is the approach taken by Koenisegg (Koenigsegg) and BST Blackstone (Cathcart). Doing so would simplify efforts to join the two sections of the mold together during the layup process since each mold would be partly laid up, simply bolted together, and then the outside of the molds would be wrapped with additional carbon fiber. Any inconsistency in the thickness of the layup would solely impact the distance between the two bead seats. Fortunately, the required tolerances for this dimension are extremely low since the tire will expand when pressurized until it presses against both walls of the bead seats.

Using aluminum molds, while expensive, would greatly increase the tolerances of the wheel and eliminate many of the manufacturing headaches that were encountered this year. These could potentially be used directly as molds, though thermal expansion analysis of the cure cycle would be necessary before this could be done with confidence. Alternatively, aluminum plugs could be used to produce carbon fiber molds, which would eliminate all thermal expansion concerns. Incorporating indicating and alignment features into the molds would increase tolerances and simplify the manufacturing process.

Producing two sets of molds would allow for two wheels to be manufactured simultaneously. If the required manpower is available, the manufacture of a second set of molds should be considered. Using a single set of aluminum plugs to produce multiple sets of composite molds may provide the most efficient means to doing this.

Manufacturing Time

The single greatest barrier to producing composite wheels is the inordinate amount of time required for the wheel layup. Due to challenging geometry of the wheel, large number of plies, and low allowable void content of the layup, laying up a single wheel took longer than the manufacture of any other component on the car, with the sole exception of the vehicle monocoque. For manufacturing CFRP wheels to be feasible, it is essential that this time be reduced. There are a variety of steps that can be taken to do this.

The existing layup schedule was deliberately made very conservative. Once testing and evaluation of the wheel stiffness and strength is complete, it will likely be possible to significantly reduce the required number of plies composing the different sections of the wheel. This would reduce the manufacturing time as well as further reduce the weight of the wheel.

It may be possible to eliminate the drop center if it is possible to mount the tires without one. If this is in fact possible, it would be highly desirable. The drop center represented the most challenging section to layup and was one of the most highly stressed sections of the wheel. Eliminating it would reduce manufacturing complexity, reduce the number of plies in this region, allow for an increase in wheel stiffness, and reduce wheel weight. Therefore, eliminating the drop center, if possible, would shorten the required manufacturing time and enhance the performance specifications of the wheel.

Using different prepreg could greatly speed the layup process. Neither the M46J and T300 carbon that was used this year were particularly tacky or conformable. This made the layup extremely challenging and time consuming. Omitting the use of unidirectional carbon and obtaining prepreg specifically intended for use on parts with complex geometries would be highly advantageous. This would likely involve using lower modulus and strength prepreg, but the reduction in manufacturing time would probably outweigh these disadvantages. Such prepreg would need to be obtained early in the school year to allow time for adequate material testing. It may also be necessary to obtain compatible adhesive and/or surface film.

Future Development

There are a variety of promising approaches to design, manufacturing techniques, and analysis that could be investigated in future years. None are strictly necessary to produce CFRP wheels, but all could potentially enhance the design and manufacture of the wheel. These are all topics the FSAE team has minimal experience with, so significant research and testing would be required to provide the confidence necessary to implement these items.

Testing and Analysis

Tire Bead Seat Load Testing

Information on the load distribution along the bead seats of the wheel is unavailable. To enhance the team's understanding of the load transfer between the tire and the wheel, the pressure distribution could potentially be measured experimentally. This would allow for the loads to be defined with far greater accuracy in the FEM simulations. It may be possible to determine the load distribution using a thin-film pressure sensor placed between the tire and the rim. The pressure distribution could then be measured as the wheel was loaded with an Instron or potentially as the car is driven.

ANSYS Model Sophistication

The ANSYS model of the wheel that was developed this year was largely based upon the monocoque M.Eng. report tutorial. See: (Wu, Badu and Tia) Extensive discussions with ANSYS's technical support team during the late spring revealed that it is possible to far increase the sophistication of the wheel model. It is possible to precisely define the ply transitions between regions of different thickness. The manner in which plies drape across curved surfaces can also be manipulated. The wheel could be

simulated as a solid, rather than a shell, which due to its thickness and the presence of out-of-plane loads may be advantageous. It is possible to simulate bonded metallic components, lug preloads, and mechanical fastening.

It is not clear that it is necessary to make any changes to the manner in which the wheel is simulated; the model may be accurate enough as is. Still, these are all potential avenues to explore if desired. Tutorials and example files of relevant models have been acquired and can be consulted. ANSYS technical support engineers, in contrast to most consumer technical support, are extraordinarily helpful and knowledgeable. Consulting with them and sending them a current wheel file would likely prove to be highly informative.

Impact and Fatigue Resistance

The impact and fatigue resistance of the wheel was neither analyzed or tested. This could be a topic for future research.

Manufacturing and Molds

Silicone Pressure Intensifier

Significant effort was invested in evaluating the suitability of silicone pressure intensifiers for use. None of the testing proved successful, but the testing was not conducted in a manner that fairly assessed the effectiveness of silicone pressure intensifiers. The team now has RTV silicone on hand and further testing could be conducted to determine if in fact silicone pressure intensifiers could be used to aid the manufacture of the wheel. If the team is to attempt to produce wheels with hollow spokes, this is one of a handful of approaches that would need to be utilized in order to do so.

Bladders

The use of bladders to apply internal pressure while curing could be investigated. Manufacturing bladders would likely prove challenging, but there is no reason to believe that bladders would not work as intended. Bladders are another approach that can be used to manufacture wheels with hollow spokes. Potentially, bladders could be formed from the uncured silicone sheet that was evaluated for use as a vacuum bag this year. It may also be possible to use a hybrid silicone pressure intensifier bladder which would consist of a hollow silicone pressure intensifier block internally pressurized with compressed air.

Core

The use of core could potentially allow the weight of the wheel to be reduced while increasing its stiffness. The team has significant experience using core, but further research would be required in order to evaluate the susceptibility of core to the cyclic loading and impacts that the wheel would be subjected to. If core were to be used, it would likely need to be a high density foam, rather than aluminum or Nomex honeycomb.

Tackifier

Vermont Composites described using a 'tackifier' solution in order to increase the tackiness of prepreg. In essence, this involves dissolving prepreg resin in solvent and then using the resulting mixture to enhance the tackiness of plies. Their instructions for doing so are included in Appendix K: Tackifier

Solution. Making and using such a solution could be tested. The use of tackifier may ease the layup process, but its impact on laminate strength would need to be evaluated.

Appendix A: Wheel Load Distribution Calculations

Despite extensive research, detailed information about the distribution of tire loads was found to be largely unavailable. Information on the distribution of radial loads was found in the following article:

W. Xu, P. O. (2008). Simplified Stress Analysis of a Large-scale Harbor Machine's Wheel. In W. J. Xiu-Tian Yan, *Global Design to Gain a Competitive Edge* (pp. 355-364). Springer.

The provided equations were used to calculate the necessary loading distribution in Mathematica. This equation was then used to define the radial load applied to the wheel in ANSYS. The Mathematica calculations are shown below:

WHEEL LOADING CALCULATIONS:

INPUTS:

Radial Load (lb):

In[167]:= $W = 1260$

Out[167]= 1260

Distribution Angle (degrees):

In[168]:= $\theta 0deg = 60$

Out[168]= 60

Bead Width (inch):

In[169]:= $b = 0.45$

Out[169]= 0.45

Bead Radius (inch):

In[170]:= $rb = 9.75 / 2$

Out[170]= 4.875

CALCULATIONS:

Distribution Angle (Radians):

In[171]:= $\theta_0 = 2 * \text{Pi} * \theta_{0\text{deg}} / 360$

Out[171]= $\frac{\pi}{3}$

Maximum Pressure (PSI):

In[172]:= $P_{\text{max}} = W * \text{Pi} / (8 * b * r_b * \theta_0)$

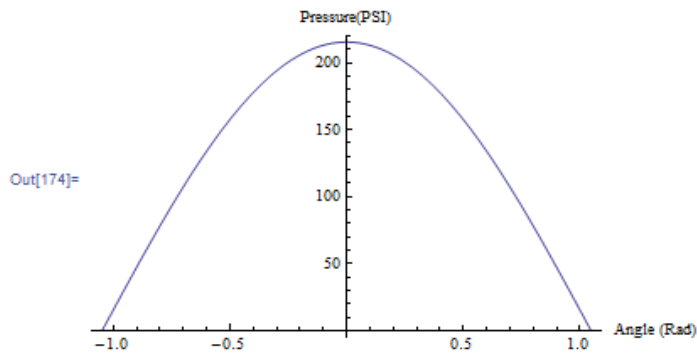
Out[172]= 215.385

Pressure Distribution in Terms of Theta:

In[173]:= $P = P_{\text{max}} * \text{Cos} [(\text{Pi} / 2) * (\theta / \theta_0)]$

Out[173]= $215.385 \text{Cos} \left[\frac{3\theta}{2} \right]$

In[174]:= `Plot[{P}, {θ, -θ0, θ0}, AxesLabel -> {"Angle (Rad)", "Pressure (PSI)"}]`



Pressure Distribution in Terms of X (inch):

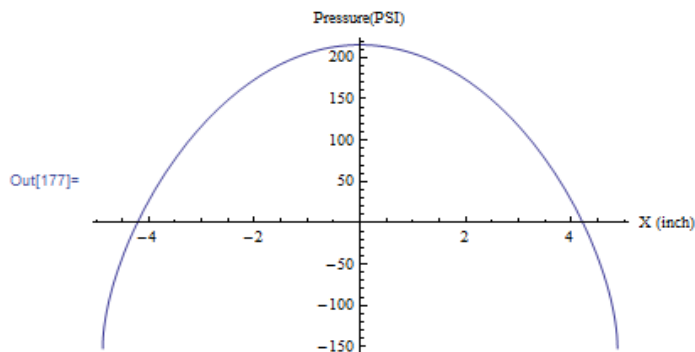
In[175]:= $Y = \text{Sqrt} [r_b^2 - X^2]$

$P / \theta \rightarrow \text{ArcTan} [X / Y]$

Out[175]= $\sqrt{23.7656 - X^2}$

Out[176]= $215.385 \text{Cos} \left[\frac{3}{2} \text{ArcTan} \left[\frac{X}{\sqrt{23.7656 - X^2}} \right] \right]$

In[177]:= `Plot[{P / θ -> ArcTan[X/Y]}, {X, -rb, rb}, AxesLabel -> {"X (inch)", "Pressure (PSI)"}]`



Appendix B: 2010 Wheel Compliance Testing

Spring 2010 Testing

"The following table and figure outline the testing results and procedure.



Figure 132: Wheel Loaded to Test Stiffness

Table 11: Spring 2010 Wheel Deflection Results

Wheel Deflection Results in thousandths of an inch				
load (lbs)	Al with Mg Center		CF with Mg Center	
	deflection on loaded side	deflection at opposite side	deflection on loaded side	deflection at opposite side
0	0	0	0	0
100	-6	4	-4	2
200	-13	8	-7	4
300	-19	12	-10	7
400	-24	17	-14	8
500	-29	22	-17	10

Table 12 - Wheel Deflection Results for Carbon Fiber and Aluminum Wheels

The table shows the results from the stiffness test which results in an average of about a 40% increase in stiffness with the carbon fiber wheels over the aluminum" (Meier 7-8).

Fall 2010 Testing

Procedure

" For the physical compliance test you need to use the large turnbuckle from the suspension bin in order to get up to 500 lbs. A racing scale is used underneath the arm of the wheel testing rig (put a small plate of aluminum between the steel arm and the racing scale in order to protect the scale). You should calculate the force you are actually applying by a sum of moments about the pivot point. I believe the long arm is around 11" and the short one around 6.5" or 5.5". You must measure this and change all of the overall loads you want to apply into the loads you will see on the scale before you start. For example, if you wish to apply 50 lbs you should see $(50 * 6.5) / 11 = 29.5$ lbs on the racing scale. Calculate all of these loads before you begin the test in order to ensure the test goes smoothly. Also make sure to place a dial indicator at the wheel center in order to find the stiffness of just the wheel flanges to compare with the finite element model results." (Rotondo, ARG11 Fall Technical Report 22-23)



Figure 133: Dial indicator on the point of maximum deflection in compliance test and predicted by ANSYS model.

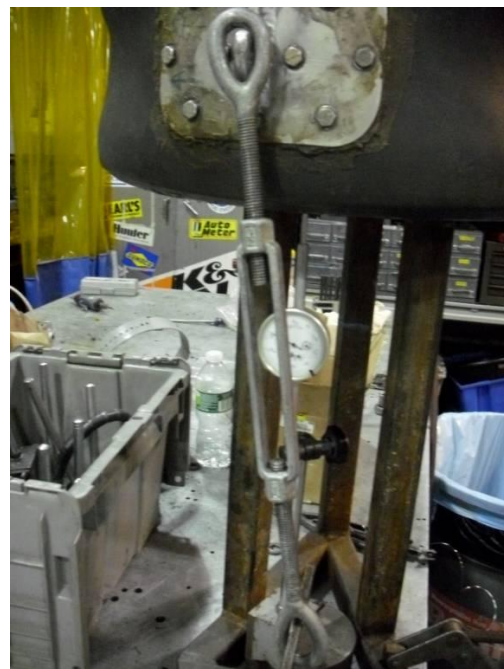


Figure 134: Location of turnbuckle. Note the small angle due to inability to align tire perfectly on wheel. With small angle approximation the effects are negligible.



Figure 135: Location of dial indicators along top of wheel during compliance test.

Results

"The wheel deflection was found to be .018" at the small flange and relatively larger on the large flange (actual wheel deflection measurement was impossible with current deflection testing jig)" (Rotondo, ARG11 Fall Technical Report 21).

Appendix C: Flexural Bending Testing

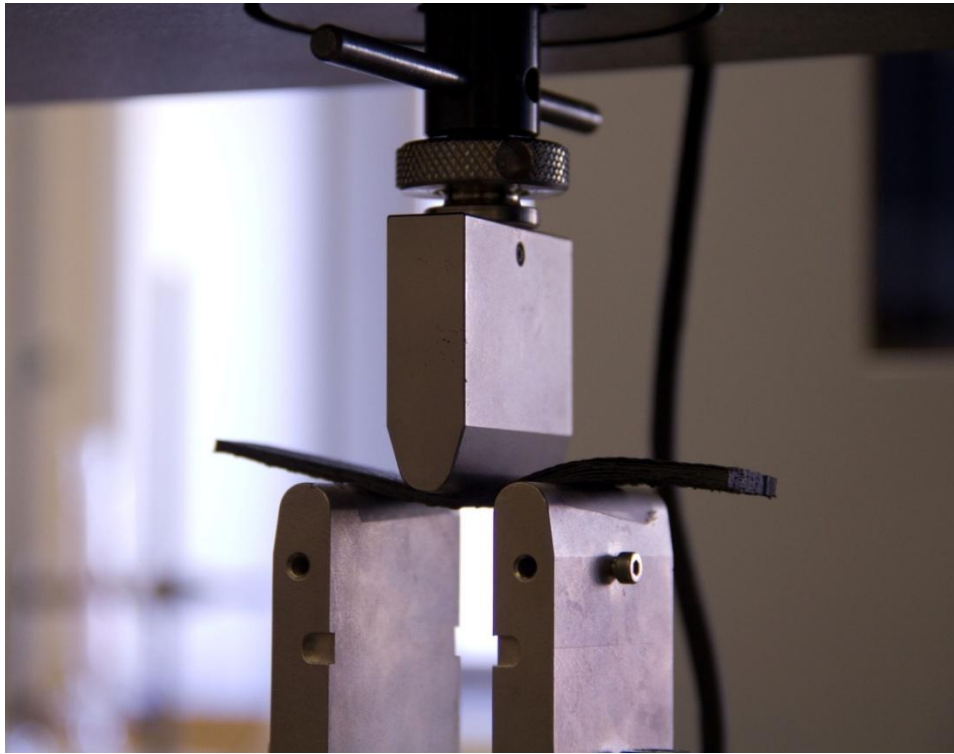


Figure 136: Flexural Bending Test Close-up (After Test)

Table 13: M46J Carbon Flexural Bending Test Results

Material	Plies*	Test #	Width (in)	Thickness (in)	Support Span (in)	Max Load (lbf)	Max Flexural Strength (PSI)
M46 UNI	10	1	1.31	0.08	1.575	511.989	144253.4
M46 UNI	10	2	1.306	0.076	1.575	523.056	163792.5
M46 UNI+Green Surfacing Film	8+2	N/A	1.34	0.0745	1.575	354.320	112536.9
M46 UNI+T300 Weave	8+2	N/A	1.331 5	0.0755	1.575	427.710	133116.4

*All layers 0 degrees

Appendix D: ANSYS Layup Optimization Results

Maximum Wheel Deflection using T800H and T800S Carbon Fiber

- ANSYS "Simple Wheel" results
- Symmetric 12-ply laminate consisting of Layers of T800H (woven) and T800S (UNI) Carbon Fiber used throughout wheel
- Only specially orthotropic layup schedules considered
- Woven fabric used as outside layer for surface finish and damage propagation reasons
- Note that for woven fabric 0=90 and -45=45
- Attempts have been made to minimize the angle between adjacent plies in order to minimize inter laminar stresses

	Attempt 1		Attempt 2		Attempt 3			
(Inch)	Deflection	0.0702	Deflection	0.0723	Deflection	0.071		
(Inch)	Thickness	0.1044	Thickness	0.0924	Thickness	0.0924		
(lb/inch ²)	Density	0.005574	Density	0.005122	Density	0.005122		
	Density*		Density*		Density*			
(lb/inch)	Deflection	3.91E-04	Deflection	3.70E-04	Deflection	3.64E-04		
	Material	Direction	Material	Direction	Material	Direction		
Outer Ply	H	0	H	45	H	45		
	H	45	S	0	S	90		
	H	0	S	0	S	90		
	H	45	S	45	S	45		
	H	0	S	-45	S	-45		
Middle Ply	H	45	S	90	S	0		
	Attempt 4		Attempt 5		Attempt 6		Attempt 7	
	Deflection	0.072	Deflection	0.0716	Deflection	0.0712	Deflection	0.0708
	Thickness	0.0948	Thickness	0.0948	Thickness	0.0948	Thickness	0.0948
	Density	0.005122	Density	0.005213	Density	0.005213	Density	0.005213
	Density*		Density*		Density*		Density*	
	Deflection	3.69E-04	Deflection	3.73E-04	Deflection	3.71E-04	Deflection	3.69E-04
	Material	Direction	Material	Direction	Material	Direction	Material	Direction
	H	0	H	45	H	0	H	0
	S	0	H	45	H	45	S	90
	S	0	S	0	S	0	S	45
	S	45	S	45	S	45	S	-45
	S	-45	S	-45	S	-45	S	0
	S	90	S	90	S	90	H	0

Attempt	8	Attempt	9	Attempt	10	Attempt	11
Deflection	0.0712	Deflection	0.0715	Deflection	0.0708	Deflection	0.0709
Thickness	0.0948	Thickness	0.0948	Thickness	0.0948	Thickness	0.0948
Density	0.005213	Density	0.005213	Density	0.005213	Density	0.005213
Density*		Density*		Density*		Density*	
Deflection	3.71E-04	Deflection	3.73E-04	Deflection	3.69E-04	Deflection	3.70E-04
Material	Direction	Material	Direction	Material	Direction	Material	Direction
H	45	H	0	H	0	H	0
S	90	S	0	S	90	S	90
S	45	S	45	S	90	S	0
S	-45	S	-45	S	45	S	45
S	0	S	90	S	-45	S	-45
H	45	H	0	H	0	H	0
Attempt	12	Attempt	13	Attempt	14	Attempt	15
Deflection	0.0712	Deflection	0.0698	Deflection	0.0698	Deflection	0.0704
Thickness	0.0924	Thickness	0.1044	Thickness	0.1044	Thickness	0.0996
Density	0.005122	Density	0.005574	Density	0.005574	Density	0.005393
Density*		Density*		Density*		Density*	
Deflection	3.65E-04	Deflection	3.89E-04	Deflection	3.89E-04	Deflection	3.80E-04
Material	Direction	Material	Direction	Material	Direction	Material	Direction
H	0	H	0	H	0	H	0
S	90	H	0	H	0	S	90
S	90	H	45	H	0	S	0
S	90	H	45	H	45	H	45
S	45	H	0	H	0	H	0
S	-45	H	45	H	45	H	45
Attempt	16						
Deflection	0.0698						
Thickness	0.1044						
Density	0.005574						
Density*							
Deflection	3.89E-04						
Material	Direction						
H	0						
H	0						
H	0						
H	0						
H	45						
H	45						

Maximum Wheel Deflection using M46J Carbon

- ANSYS "Simple Wheel" results
- Even symmetric laminates consisting of layers of M46J (UNI) carbon fiber
- Only specially orthotropic layup schedules considered
- Minimum allowable Tsia-Wu failure criterion: 0.25

Main Cylinder (Optimized 1st)

	Attempt 1		Attempt 2		Attempt 3			
(Inch)	Deflection	0.0622	Deflection	0.0622	Deflection	0.0622		
(Inch)	Thickness	0.096	Thickness	0.096	Thickness	0.096		
(lb/inch ²)	Density	0.005184	Density	0.005184	Density	0.005184		
	Density*		Density*		Density*			
(lb/inch)	Deflection	3.22E-04	Deflection	3.22E-04	Deflection	3.22E-04		
	Direction		Direction		Direction			
Outer Ply		0		90		0		
		90		0		45		
		45		45		-45		
		-45		-45		90		
		0		0		0		
Middle Ply		90		90		90		
Attempt 4		Attempt 5		Attempt 6		Attempt 7		
Deflection	0.0623	Deflection	0.0622	Deflection	0.0622	Deflection	0.0622	
Thickness	0.096	Thickness	0.096	Thickness	0.096	Thickness	0.096	
Density	0.005184	Density	0.005184	Density	0.005184	Density	0.005184	
Density*		Density*		Density*		Density*		
Deflection	3.23E-04	Deflection	3.22E-04	Deflection	3.22E-04	Deflection	3.22E-04	
	Direction		Direction		Direction		Direction	
	0		0		90		45	
	90		0		90		-45	
	0		45		45		0	
	45		-45		-45		90	
	-45		0		0		0	
	90		90		90		90	

Attempt	8	Attempt	9	Attempt	10
Deflection	0.0626	Deflection	0.0623	Deflection	0.0622
Thickness	0.096	Thickness	0.096	Thickness	0.096
Density	0.005184	Density	0.005184	Density	0.005184
Density*Deflection	3.25E-04	Density*Deflection	3.23E-04	Density* Deflection	3.22E-04
	Direction		Direction		Direction
	45		0		0
	-45		90		90
	0		0		45
	90		90		-45
	45		45		90
	-45		-45		0

Inner Rim (Optimized 2nd)

	Attempt	1	Attempt	2	Attempt	3
(Inch)	Deflection	0.0544	Deflection	0.0536	Deflection	0.0536
(Inch)	Thickness	0.224	Thickness	0.224	Thickness	0.224
(lb/inch ²)	Density	0.012096	Density	0.012096	Density	0.012096
	Density*		Density*		Density*	
(lb/inch)	Deflection	6.58E-04	Deflection	6.48E-04	Deflection	6.48E-04
	Direction		Direction		Direction	
Outer Ply		0		0		0
		90		90		0
		45		0		90
		-45		90		0
		0		0		0
		90		90		90
		45		45		45
		-45		-45		-45
		0		0		0
		90		90		90
		45		45		45
		-45		-45		-45
		0		0		0
Middle Ply		90		90		90

Attempt	4	Attempt	5	Attempt	6	Attempt	7
Deflection	0.0536	Deflection	0.0536	Deflection	0.0552	Deflection	0.0552
Thickness	0.224	Thickness	0.224	Thickness	0.208	Thickness	0.208
Density	0.012096	Density	0.012096	Density	0.011232	Density	0.011232
Density*		Density*		Density*		Density*	
Deflection	6.48E-04	Deflection	6.48E-04	Deflection	6.20E-04	Deflection	6.20E-04
Direction		Direction		Direction		Direction	
	0		0		N/A		N/A
	90		0		0		0
	0		90		90		90
	90		0		0		0
	45		45		45		90
	-45		-45		-45		0
	0		0		0		45
	90		90		90		-45
	0		0		0		0
	90		90		90		90
	45		45		45		45
	-45		-45		-45		-45
	0		0		0		0
	90		90		90		90

Attempt	8	Attempt	9	Attempt	10
Deflection	0.0571	Deflection		Deflection	0.0571
Thickness	0.192	Thickness	0.192	Thickness	0.192
Density	0.010368	Density	0.010368	Density	0.010368
Density*		Density*		Density*	
Deflection	5.92E-04	Deflection	0.00E+00	Deflection	5.92E-04
	Direction		Direction		Direction
	N/A		N/A		N/A
	N/A		N/A		N/A
	0		0		0
	90		0		90
	0		90		45
	90		0		-45
	45		45		0
	-45		-45		90
	0		0		0
	90		90		90
	45		45		45
	-45		-45		-45
	0		0		0
	90		90		90

Outer Rim (Optimized 3rd)

	Attempt 1	Attempt 2	Attempt 3
(Inch)	Deflection 0.04	Deflection 0.04	Deflection 0.04
(Inch)	Thickness 0.32	Thickness 0.32	Thickness 0.32
(lb/inch ²)	Density 0.01728	Density 0.01728	Density 0.01728
	Density*	Density*	Density*
(lb/inch)	Deflection 6.91E-04	Deflection 6.91E-04	Deflection 6.91E-04
	Direction	Direction	Direction
Outer Ply	0	0	0
	90	90	90
	45	45	45
	-45	-45	-45
	0	0	0
	90	90	90
	0	0	0
	90	90	90
	45	0	0
	-45	90	90
	0	45	45
	90	-45	-45
	0	90	0
	90	0	90
	45	90	0
	-45	0	90
	0	45	45
	90	-45	-45
	0	90	0
Middle Ply	90	0	90

Maximum Wheel Deflection using M46J Carbon and T300 Carbon

- ANSYS "Simple Wheel" results
- Even symmetric laminates consisting of layers of M46J (UNI) carbon fiber and T300 plain weave carbon fiber
- T=T300, M= M46J
- Only specially orthotropic layup schedules considered
- Minimum allowable Tsia-Wu failure criterion: 1.66
- Revised layup updated to allow for increased ease of layup by accounting for the inability to M46J to conform to the mold surface along the inner and outer rims
- T300 used as an outer layer for the main cylinder and for all layers of the inner and outer rims

Main Cylinder (Optimized 1st)

	Attempt	1
(Inch)	Deflection	0.0299
(Tsia-Wu)	Max Failure Criteria	0.143
	Material	Direction
Outer Ply	T	45
	M	0
	M	45
	M	90
	M	0
	M	90
Middle Ply	M	-45

Inner Rim (Optimized 2nd)

	Attempt	1	Attempt	2	Attempt	3
(Inch)	Deflection	0.0299	Deflection	0.0303	Deflection	0.299
(Tsia-Wu)	Max Failure Criteria	0.143	Max Failure Criteria	0.142	Max Failure Criteria	0.143
	Material	Direction	Material	Direction	Material	Direction
Outer Ply	T	45	T	45	T	45
	T	0	T	0	T	0
	T	45	T	45	T	0
	T	0	T	0	T	45
	T	0	T	45	T	0
	T	0	T	45	T	0
	T	45	T	45	T	45
	T	0	T	0	T	0
	T	45	T	45	T	45
	T	0	T	0	T	0
Middle Ply	T	45	T	45	T	45

Attempt	4
Deflection	0.296
Max Failure	
Criteria	0.143
Material	Direction
T	45
T	0
T	0
T	45
T	0
T	0
T	45
T	0
T	0
T	45
T	0

Outer Rim (Optimized 3rd)

	Attempt	1	Attempt	2
(Inch)	Deflection	0.296	Deflection	0.0294
(Tsia-Wu)	Max Failure		Max Failure	
	Criteria	0.143	Criteria	0.142
	Material	Direction	Material	Direction
Outer Ply	T	45	T	45
	T	0	T	0
	T	45	T	0
	T	0	T	45
	T	0	T	0
	T	0	T	0
	T	45	T	45
	T	0	T	0
	T	0	T	0
	T	0	T	45
	T	45	T	0
	T	0	T	0
	T	45	T	45
	T	0	T	0
	T	0	T	0
	T	0	T	45
Middle Ply	T	0	T	0

Appendix E: Layup Schedule Development

Wheel Layup Schedule v1

NOTE: (**INCORRECT** Wheel Offset Used)

Section	Number of Plies	Thickness (in)	Laminate Code
Center	42	0.336	$[0_T/45_T/(0/20/40/60/\pm 80/-60/-40/-20)_2/\bar{0}]_s$
Spokes	24	0.192	$[0_T/45_T/0/20/40/\pm 80/-60/-40/-20/\bar{0}]_s$
Inner Rim	24	0.192	$[(0/90/\pm 45/0/90)_2]_s$
Outer Rim	40	0.32	$[0/90/\pm 45/(0/90)_3/\pm 45/(0/90)_2/\pm 45/0/90]_s$
Main Cylinder	12	0.096	$[0/90/\pm 45/0/90]_s$

*T=T300 Weave

**M46J unless otherwise specified

***Surfacing film not included

- **Note: Incorrect wheel offset**
- **Total number of pieces: 94**
- **ANSYS Weight Estimate: 1.61 kg (3.55 lb)**
- **Rough Estimate of Carbon Usage: 60 ft²**

Wheel Layup Schedule v2

Section	Number of Plies	Thickness (in)	Laminate Code
Center	28	0.224	$[0_T/45_T/(0/30/60/90/-60/-30)_2]_s$
Spokes	16	0.128	$[0_T/45_T/0/30/60/90/-60/-30]_s$
Inner Rim	20	0.160	$[0/90/\pm 45/(0/90)_2/\pm 45]_s$
Outer Rim	32	0.256	$[0/90/\pm 45/(0/90)_3/\pm 45/(0/90)_2]_s$
Main Cylinder	12	0.096	$[0/90/\pm 45/0/90]_s$

*T=T300 Weave

**M46J unless otherwise specified

***Surfacing film not included

- **Note: Wheel offset corrected**
- **Total number of pieces: 66**
- **ANSYS Weight Estimate: 1.37 kg (3.02 lb)**
- **Rough Estimate of Carbon Usage: 50 ft²**
- **Max Deflection for Extreme Load Case: 0.0226 in**

Wheel Layup Schedule v3

Section	Number of Plies	Thickness (in)	Laminate Code
Center	28	0.224	$[0_T/45_T/(0/30/60/90/-60/-30)_2]_s$
Spokes	16	0.128	$[0_T/45_T/0/30/60/90/-60/-30]_s$
Inner Rim	20	0.160	$[45/(0/90)_2/-45/0/45/90/-45]_s$
Outer Rim	32	0.256	$[45/(0/90)_2/-45/0/90/0/+45/90/-45/(0/90)_2]_s$
Main Cylinder	12	0.096	$[45/(0/90)_2/-45]_s$

*T=T300 Weave

**M46J unless otherwise specified

***Surfacing film not included

- **Note: Rim optimized for damage tolerances and bearing loads**
- **Total number of pieces: 66**
- **ANSYS Weight Estimate: 1.37 kg (3.02 lb)**
- **Rough Estimate of Carbon Usage: 50 ft²**
- **Max Deflection for Extreme Load Case: 0.0227 in**

Wheel Layup Schedule v4

Total Plies

Section	Number of Plies	Thickness (in)	Laminate Code
Center	28	0.225	$[0_T/45_T/(0/30/60/90/-60/-30)_2]_s$
Spokes	16	0.129	$[0_T/45_T/0/30/60/90/-60/-30]_s$
Inner Rim	22	0.177	$[45_T/0/45/90/0/90/-45/0/45/90/-45]_s$
Outer Rim	34	0.273	$[45_T/0/45/90/0/90/-45/0/90/0/+45/90/-45/(0/90)_2]_s$
Main Cylinder	14	0.113	$[45_T/0/45/90/0/90/-45]_s$

Independent Plies

Center	12		$[0/30/60/90/-60/-30]_s$
Spokes	16		$[0_T/45_T/0/30/60/90/-60/-30]_s$
Inner Rim	8		$[0/45/90/-45]_s$
Outer Rim	20		$[0/90/0/+45/90/-45/(0/90)_2]_s$
Main Cylinder	14		$[45_T/0/45/90/0/90/-45]_s$

*T=T300 Weave

**M46J unless otherwise specified

***Surfacing film not included

- **Note: T300 weave added to rim for damage resistance**

- Total number of pieces: 68
- ANSYS Weight Estimate: 1.49 kg (3.29 lb)
- Rough Estimate of Carbon Usage: 53 ft²
- Max Deflection for Extreme Load Case: 0.0212 in

Wheel Layup Schedule v5

Total Plies

Section	Number of Plies	Thickness (in)	Laminate Code
Center	28	0.225	$[0_T/45_T/(0/30/60/90/-60/-30)_2]_s$
Spokes	16	0.129	$[0_T/45_T/0/30/60/90/-60/-30]_s$
Inner Rim	22	0.187	$[(45_T/0_T/0_T)_3/45_T/0_T]_s$
Outer Rim	34	0.289	$[(45_T/0_T/0_T)_5/45_T/0_T]_s$
Main Cylinder	14	0.113	$[45_T/0/45/90/0/90/-45]_s$

Independent Plies

Center	12		$[0/30/60/90/-60/-30]_s$
Spokes	16		$[0_T/45_T/0/30/60/90/-60/-30]_s$
Inner Rim	20		$[0_T/0_T/(45_T/0_T/0_T)_2/45_T/0_T]_s$
Outer Rim	32		$[0_T/0_T/(45_T/0_T/0_T)_4/45_T/0_T]_s$
Main Cylinder	14		$[45_T/0/45/90/0/90/-45]_s$

*T=T300 Weave

**M46J unless otherwise specified

***Surfacing film not included

- Note: Rims entirely composed of T300 to increase ease of manufacture – using M46J for rims proved unfeasible during first layup
- Total number of pieces: 94
- ANSYS Weight Estimate: 1.51 kg (3.33 lb)
- Rough Estimate of Carbon Usage: 53 ft²
- Max Deflection for Extreme Load Case: 0.0294 in

Appendix F: Final Layup Checklist

Ply #	1	2	3	4	5	6	7	8	9	10	11	12	13	14	15	16	17	18	19	20
Center	0	30	60	90	-60	-30	-30	-60	90	60	30	0								
Spokes	OT	45T	0	30	60	90	-60	-30	-30	-60	90	60	30	0	45T	OT				
Inner Rim	OT	OT	45T	OT	OT	45T	OT	OT	45T	OT	OT	45T	OT	OT	45T	OT	OT	45T	OT	OT
Outer Rim + Drop Center	OT	OT	45T	OT	OT	45T	OT	OT	45T	OT	OT	45T	OT	OT	45T	OT	OT	45T	OT	OT
Main Cylinder	0	45	90	0	90	-45	-45	90	0	90	45	0								
Entire Rim	AF	45T	45T																	

Step #	1	2	3	4	5	6	7	8	9	10	11	12	13	14	15	16	17	18	19	20
Center									0	30	60	90	-60	-30	-30	-60	90	60	30	0
Spokes	OT	45T	0	30	60	90	-60	-30												
Inner Rim				OT	OT			45T	OT			OT	45T			OT	OT			45T
Outer Rim + Drop Center				OT	OT	45T		OT	OT	45T		OT	OT	45T		OT	OT	45T		OT
Main Cylinder			0				45				90				0					90
Entire Rim	AF	45T																		

21	22	23	24	25	26	27	28	29	30	31	32
45T	OT	OT	45T	OT	OT	45T	OT	OT	45T	OT	OT

21	22	23	24	25	26	27	28	29	30	31	32	33	34	35	36	37	38	39	40	41	42	43	44	45	
-30																									
OT									OT	45T				OT	OT				45T	OT				OT	
OT	45T		OT						45T	OT	OT			45T	OT	OT			45T	OT	OT			45T	
		-45															0						90		

46	47	48	49	50	51	52	53	54	55
			45T						OT
45T				OT	OT				
OT	OT			45T	OT	OT			
		45				0			
								45T	

KEY:
<u> </u> = Symmetric Mirror
AF = Adhesive Film
T = T300 Weave
Else, M46J UNI

Notes:

- Transition areas must be tapered with angle of >10 degrees. To achieve adequate angle, stagger the edges of each ply >0.05"
- Inner Rim plies must extend at least 1/2" beyond bead seat and overlap the Main Cylinder plies
- Outer Rim + Drop Center plies must extend at least 1/2" beyond drop center and overlap the Main Cylinder plies
- Spoke plies applied after the molds are bolted will not extend onto the wheel rim Outer Rim + Drop Center and Entire Rim plies applied after the molds are bolted will extend at least 1" onto wheel center

Appendix G: Ryan Kennett Emails

Ryan,

I have a few technical composite related questions that I have been unable to satisfactorily answer and I was hoping you might know the answer to some of them.

Mechanical Properties of Woven vs. Unidirectional Fabric

I understand that unidirectional fabric should have greater in-plane strength and stiffness due to the absence of fiber crimp. I also understand that unidirectional fabrics are more susceptible to damage propagation, fatigue, and edge effects because the fibers are not interlocking. I have been unable to determine, in practice, however, how significant these differences are. This would be relevant for the side faces of the wheels which have a large number of brake cooling holes (lots of edges) and the holes for the wheel lugs (highly concentrated cyclic loading). Do you have any sense how important it would be to use woven fabric in these areas?

Sealing

I have been told that the past CU FSAE carbon rims suffered from porosity issues. I am not entirely convinced that this was or will be a problem, but, in the event that it is, we would need to seal the wheels. I can think of a variety of different sealants that may work, but I have been unable to find any product, with the exception of gas tank sealant, that is actually intended to seal porous composite parts. Are you aware of any sealant that is used to seal pressurized composite components or is this simply never a problem to begin with?

Mechanical Joining

In industry, how are mechanical composite joints evaluated? I have seen some rough guides to calculate the number and type of bolts required and I have seen complex FEM simulations of individual bolts with pre-tension loads applied. The rough guides are inadequate in this case because the number and type of bolts (the wheel lugs) are already specified and not what would typically be recommended. The FEM simulations, in contrast, seem absurdly involved for something so commonly utilized. Also the FEM simulations typically focus on bearing loading, rather than frictional loading, which in this case, I believe would be the preferred method of transferring the required loads. Up to now, I have been simulating the wheel lugs simply by fixing the areas underneath the bolt heads, which is, of course, a very rough approximation.

Thanks for your help! I hope you are having an excellent holiday season.

Sincerely,
Nathaniel Gilbert

As far as weave vs. uni, I wouldn't worry to much. You guys have a bunch of m46j so I'd lay up the wheel with that. I'd put a face sheet of weave on the outside too look cool and add some durability. The problem with weave is that once you nick and edge and start pulling off a face sheet, you'll pull off a whole chunk. So to save you from trying (and most likely failing) to keep the clowns on the team from fucking them up, I'd take the negligible weight hit and put a ply of weave on the inside and outside. If you are in the situation where you have two different resin systems and are worrying about mixing (which I think you may be) I'd call the supplier and see what they say. They may give you an immediate answer and save you some time. If they don't know which is possible, just do a quick test panel and see what happens. worst case scenario, you lay up with all uni... which is a little scary but I think you'd be fine.

Seal will almost certainly be a problem if you repeat what we did. I guess you're planning on using a pressure intensifier which in theory could help but I'm not convinced of that either. Adding pressure will decrease porosity but by how much.... on a really shitty lay up (no pressure) maybe 80% (all figures made up) but on a vacuum bag cure maybe only 5%. I really don't know. You could test it though. Just make some squares using the same carbon and see if you can pull air through them. My guess is that the resin content in your carbon is low enough to cause you problems so you should investigate a sealer or do some testing with putting a bunch of surfacing film on one side of your layup. As far as products, I don't really know any. I'll ask around work, but my guess is you could use a latex paint or something like that as well. The gas tank sealer does sound nice because it probably won't get angry with brake fluid and other stupid shit the team will inevitably pour on it.

As far as joints, you just need to do a test. No one in industry trusts shit like this using FEA (at least without a huge safety factor). I'd just figure out the worst case load (well at least the worst case you can feasibly replicate on the instron) intuitively and try to replicate it on the instron. Definitely think about it first and try to predict the failure mode with an FEA model or some hand calcs. don't just throw it on and pull it. Fixing the bolt holes is definitely an approximation and is unconservative, but it isn't so unconservative that it will give you the wrong failure mode (well at least it doesn't seem like it will....). So just put make a model and apply a moment to the thing (you won't be able to test the torsional case easily so I'd just start with you hard corner case). then make a rig that will apply the same moment on the instron. Then just figure out a scaling factor to look at your torsion case. I'd assume if you're designing this thing to be stiffer than a kiezer, strength will not be an issue, but you should definitely do some sketchy instron work for a sanity check and so the judges don't shit on you.

Sorry if this email isn't clear. I am notorious for shitty grammar and sentences that don't make sense so feel free to tell me my shit doesn't make sense. Also sorry if I assumed you are less intelligent than you are. I think I aired on the side simple in writing this email because I've just never talked to you and don't know what's obvious and what's not.




But hope this helps a little maybe. Let me know if you'd like more on something and I'll try to elaborate or just find someone smarter than I.

-kennett

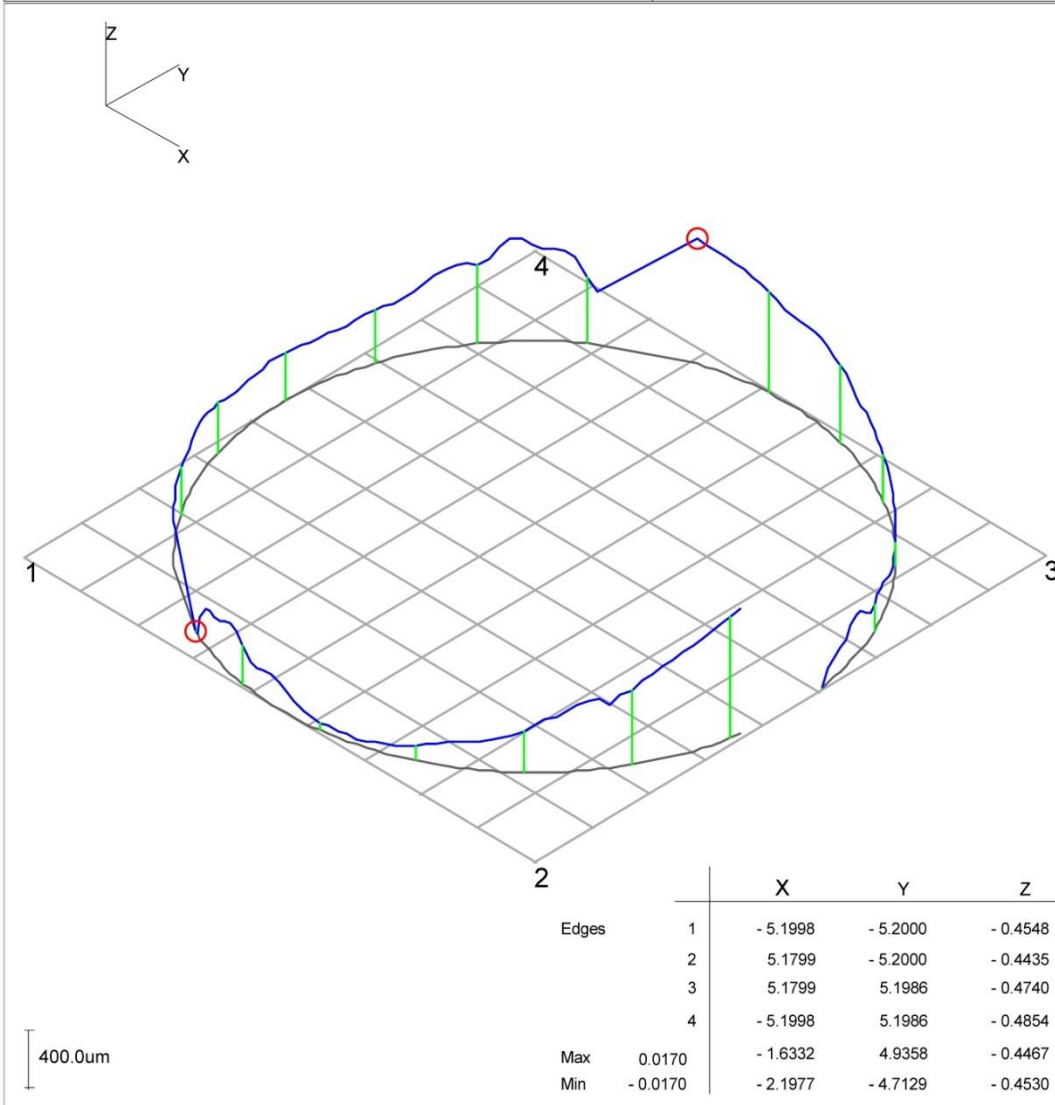
Appendix H: Wheel Rim Mold CMM Results

Results were measured using the LEPP ZEISS CMM (Coordinate Measuring Machine). The rim mold was measured during initial assembly. These results reflect the dimensions after the final adjustment of the rim mold section alignment.

Outer Rim Bead Surface

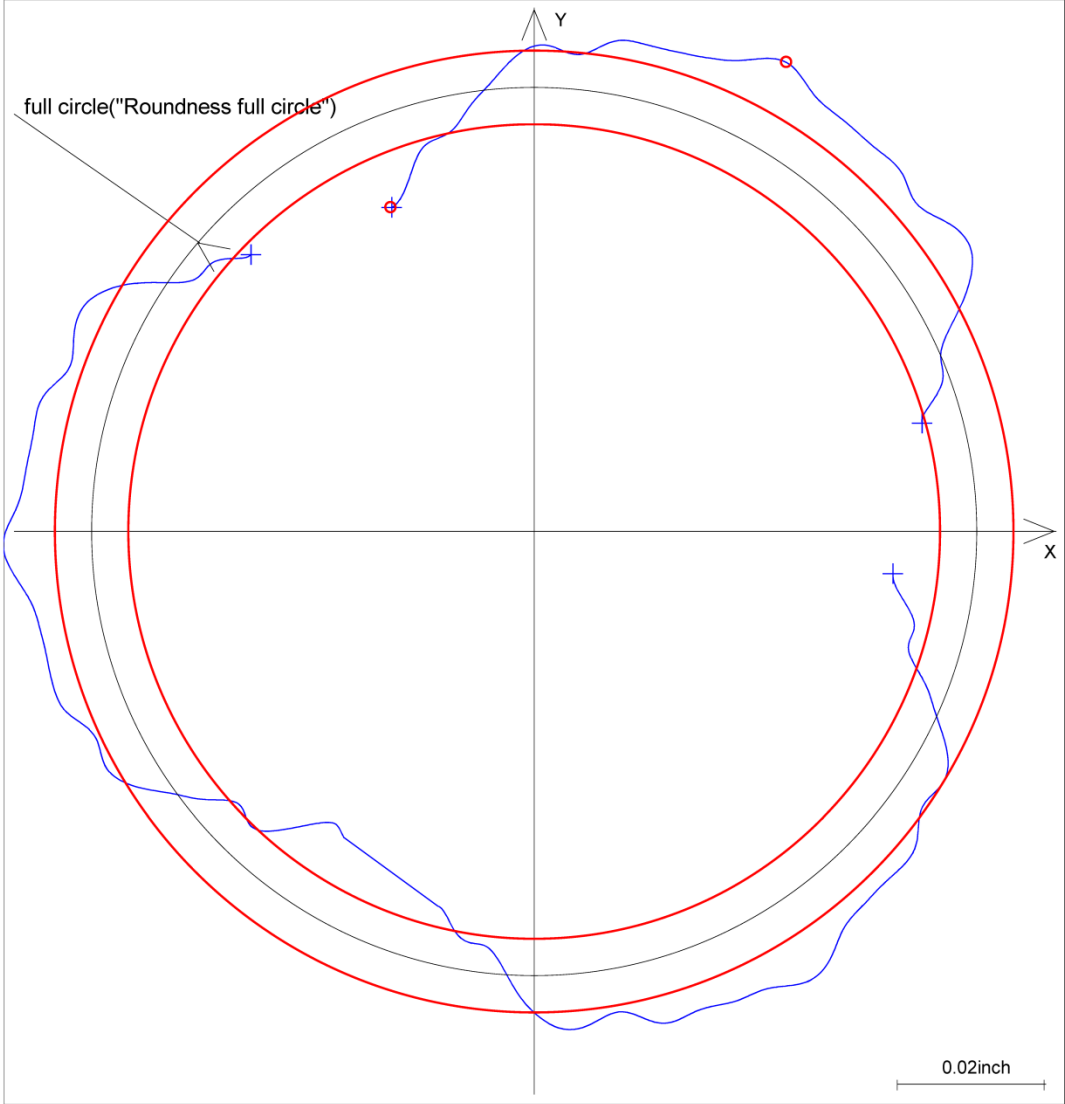
ZEISS Calypso							
Measurement Plan FSAE Wheel Mold		Date January 20, 2014					
Drawing No.		Time 4:16:54 pm				Order * order *	
Operator Master		CMM C32Bit				Incremental Part Number 10	
	Actual	Nominal	Upper Tol.	Lower Tol.	Deviation		
	Overall Result						
		1					
		0					
		1					
		0					
		0					
		0					
		0					
		0					
		0					
		0					
	Diameter full circle						
	9.9221	9.8230	0.0100	-0.0100	0.0891		
					0.0991		

ZEISS Calypso 5.4.16		Carl Zeiss		Date January 20, 2014
Part Number 9		CMM ACCURA	Drawing No.	Order * order *
Measurement Plan FSAE Wheel Mold			Department: Operator Signature: Master	
			Flatness1	



						Magnification		25	
No	Identifier	Actual	Tol.	Number of	Speed	Stylus Radii	F.Typ	L-C	UPR
1	Flatness1	0.0340	0.0000	182	1	0.0591			

ZEISS Calypso 5.4.16		Carl Zeiss		Date January 20, 2014
Part Number 9		CMM ACCURA	Drawing No.	Order * order *
Measurement Plan FSAE Wheel Mold			Department: Operator Signature: Master	
			Roundness full circle	



Magnification 50									
No	Identifier	Actual	Tol.	Number of	Speed	Stylus Radi	F.Type	L-C	UPR
1	Roundness full circle	0.0243	0.0100	1238	1	0.0591	Spline		50

Inner Rim Bead Surface

ZEISS Calypso



Measurement Plan
FSAE Wheel Mold BAcK Side

Date
January 20, 2014

Drawing No.
* drawingno *


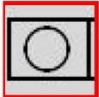

Time
4:30:23 pm

Order
* order *

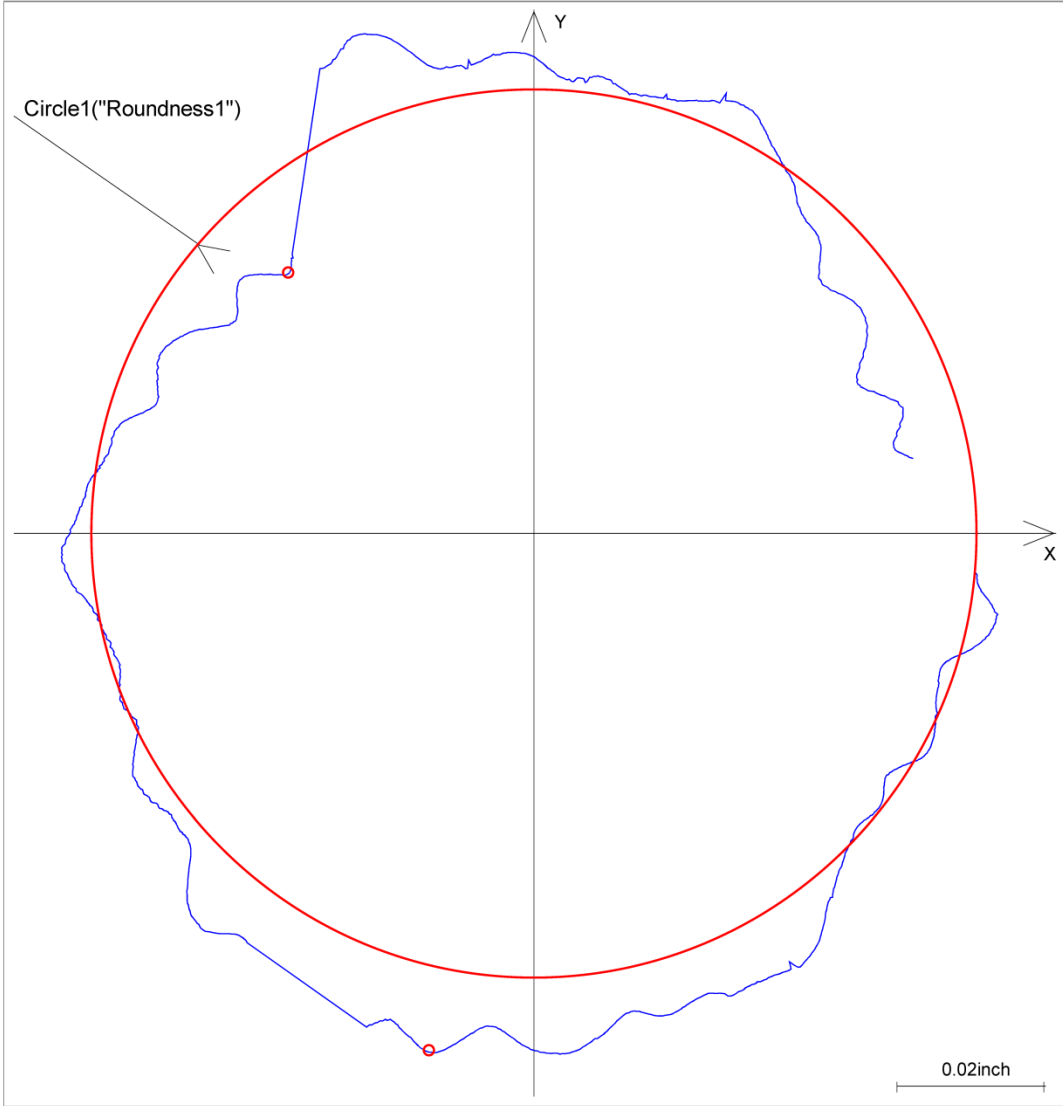
Operator
Master

CMM
C32Bit

Incremental Part Number
2

	Actual	Nominal	Upper Tol.	Lower Tol.	Deviation
 Overall Result					
All Characteristics:		2			
...in Tolerance:					1
...Out of tolerance:					1
...Over Warning Limit:					0
...Not Calculated:					0
Total Coord. systems:					0
...Not Calculated:					0
Total Text elements:					0
 Roundness1					0.0233
	0.0233	0.0000	0.0000		0.0233
 Diameter Circle1					----
	9.9124	9.9189	0.0079	-0.0079	-0.0065

ZEISS	Calypso 5.4.16	Carl Zeiss		Date January 20, 2014
				Order * order *
Part Number 1	CMM ACCURA	Drawing No. * drawingno *	Department: Operator Signature:	Master
Measurement Plan FSAE Wheel Mold BAck Side			Roundness1	



Magnification 50

No	Identifier	Actual	Tol.	Number of	Speed	Stylus Radii	F.Type	L-C	UPR
1	Roundness1	0.0233	0.0000	1235	1	0.0591			

Appendix I: Noodle Instructions

An extensive internet and literature search found only passing references to materials intended to fill the deltoid gaps (such as that which existed at the joint between the rim and wheel center). These were described as adhesive radius filler, gusset filler, deltoid noodle, radius noodle, radius filler, and/or braided fillet. A discussion the use and manufacture of deltoid noodle with engineers and technicians at Boeing's Philadelphia facility has been included below.

<John.H.Harris6@boeing.com> wrote:

That third item you need is called a noodle, we use them here in the factory on quite a few parts. I don't know if they have an expiration date or not (which determines whether or not we'll be able to find some for you), but I'm sure Karl will know. He may also be able to give a recommendation on how to use them properly.

Thanks

John

<karl.r.bernetich@boeing.com> wrote:

Re: noodle filler

One size does not fit all ... we shape each piece for the application. (It's a bad area for a defect on an aerospace part.) The cross sectional area of the noodle ... should equal ... the ply thickness * the ply width. We generally overstuff the noodle by 10% to 20% (A little too much is OK. Too little material is bad.) We use parent material (uni tape) and compact it to the required shape. If it's formed straight and bend it, it will kink and cause us problems. The boat industry typically fills that area with paste adhesive (or resin and microballoons) and sweeps the putty with a tongue depressor to form the radius and then wet tabs on close out plies. Some companies use film adhesive rolled up to fill that area. Too big an area and the film adhesive may shrink and form cracks. You could probably use dry tow and wet it out with (EA9396 or similar) and stuff that into the gap.

Karl,

From what you described, I gather that the first process you mentioned involves cutting uni fabric/tape along the fiber direction into thin strips/bundles of fibers and then individually packing these strips into the desired space. Does that generally describe the process? I assume that the "the ply thickness * the ply width" that you mentioned refers to the quantity uni material used to make the noodle. Is that correct? Are there any particular techniques for packing the fibers or steps which may not be obvious? Would it be advantageous to additionally pack

some adhesive film into the area to locally increase resin content? Is there any disadvantage of using this method or shortfalls we should be aware of?

Thank you for all of your help. I greatly appreciate it.

Sincerely,
Nathaniel Gilbert

<karl.r.bernetich@boeing.com> wrote:

From what you described, I gather that the first process you mentioned involves cutting uni fabric/tape along the fiber direction into thin strips/bundles of fibers and then individually packing these strips into the desired space. Does that generally describe the process? If it's uni tape, it will naturally fold, roll, accordion, etc.

Or we use pre slit uni prepreg in 1/8" strands. Would not suggest graphite fabric for the application. That will need to be slit into 1/8" to 1/4" in widths and the cross thread will inhibit good forming. If fabric is the only thing you have, maybe +/-45 would be better. If you have glass prepreg, that's usually a much finer weave (7781, 120 glass) and will work in 0/90 or +/-45 thin strips.

I assume that the "the ply thickness * the ply width" that you mentioned refers to the quantity uni material used to make the noodle. Is that correct?

Yes ... cross sectional area of 1 uni ply (ply thickness * width) = cross sectional area of the noodle.

Are there any particular techniques for packing the fibers or steps which may not be obvious?

No ... we pull thru a plastic die with the shape cut out. A lot of folks pack into a trough and compress.

Only technique is attention to detail.

Would it be advantageous to additionally pack some adhesive film into the area to locally increase resin content?

Don't know if it'd be advantageous or not ... we don't.

Is there any disadvantage of using this method or shortfalls we should be aware of ?

What method ? extra adhesive ??? Narrow window between 100% and a little extra. Too – too much is not good either ... distorts plies in final part.

Karl,

We are making the part using M46J uni carbon. That splits easily into 0 degree strips. It sounds like we should split some of the M46J into 1/8" wide strips and then pack those strips into the corner of the part during the layup to create a radius (with 0 degrees orientated parallel to the corner being filled). Does that sound reasonable? I am just trying to confirm that I am understanding your description correctly.

Thank you for all of your help.

Sincerely,
Nathaniel Gilbert





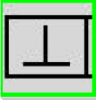
<karl.r.bernetich@boeing.com> wrote:

For a straight run, and only a couple of noodles, I would fold/roll into a tight circle (but that will kink on you as you bend into a hoop). You probably do need to cut into 1/8" strips to go around the hoop.

It's a very hard area to impart final cure pressure on when everything is "live prepreg" and co-cured together. So for that complex of a shape, I would form and compact the noodle, to final shape, separately. (but again, our detects may be more critical.)

I think you will have a hard time pack(ing) the correct amount of those strips into the corner of the part during the layup. It is very hard to remove a defect (that has been hand laid up in the noodle) during processing.

Appendix J: Wheel CMM Results

		ZEISS Calypso				
Measurement Plan FSAE Carbon Wheel	Date April 19, 2014					
Drawing No.	Time 3:03:01 pm	Order * order *				
Operator Master	CMM C32Bit	Incremental Part Number 1				
		Actual	Nominal	Upper Tol.	Lower Tol.	Deviation
	Overall Result					
	All Characteristics:	3				
	...in Tolerance:	1				
	...Out of tolerance:	2				
	...Over Warning Limit:	0				
	...Not Calculated:	0				
	Total Coord. systems:	0				
	...Not Calculated:	0				
	Total Text elements:	0				
	Diameter Circle1					-0.0020
	9.9080	9.9200	0.0100	-0.0100		-0.0120
	Diameter Circle2					-0.0359
	9.8741	9.9200	0.0100	-0.0100		-0.0459
	Perpendicularity1					---
	0.0310	0.0000	0.0500			0.0310

Appendix K: Tackifier Solution

Vermont Composites mentioned that they use a "tackifier" solution to enhance the tackiness of prepreg and make laying up easier. We did not attempt to use tackifier this year, but it may be worth investigating further. Instructions for making and using tackifier are included below.

Subject: Re: FW: FW: Question about our monocoque cure plan

Hi Nick, Traig,

Thanks again for your help these past weeks! Nick, I believe you mentioned to Jesse a product like acetone that you could use to somehow increase the tack of prepreg that is losing it's tack, could you remind us what that method was?

Thanks,

Alex Hsia

<Nicholas.Pratt@kaman.com> wrote:

Alex-

I have pasted in the text from one of our procedure on making and using tackifier solution. Try to make the tackifier from your prepreg, if it does not dissolve fully it will not be acceptable. If that is the case, you can try using a 350° curing epoxy resin. It is best to apply tackifier in trim areas or to the tool (i.e. not between plies), if you do apply it between layers I do not think you will have any problems, that guideline is more for structures where you would not have qualification test data to say that you are not affecting the strength by putting tackifier between layers.

You could also try adding heat to get the material more tacky. We use heatguns that are calibrated and have a digital temperature readout to limit the temperature to about 140°F. If you do not have a calibrated heat gun, just keep it on low and keep it moving. The idea is to warm the resin a little without curing it.

Text of Resin Tackifier and Application Procedure:

1.0 Overview

1.1 Purpose

This procedure describes the general use and preparation of tackifiers during lay up of composite parts.

1.2 Scope

This procedure details how to manufacture and apply a resin tackifier to aid in the layup of composite parts. Tackifiers are typically applied to mold tool surfaces to aid first ply placement, metallic mesh, or to prepreg to aid in the placement of core components and other dry materials.

1.3 Skills Required

Manual skills

Familiarity with Layup Room Procedures

2.0 Preparation of Tackifier Solution

2.1 Obtain pieces of prepreg, a metal paint can or similar, and acetone. Be sure to wear acetone and resin resistant gloves, such as latex or nitrile. Use the same resin system as the part to be laid up unless otherwise noted. Whenever possible, use discarded off cuts from ply kits.

2.2 Prepreg shall not be more than 6 months expired for use in a tackifier solution.

2.3 If resin cannot be fully dissolved in the acetone, the solution is not acceptable for use and shall be discarded.

- 2.4 Identify the can with "Tackifier" or "Tackifier Solution". Record the prepreg material, lot number, and date of solution preparation on the container. Only use prepreg with the same lot number for a given solution.
- 2.5 It is suggested to start with a 3:1 ratio of acetone to prepreg, by weight.
- 2.6 The ratio may be adjusted to achieve the desired level of tack.
- 2.7 Cover the solution and allow the acetone to fully soak the prepreg. Stirring the solution will help to dissolve the resin. Wash the prepreg and squeeze out acetone/resin from the reinforcement
- 2.8 If necessary add additional acetone, prepreg, or allow acetone to evaporate to achieve desired consistency and tack.
- 2.9 Tackifier may be stored at room temp in a sealed container for 30 days. Acetone may be added as required. Do not add additional prepreg after the initial preparation.
- 3.0 Application of Tackifier Solution
- 3.1 Wet the area to be treated with a thin even coating of the tackifier. A brush is a suitable means of application. Avoid pooling.
- 3.2 Allow the acetone to evaporate from the tackified surface for 10 minutes minimum before application of additional plies or materials.
- 3.3 Record the pre-preg material, lot number, and date of solution preparation on the traveler.

Bibliography

- Airtech International Inc. "Pressure Strip." Data Sheet. 2013. 2014.
- Alexandru Valentin Radulescu, Sorin Cananau, Irina Radulescu. "Mechanical Testing Methods Concerning the Stress Analysis for a Vehicle Wheel Rim." *Mechanical Testing and Diagnostics* (2012): 33-39.
- Andreas Norbert Rupp, André Heinrietz, Oliver Ehl. "Simulation of the Experimental Proof Out of Wheels and Hubs." *SAE 2002 World Congress*. Detroit: SAE International, 2002.
- B. Riley, A. George. *Design, Analysis and Testing of a Formula SAE Car Chassis*. Warrendale, PA: SAE International, 2002.
- "Beginners' Guide to Out-of-Autoclave Prepreg Carbon Fibre." Guide. n.d.
- Black, Sara. "Getting To The Core Of Composite Laminates." 1 October 2003. *Composites World*. 2013. <<http://www.compositesworld.com/articles/getting-to-the-core-of-composite-laminates>>.
- Carbon Revolution Pty Ltd. *The World's First One-Piece Carbon Fiber Wheel*. 2013. May 2014. <<http://carbonrev.com/>>.
- Cathcart, Alan. "BST Blackstone: Black Gold!" *FIM Magazine* February March 2011: 45-51.
- Chapman, LT Matthew K. "Development of a Composite Wheel Rim for an FSAE Car." Undergraduate Thesis Report. 2011.
- Compositech. "Carbon Fiber Car Wheel." n.d.
- COMSOL. "Fatigue Analysis of an Automobile Wheel Rim Solved with COMSOL Multiphysics 3.5a." 2008.
- Cremens, Walter S. "Thermal Expansion Molding Process for Aircraft Composite Structures." *Turbine Powered Executive Aircraft Meeting*. Phoenix: SAE Inc., 1980.
- Crouchen, Mark. "The Use of Thermal Expansion Cores for Non-Autoclave Processing of Pre-Preg Materials." Rockwood Composites Ltd, n.d.
- Cytec Industrial Materials. "De-bulking Guidelines." n.d.
- Cytec Industrial/Aerospace Materials. "MTM 45-1." Data Sheet. n.d.
- David Banis, J. Arthur Marceau, Michael Mohaghegh. "Design for Corrosion Control." n.d. *Aero Magazine*. Boeing. 2013. <http://www.boeing.com/commercial/aeromagazine/aero_07/corrosn.html#table01>.
- Dhananjayan, Vinoth Kumar. "Design and Analysis of a Compression Molded Carbon Composite Wheel Center." Master's Thesis. 2013.

E Reissner, M Stein. "Torsion and Transverse Bending of Cantilever Plates." n.d.

Ellsworth Adhesives. *Surface Preperation Guide*. 2014. 2014.
<<http://www.ellsworth.com/resources/surface-preparation-guide/#stainless-steel>>.

Federal Aviation Administration. "Advanced Composite Materials." *Aviation Maintenance Technician Handbook*. n.d. (7)1-(7)58.

Gardiner, Ginger. "Out-of-autoclave prepregs: Hype or revolution?" *High Performance Composites* 1 January 2011. <<http://www.compositesworld.com/articles/out-of-autoclave-prepregs-hype-or-revolution>>.

Gerhard Fischer, Vatroslav V. Grubisic. "Design Criteria and Durability Approval." *International Truck and Bus Meeting and Exposition*. Indianapolis: SAE International, 1998.

GMT Composites. *The Autoclave Myth*. n.d. 27 April 2014.
<<http://www.gmtcomposites.com/why/autoclave>>.

Hawkeye Industries Inc. "Duratec Polyester Surfacing Primer." Data Sheet. n.d.

Heisler, Heinz. "Advanced Vehicle Technology." 1989.

Henkel Corporation. *Porosity Sealing by Design*. Madison Heights, 2005.

Henkel Corporation Aerospace Group. *Hysol® Surface Preparation Guide*. Guide. Bay Point, n.d.

Herakovich, Carl T. *Mechanics of Fibrous Composites*. New York: John Wiley & Sons, Inc., 1998.

Hoke, Michael J. "Adhesive Bonding of." Presentation. n.d.

"Hysol E-40HT." Technical Data Sheet. 2008.
<[https://tds.us.henkel.com/NA/UT/HNAUTTDS.nsf/web/7F948428635DFC62852573B600685299/\\$File/HYSOL%20E-40HT-EN.pdf](https://tds.us.henkel.com/NA/UT/HNAUTTDS.nsf/web/7F948428635DFC62852573B600685299/$File/HYSOL%20E-40HT-EN.pdf)>.

Hysol Surface Preperation Guide. Guide. Bay Point: Henkel Corporation, n.d.

IIT Kanpur. *Module 5: Laminate Theory. Lecture 17: Laminate Constitutive Relations*. n.d. 2013.
<http://nptel.ac.in/courses/101104010/lecture17/17_1.htm>.

J.E. Jam, N.O. Ghaziani. "Numerical and experimental investigation of bolted joints." *International Journal of Engineering, Science and Technology* 3.8 (2011): 285-296.

Jack E. Gieck, William D. Noil. "Composite Wheels." *Congress and Exposition*. Detroit: SAE International, 1980.

Kinstler, John. "The Science and Methodology of SAE Wheel Fatigue Test Specifications." *2005 SAE World Congress*. Detroit: SAE International, 2005.

- Little, P.K. Mallick and R.E. "Design of Mechanically Fastened (Bolted) Joints in Automotive Composites." *International Congress & Exposition*. Detroit: SAE International, 1994.
- Loctite Structural Adhesives Selector Guide*. Guide. Rocky Hill: Henkel, n.d.
- Luxmoore, Joe. "Analysis of Composite Structures with ACP." ANSYS, Inc., 24 June 2013.
- M. Chawla, D. Homa B.F. Spencer Jr., D.J. Kirkner, E.E. Schudt. "Experimental Verification of an Algorithm for." *Aerospace Atlantic Conference*. Dayton: SAE International, 1995.
- Maduskuie, Andrew. "Spring 2008 Carbon Wheels Technical Report." 2008.
- Making 280mph Capable Carbon Fiber Wheels - Inside Koenigsegg*. Koenigsegg. 2014.
<<https://www.youtube.com/watch?v=PGGiuaQwcd8>>.
- Mason, Stephen. *The Effects of Rotational Inertia on Automotive Acceleration*. n.d. May 2014.
<<http://stephenmason.com/cars/rotationalinertia.html>>.
- matt#corse. *Warning dymag carbon wheel single sided swingarm*. 2013. 10 April 2014.
<<http://www.ducati.ms/forums/11-ducatti-motorcycle-chat/272025-warning-dymag-carbon-wheel-single-sided-swingarm.html>>.
- McClendon, Julien L.H. "Determine Bearing Stress Distribution in Composite." Final Project Report. 2011.
- McElroy, John. *Manufacturing advances bring carbon fiber closer to mass production*. 27 November 2012. 2014. <<http://www.autoblog.com/2012/11/27/manufacturing-advances-bring-carbon-fiber-closer-to-mass-product/>>.
- Meier, Kyle. "Spring 2010 Carbon Fiber Wheels Technical Report." 2010.
- Mindlin, R D. "Influence of Rotatory Inertia and Shear on Flexural Motions of Isotropic, Elastic Plates." n.d.
- Mosites Rubber Company, Inc. *Silicone Rubber Fabrications*. 2014. 2014.
<<http://www.mositesrubber.com/products/silicone-rubber-fabrications.htm>>.
- . *Silicone Rubber Technical Information*. n.d. 2014. <<http://mositesrubber.com/technical/silicone-rubber.htm>>.
- N. T. Tseng, R. O. Pelle and J. P. Chang. "Numerical Simulation for the Tire..Rim." *International Congress and Exposition*. Detroit: SAE International, 1989.
- Niederer, Bruce. "If you can't take the heat... Understanding the effects of high temperatures on cured epoxy." *EPOXYWORKS* 2006: 1-2. <<http://www.westsystem.com/ss/assets/Uploads/04-Heat.pdf>>.

- Niu, Michael C.Y. *Composite Airframe Structures: Practical Design Information and Data*. Third. Hong Kong: Hong Kong Conmilit Press Ltd., 2010.
- P. Seaburg, C. Carter. *Torsional Analysis of Structural Steel Members*. Chicago, IL: American Institute of Steel Construction, 1997.
- Pandey, P. C. "NPTEL: Composite Materials." 2004. *National Programme on Technology Enhanced Learning*. 2013.
- Peters, S.T. "Ten Common Mistakes in Composite Design and Manufacture and How to Avoid Them." *SAMPE Journal* (2006): 53-58.
- Ramsey, Jonathon. *BMW to offer carbon fiber wheels in a year or two*. 23 February 2014. May 2014. <<http://www.autoblog.com/2014/02/23/bmw-carbon-fiber-wheels/>>.
- Reddy, J N. "Theory and Analysis of Elastic Plates and Shells." n.d.
- Rotondo, Megan. "ARG11 Fall Technical Report." 2010.
- . "ARG11 Spring 2011 Technical Report." 2011.
- S. Heimbs, M. Pein. *Failure Behavior of Honeycomb Sandwich Corner Joints and Inserts*. Munich, Germany: Elsevier, 2009.
- S. Venkateswarlu, K. Rajasekhar. "Modelling and Analysis of Hybrid Composite Joint Using Fem in Ansys." *IOSR Journal of Mechanical and Civil Engineering* 6.6 (2013): 1-6.
- SAE International. "2014 Formula SAE Rules." 2013.
- Sloan, Jeff. "High-speed press cure for high-speed racers." 1 July 2011. *Composites World*. High-Performance Composites. 2013. <<http://www.compositesworld.com/articles/high-speed-press-cure-for-high-speed-racers>>.
- . "High-speed press cure for high-speed racers." *High Performance Composites* July 2011. <<http://www.compositesworld.com/articles/high-speed-press-cure-for-high-speed-racers>>.
- . "Machining carbon composites: Risky business." March 4 2010. *Composites World*. 2013. <<http://www.compositesworld.com/articles/machining-carbon-composites-risky-business>>.
- Smooth-On, Inc. *Preparation of Surfaces for Epoxy Adhesive Bonding*. 2011. 2014. <<http://www.smooth-on.com/Adhesive-Bonding/c16/p43/Preparation-of-Surfaces-for-Epoxy-Adhesive-Bonding/pages.html>>.
- SP Gurit. "Guide to Composites." n.d.
- Strong, A. Brent. *Fundamentals of Composites Manufacturing: Materials, Methods and Applications*. Society of Manufacturing Engineers, 2007.

- Su, Fang-Yu and Xiao-Qing Wu. "Experimental Study on Silicone Rubber Mold Design for Thermal Expansion RTM." *Reinforced Plastics and Composites* (2010): 1-5.
- Th. Kermanidis, G. Labeas, K.I. Tserpes and Sp. Pantelakis. "Finite Element Modeling of Damage Accumulation in Bolted Composite Joints Under Incremental Tensile Loading." *European Congress on Computational Methods in Applied Sciences and Engineering*. Barcelona: ECCOMAS, 2000.
- The Microseal Co. *Brochure*. n.d. 2014. <<http://www.microleak.com/brochnew.htm>>.
- The Tire and Rim Association. "5 Degree Drop Center Rim Contours JA Contour for 10, 12, 14, and 15 Rim Diameter Codes." 2010.
- Thryft, Ann R. *One-Piece Carbon Composite Wheel Drives Cars*. 13 August 2012. 2014. <http://www.designnews.com/author.asp?doc_id=248043>.
- U. Kocabicak, M. Firat. "Numerical Analysis of Wheel Cornering Fatigue Tests." *Engineering Failure Analysis* (2001): 339-354.
- UMECO. "Introduction to Advanced Composites and Prepreg Technology." n.d.
- United, Nations. "Uniform Provisions Concerning the Approval of Wheels for Passenger Cars and their Trailers." Agreement. 2007.
- Vermont Composites. "Design Guide for Composite Enclosures." n.d. <http://www.vtcomposites.com/Images/UserDir/PDF/VCI_CarbonFiberDesignGuide.pdf>.
- Wei, Daniel C. "Ram Section Fatigue Results of Aluminum and Steel Wheels." *International Congress & Exposition*. Detroit: SAE International, 1982.
- West System. *105 Epoxy Resin® / 207 Special Clear Hardener*. Technical Data Sheet. Bay City: Gougeon Brothers Inc., 2013.
- Whitcomb, John and Xiaodong Tang. "Effective Moduli of Woven Composites." *Journal of Composite Materials* (2001): 2127-2144.
- Woinowsky-Krieger, S. Timoshenko and S. *Theory of plates and shells*. NY: McGraw-Hill, 1959.
- Wrightson, Cole. *ARG11_Frame_Technical_Report_Spring_2011*. Ithaca, NY: Cornell University, 2011.
- Wu, James, Owusu A. Agyeman Badu and Yongcheng Tia. "Design, Analysis and Testing of an Automotive Carbon Fiber Monocoque Chassis." Meng Project Report. Cornell University, 2013.
- Wubin Xu, Peter J Ogrodnik, Bing Li, Jian Li, Shangping Li. "Simplified Stress Analysis of Large-scale." (n.d.): 355-364.
- X. Yang, O. A. Olatunbosun and E. O. Bolarinwa. "Materials Testing for Finite Element Tire Model." *SAE International Journal of Materials Manufacturing* 3.1 (2010): 211-220.

Zander, B. *Carbon Fiber Monocoque: Design, Analysis and Validation*. Ithaca, NY: Cornell University, 2011.

Zipp Speed Weaponry. *Woven Carbon vs. Unidirectional*. n.d. 2014.
<<http://www.zipp.com/technologies/composite/woven.php>>.